Available online at www.sciencedirect.com
ScienceDirect
Tetrahedron 64 (2008) 261–298
Tetrahedron

Tetrahedron report number 820

(+)-Discodermolide: total synthesis, construction of novel analogues, and biological evaluation

Amos B. Smith, III* and B. Scott Freeze

Department of Chemistry, Monell Chemical Senses Center, Penn Center for Molecular Discovery, and Laboratory for Research on the Structure of Matter, University of Pennsylvania, Philadelphia, PA 19104-6323, USA

Received 9 September 2007
Available online 12 October 2007

Contents

* Corresponding author. Tel.: +1 215 898 4860; fax: +1 215 898 5129; e-mail: smithab@sas.upenn.edu

doi:10.1016/j.tet.2007.10.039

1. Introduction

Natural products have a well-proven track record as cancer chemotherapeutic agents.[1] Beginning in the late 1960s with the approval of the Vinca alkaloids vinblastine and vincristine for the treatment of a number of cancers, natural products have emerged both as treatments and as leads for further drug development. Without a doubt, the most important cancer chemotherapeutic agent to arise from a natural source is paclitaxel (Taxol®, Fig. 1),[2] a complex diterpene originally isolated from the bark of the Pacific yew *Taxus brevifolia*. Paclitaxel has met with considerable clinical success for ovarian, breast, and lung carcinomas, but the relative paucity of paclitaxel available from the Pacific yew (4000 trees were sacrificed to furnish 360 g of the drug) nearly prevented the drug from being developed. The supply problem was ameliorated with the discovery that a structurally similar compound, 10-deacetylbaccatin III, could be extracted readily in much larger quantities from the renewable foliage of the European yew *Taxus baccata* that, in turn, could be converted chemically to paclitaxel or to the more potent synthetic congener Taxotere (Fig. 1).

Paclitaxel comprises the first member of an ever-growing class of natural products that induce the polymerization of the ubiquitous cellular protein tubulin and suppress microtubule dynamics,[2a] thus preventing effective cell division. The second entry to this class, epothilones A and B (Fig. 1),[3] also hold considerable promise as lead anticancer agents in part because, unlike paclitaxel, the epothilones showed efficacy against several multi-drug-resistant (MDR) cell lines.[4] However, the most interesting compounds to result from the epothilone studies are the structurally related synthetic analogues. For example, Danishefsky and co-workers discovered that 12,13-desoxyepothilone B (Fig. 1), a late-stage intermediate in the total synthesis of epothilone B, displayed in vivo tumor growth suppression superior to that of the natural product in mice bearing human xenograft tumors.[4c] More importantly, 12,13-desoxyepothilone B (now termed epothilone D) exhibited little to no general cytotoxicity, whereas epothilone B often proved to be fatal to the treated mice. Further optimization ultimately led the Danishefsky team, in collaboration with Kosan Biosciences, to 26-trifluoro-*E*-9,10-dehydro-12,13-deoxyepothilone B (Fludelone, Fig. 1), an orally available agent that led to complete tumor remission in two tumor xenograft models, with no relapse evident even after 200 days![5] This synergy between total synthesis and drug optimization is not solely academic; in 2005, a joint Kosan/Roche venture entered epothilone D into Phase II clinical trials[6] for the treatment of breast, lung, and prostate cancer. Earlier this year that trial was halted in order to focus resources on a second, more promising epothilone B congener (9,10-didehydro-12,13-desoxyepothilone B, Fig. 1)[6] that was recently introduced into Phase II. Elsewhere, Bristol–Myers Squibb Company has completed Phase III clinical trials on Ixabepilone (another epothilone

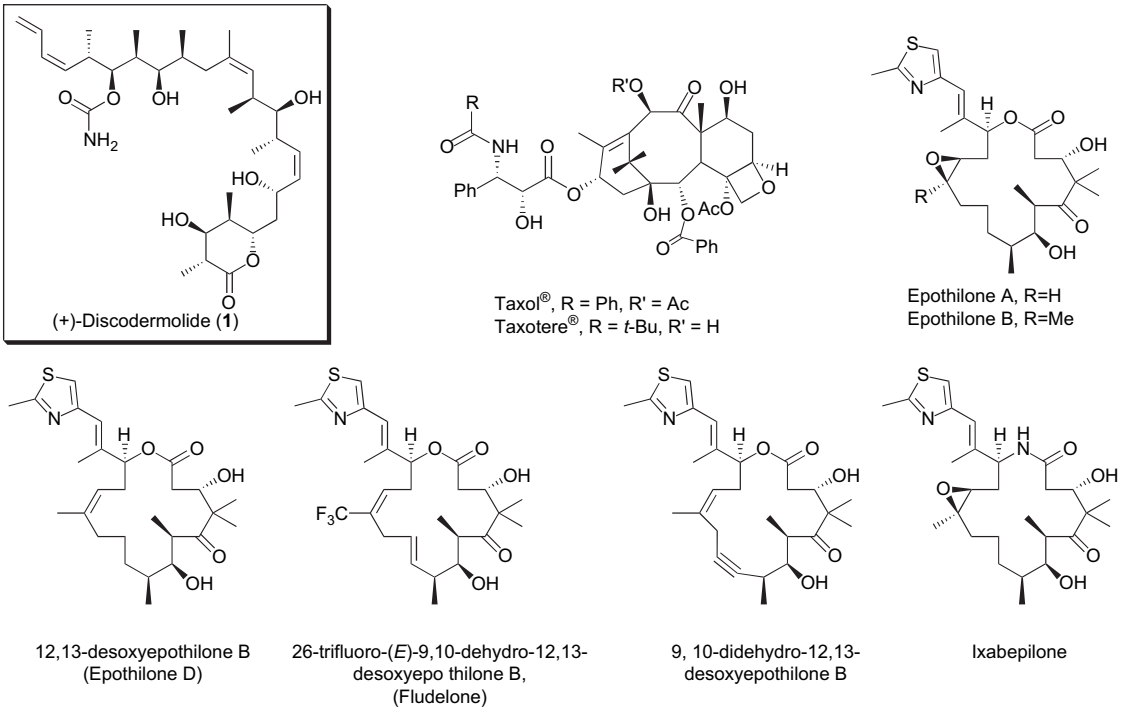

Figure 1. Natural and non-natural microtubule-stabilizing agents.

B analogue),[7] and in June 2007 applied for a New Drug Application for the monotherapy treatment of metastatic or locally advanced breast cancer in patients whose tumors are resistant or refractory to anthracyclines, taxanes, and capecitabine. On October 16th, 2007, ixabepilone was approved by the FDA for this indication under the trade name Ixempra.

A third structurally distinct microtubule-stabilizing natural product, (+)-discodermolide (**1**, Fig. 1), was isolated in 1990 by Gunasekera and co-workers at the Harbor Branch Oceanographic Institute from the deep-sea marine sponge *Discodermia dissoluta*.[8] Employing a battery of NMR experiments, including ^{1}H, ^{13}C, COSY, long-range COSY, and several 2D correlation experiments, the Gunasekera team determined that (+)-discodermolide comprises a linear polypropionate backbone, punctuated by *Z*-olefinic linkages at C(8,9) and C(13,14), a terminal *Z*-diene substituent at C(21–24), 13 stereogenic centers (including 4 secondary hydroxyls and 7 methyl substituents), a carbamate, and a fully substituted D-lactone. While the relative stereochemistry was determined by X-ray crystallography, the absolute stereochemistry of (+)-discodermolide remained unknown until 1993, when Schreiber and co-workers reported the first total synthesis in the discodermolide area,[9a] which unfortunately proved to be the unnatural antipode. The Schreiber group then prepared the natural congener.[9c]

(+)-Discodermolide, like the epothilones, retains tumor cell growth inhibitory activity against several MDR cancer cell lines. However, (+)-discodermolide exhibits a number of characteristics unique among the microtubule-stabilizing agents, including a linear (not macrocyclic) framework, immunosuppressive properties both in vitro[10a] and in vivo,[10b] potent induction of an accelerated senescence phenotype,[11] and synergistic antiproliferative activity in combination with paclitaxel.[12] Importantly, despite the discovery of several additional microtubule-stabilizing natural products—including eleutherobin,[13] sarcodictyins A and B,[14] laulimalide and isolaulimalide,[15] dictyostatin,[16] peloruside A,[17] FR182876,[18] WS9885B,[19] taccalonolides,[20] and the coumarins[21]—discodermolide remains the most potent natural promoter of tubulin assembly yet discovered.[22] The intriguing biological activity profile has prompted a number of efforts directed toward the total synthesis of (+)-discodermolide as well as toward the production and evaluation of synthetic analogues. The sections to follow present a detailed account of each of these aspects of discodermolide research.

2. Biological activities of (+)-discodermolide

2.1. (+)-Discodermolide: immunosuppressive properties

Initial biological evaluation, carried out by researchers at Harbor Branch, demonstrated that (+)-discodermolide (**1**) is a highly potent immunosuppressive agent, with activity comparable to that of the clinically proven immunomodulator cyclosporin A, both in vitro[10a] and in vivo.[10b] Specifically, (+)-discodermolide was found to suppress the two-way mixed lymphocyte reaction (MLR) in both human peripheral blood leukocytes (PBL) and murine splenocytes. Mitogenic response of PBL in the presence of the immunostimulators concavalin A (ConA) or phytohemagglutinin (PHA) was similarly suppressed by (+)-discodermolide, with IC_{50} values in the low micromolar range. Importantly, the immunosuppression response is observed at concentrations of (+)-discodermolide that are essentially non-toxic in vitro.

Follow-up experiments probed the efficacy of (+)-discodermolide as an in vivo immunosuppressant, utilizing the parental-F_1 graft-versus-host reaction model for splenomegaly. At daily dosage levels of 1.25 and 5.0 mg/kg, discodermolide suppressed the splenomegaly response by 93 and 219%, respectively, which is 100- to 1000-fold more potent than cyclosporin A, and on par with the powerful immunosuppressant FK506.[10b] Mechanistic investigations, by researchers at Harbor Branch in collaboration with Roche and Merck, demonstrated that the immunosuppressive activity of discodermolide was largely due to a general antiproliferative effect on lymphoid cells, including PHA- and ConA-induced T cells, at low-nanomolar concentrations.[23] This antiproliferative activity was not limited to lymphoid cells, as (+)-discodermolide was demonstrated to maintain potent antiproliferative effects in several non-lymphoid cell lines.[23]

2.2. (+)-Discodermolide: antiproliferative/antimitotic properties

Cell cycle studies designed to probe the general antiproliferative activity of (+)-discodermolide (**1**), first reported in 1993 by a collaboration between Harbor Branch, Roche, and Merck, demonstrated that discodermolide prevented murine DO11.10 T hybridoma cells from cycling normally through the phases of the cell cycle.[23] In untreated controls, 68% of cells were found to comprise the G_1 phase of the cell cycle, 31% were found at the S phase, and less than 1% could be seen at the G_2/M phase. After treatment for 3 h with discodermolide, the characteristic percentages shifted to 52% at the G_1 phase, 40% at the S phase, and 8% at the G_2/M phase. After 24 h, an even more marked difference was noted, with only 25% of cells now comprising the G_1 phase, 16% at the S phase, and 58% at the G_2/M phase, indicating that discodermolide blocks the cell cycle at the G_2/M phase. The cell cycle effect is reversible, as cells will resume normal cycling within 48 h after the removal of discodermolide from the medium.[23]

Subsequently (1996), ter Haar and co-workers, in collaboration with the Harbor Branch team, disclosed that discodermolide arrests mitosis via binding and stabilization of the microtubule network,[24] findings that were confirmed by the Schreiber laboratory shortly thereafter.[25]

2.3. (+)-Discodermolide: a potent microtubule-stabilizing agent

ter Haar and co-workers[24] demonstrated that, under every reaction conditions studied, tubulin polymerization was substantially more rapid upon treatment with discodermolide than with equimolar concentrations of paclitaxel. Indeed, discodermolide at a concentration of 10 μM proved to be able to promote assembly of microtubules at 37 °C even in the absence of microtubule-associated proteins (MAPs)

and/or GTP, conditions under which paclitaxel is inactive. With assistance from MAPs or GTP, 10 μM discodermolide is able to initiate tubulin polymerization at temperatures as low as 0 °C; again, Taxol is inactive under these conditions. Stability to depolymerization was also markedly superior in discodermolide-induced tubulin polymers. Specifically, addition of up to 5 mM $CaCl_2$ to polymers at 0 °C, in the presence *or absence* of MAPs and/or GTP, had no effect on the extent of assembly for the discodermolide-treated microtubule system. Taxol-induced polymers, on the other hand, began to disassociate in the presence of only 0.6 mM $CaCl_2$, even in the presence of MAPs and GTP. A final point of comparison examined by ter Haar and co-workers was the average number and length of the tubulin bundles induced upon treatment with either of the two anti-tubulin agents, at temperatures ranging from 0 to 37 °C. Discodermolide-induced systems consistently displayed large numbers of very short polymers, with an average length between 0.5 and 0.6 μm; this result proved to be independent of temperature. On the other hand, Taxol-induced microtubules were fewer in number and grew much longer in lengths on an average. At 10 °C, polymers initiated by Taxol averaged 0.7 μm in length, with those observed at 20 or 37 °C averaging over 1.60 μm. These results highlight the extraordinary ability of discodermolide to hypernucleate tubulin assembly.

In a parallel series of experiments, the Schreiber group explored the competitive binding of paclitaxel and discodermolide, as well as the stoichiometry of the tubulin polymerization event;[25] in the process, the Harvard group confirmed many of the ter Haar results. For example, pure tubulin dimers (10 μM) undergo polymerization in the presence of 10 μM Taxol, ensuring that each of the dimers is occupied with Taxol. Radiolabeled [^{3}H]-discodermolide was then added in various concentrations, and the fraction of tubulin bound with discodermolide measured. Under these conditions, discodermolide binding proceeded with a 1:1 stoichiometry, reaching a saturation point at 10 μM. This result clearly demonstrated that the presence of bound Taxol does not interfere with the binding of discodermolide; however, whether discodermolide competes with Taxol or instead binds at a distinct site remained to be determined. Initially, this question was addressed via a series of competitive binding experiments, utilizing tritiated Taxol and discodermolide as a means to quantify their respective binding. These experiments demonstrated that discodermolide does indeed competitively displace [^{3}H]Taxol from microtubules. Conversely, tubulin polymers bound with discodermolide remained largely unchanged even upon treatment with super-stoichiometric concentrations of Taxol. Taken together, these results indicate that Taxol and discodermolide bind in a mutually exclusive manner to microtubules, implying the same or overlapping binding sites.[25]

In early 2006, in collaboration with Horwitz and co-workers, we disclosed the results of a series of radiolabeling–digestion experiments directed toward the elucidation of the precise discodermolide binding domain of tubulin.[26] The study employed a radiolabeled discodermolide analogue bearing a benzophenone photoaffinity probe.[27] Photoincorporation of the probe to tubulin was followed by formic acid hydrolysis, immunoprecipitaion experiments, and subtilisin digestion, as well as Asp–N and Arg–C digestions. These experiments implicated amino acid residues 355–359 as the site of photoincorporation, residues that lie very near the known Taxol binding domain on the β-tubulin monomer. More specifically, residues 355–359 were found to comprise a subpocket within the taxoid binding site, an observation that guided the development of a model for discodermolide binding wherein the discodermolide skeleton occupies the Taxol binding site and the benzophenone appendage extends into the adjacent subpocket. It should be noted, however, that the precise mode and orientation of discodermolide binding at the molecular level remain speculative, in spite of extensive NMR and modeling studies.[28,29]

2.4. Discodermolide: retention of cytotoxicity against both taxol-resistant and multi-drug-resistant cell lines

In 1997, the Harbor Branch group assayed (+)-discodermolide against two multi-drug-resistant cell lines (including Taxol-resistant lines) that overexpress the *P*-glycoprotein transporter.[30] The relative resistance factor was evaluated as the ratio between the IC_{50} in the drug-resistant cell lines and the IC_{50} in the parent drug-sensitive cell lines. The results indicate that while the SW620AD-300 colon carcinoma line displays a 930-fold increased resistance to paclitaxel relative to the drug-sensitive variant SW620, discodermolide is only 25-fold less potent in the resistant cell line. Even more strikingly, paclitaxel diminishes in potency by a factor of 2800 in the drug-resistant A2780AD ovarian carcinoma cell line versus the parent 1A9 cell line, while the resistance factor of discodermolide is only 89.

Discodermolide was also evaluated against two 1A9-derived cell lines bearing β-tubulin mutations that render the cells resistant to treatment with Taxol. In both cases, the mutant cell line was over 20-fold less sensitive to Taxol than the wild-type 1A9. Conversely, complete sensitivity to discodermolide was retained in both mutant cell lines, a phenomenon that is thought to be the result of the superior hypernucleation activity of discodermolide relative to paclitaxel.[30]

2.5. Discodermolide and paclitaxel: a synergistic drug combination

Although paclitaxel has proven to be a highly successful chemotherapeutic, both alone and in combination with cisplatin, the growing incidence of clinical resistance to paclitaxel has prompted a search for new drugs and/or drug combinations. Traditionally, combination therapies utilize drugs whose mechanisms of action are distinct from one another, with the goal of targeting two independent disease-related pathways. However, therapies combining drugs with similar molecular targets (for example, paclitaxel and vinorelbine)[7] have advanced into Phase I/II clinical trials, indicating that this tactic holds considerable promise. With this in mind, Horwitz and co-workers at the Albert Einstein College of Medicine, in collaboration with the Smith and Danishefsky groups, began to explore the effects of alternate microtubule-stabilizing agents against several carcinoma cell lines.[12a]

These studies began with evaluation of several known microtubule-stabilizing agents, including paclitaxel, discodermolide, eleutherobin, and epothilones A and B, against

a variety of *P*-glycoprotein expressing and non-*P*-glycoprotein expressing cell lines. By and large, cell lines that were sensitive to paclitaxel were also sensitive to the other four agents. However, paclitaxel-resistant cell lines that overexpress *P*-glycoprotein tend to display cross-resistance to eleutherobin, but remain sensitive to the epothilones and discodermolide. Horwitz and co-workers also discovered a mutant cell line, termed A549-T12, that does not overexpress *P*-glycoprotein, displays 9-fold resistance to paclitaxel, and in fact *requires* low levels of paclitaxel in order to cycle smoothly through the G_2/M phase of the cell cycle. With the required low concentration of paclitaxel, this cell line exhibits cross-resistance to epothilones A and B, and eleutherobin, but not to discodermolide, making discodermolide the only agent tested that retains potent cytotoxicity. Low concentrations of epothilone A, epothilone B, or eleutherobin were also able to maintain the viability of the A549-T12 cell line in the absence of paclitaxel, whereas discodermolide proved unable to prevent the G_2/M-phase blockage at any concentration. Perhaps most interestingly, A549-T12 cells proved to be 20-fold *more sensitive* to discodermolide in the presence of low concentrations of paclitaxel (~2 nM) than in the absence, a result that is counterintuitive given the paclitaxel-dependence of the cell line.

The synergistic cytotoxicity of the discodermolide/paclitaxel combination in the A549-T12 cell line prompted Horwitz and Smith to investigate the phenomenon, with a paclitaxel/epothilone B combination serving as the control.[12] Four carcinoma cell lines (A549, SKOV3, MCF-7, and MDA-MB-231) were treated with each of the two drug combinations; a *C*ombination *I*ndex (CI) value was calculated, according to the method of Chou and Talalay,[31] to determine whether the combination acts synergistically (CI<1), additively (CI=1), or antagonistically (CI>1). The outcome clearly revealed a high degree of synergy between paclitaxel and discodermolide; the calculated CI values were significantly less than 1 in all four cell lines, across a 3- to 4-fold log concentration of the drugs. In contrast, only additive interactions were observed for the combination of paclitaxel and epothilone B.

Follow-up studies[12b] demonstrated that most of the microtubule dynamic instability parameters (growth rate, shortening rate, growth duration, shortening duration, pause duration, growth length, shortening length, % time spent growing, % time spent shortening, % pause time, and overall dynamicity) were synergistically altered by the paclitaxel/discodermolide combination, with CI values ranging from 0.20 to 0.41. Additionally, the cell cycle progression was synergistically blocked at the G_2/M phase with a CI of 0.59. Apoptosis was also enhanced cooperatively, although to a lesser degree (CI=0.85). The overall degree of synergy is quite surprising, given that paclitaxel and discodermolide appear to share both a common binding site and mechanism of action.[12b]

Synergism of paclitaxel and discodermolide was also observed in vivo using SKOV3 human tumor xenograft models.[32] In fact, combination treatment suppressed angiogenesis and induced *tumor regression* at drug concentrations that independently led to only minimal tumor growth suppression. A closer look revealed that at low concentrations, treatment with paclitaxel or discodermolide resulted in drug-induced aneuploidy, while at higher concentrations, single-agent treatment resulted instead in mitotic arrest. The synergistic effect of combination treatment was most profound when administering relatively low concentrations of paclitaxel and discodermolide (i.e., a drug regimen that induced aneuploidy, but not mitotic arrest). Importantly, the combination of discodermolide and paclitaxel was remarkably well-tolerated in the treated mice, with no toxicity noted at efficacious levels. While the precise mechanism of the observed synergism remains unknown, Horwitz and Smith speculate that the two agents might preferentially target different tubulin isotypes, despite exhibiting mutually exclusive binding to a likely common tubulin binding site. Additionally, discodermolide, but not paclitaxel, has been shown to induce an accelerated senescence phenotype (which will be the subject of the following section), providing a second potential mechanism for synergy. Efforts to elucidate the exact nature of this effect continue.

2.6. (+)-Discodermolide: a powerful inducer of accelerated senescence

In 2005, Horwitz and co-workers, in collaboration with the Smith group, isolated an A549-derived cell line that proliferated in 8 nM discodermolide, a concentration approximately one-third the IC_{50} value for parental A549 cells.[11] Further examination of this cell line, which was termed A549.Disco8, revealed that short-term exposure to the IC_{50} concentration (24 nM) of discodermolide results in both an alteration of cellular morphology and the expression of senescence-associated β-galactosidase (SA-β-gal) activity, both characteristic of an accelerated senescence phenotype. Hallmarks of senescence, which commonly occurs in cells that have undergone a series of cell divisions, include the following: a cessation of proliferation, an overall flattening of the cellular structure, an increased cytoplasmic area, and the onset of significant SA-β-gal activity.[33] Although many antitumor treatment regimens are known to induce the senescence phenotype, this phenomenon had not been observed previously with microtubule-stabilizing agents.

To explore the generality of this effect, Horwitz and co-workers separately treated HeLa, MDA-MB-231, HCT-116, and parental A549 cells with discodermolide, paclitaxel, and the known senescence-inducing agent doxorubucin (25 nM each). As expected, doxorubicin produced consistently high levels of SA-β-gal activity in all four cell lines. Discodermolide-treated cells also exhibited moderate to high levels of SA-β-gal activity across the panel, while paclitaxel induced far less, if any SA-β-gal activity.[11]

Investigation of the expression and activity of several proteins known to be associated with senescence found several differences between discodermolide-treated cells and those treated with paclitaxel, providing a basis for the disparity in the effects of the two antimicrotubule agents. Most notably, discodermolide induced substantial up-regulation and/or activation in three proteins (p66Shc, Erk1, and Erk2) involved in the mitogenic activation signaling pathway; in contrast, little or no increase in activity was noted upon paclitaxel treatment. Several other cellular pathways were found to require a much higher concentration of paclitaxel than discodermolide (relative to IC_{50}) to promote the senescence-related

response. The longevity and/or intensity of the response induced by the two agents also tended to differ.[11]

2.7. Discodermolide: a potential neuroprotective agent

Traditionally, the search for the treatment of Alzheimer's and related neurodegenerative diseases has focused on the prevention of the amyloid plaques and neurofibrillary tangles that are the hallmarks of these disorders.[34] Recently, however, a new therapeutic approach to neurodegenerative diseases was validated by Lee and Trojanowski at the University of Pennsylvania that entailed the in vivo use of microtubule-stabilizing drugs to restore function to neurons that have been disrupted by the β-amyloid-induced sequestration of the microtubule-associated tau protein.[35]

In healthy neurons, the function of tau protein is to stabilize the microtubule network, which serves as the 'railroad track' upon which actin, tubulin, mitochondria, neurotransmitter-related enzymes, and vesicles carrying messenger proteins are delivered between the nucleus and the extremities of the elongated cell.[36] The presence of amyloid-β, however, has been demonstrated to lead to hyperphosphorylation and aggregation of tau protein into neurofibrillary tangles,[37] rendering tau protein ineffective at stabilizing the microtubule network.[38] These 'tauopathies' result in a functional loss of axonal transport, leading to reduced microtubule numbers, and in turn, neurodegeneration and motor weakness.[39] Utilizing a transgenic mouse model for human tauopathy, the Penn team demonstrated that exogenous paclitaxel stabilizes microtubules, and thereby restores fast axonal transport and microtubule numbers to physiologically viable levels, thus offsetting the loss of function caused by the hyperphosphorylation, misfolding, and aggregation of tau protein.[35] Most importantly, motor-impaired mice exhibited a complete recovery of normal movement upon treatment with paclitaxel!

In a concurrent study, Georg and co-workers examined the use of microtubule-stabilizing compounds as neuroprotective agents in vitro, using cortical neurons that had been exposed to amyloid-β.[40] They found that the neuroprotective effects of paclitaxel, as measured by the neuron survival rate in treated cells versus untreated cells, were general for a variety of microtubule-stabilizing agents, including epothilone A, discodermolide, and the paclitaxel analogue docetaxel. The effective concentration (EC_{50}) of the neuroprotective agents evaluated appears to mirror closely the tubulin assembly activity (see Section 2.3), with discodermolide proving to be almost an order of magnitude more potent than paclitaxel (EC_{50} 1.7 and 13 nM, respectively); epothilone A also proved to be superior to paclitaxel, with an EC_{50} of 3.3 nM. Taken together, the promising in vivo efficacy of paclitaxel,[35] coupled with the superior in vitro potency of discodermolide and epothilone A,[40b] indicate that further evaluation of these natural products and related analogues as neuroprotective agents is warranted.

3. (+)-Discodermolide: synthetic approaches

The impressive biological profile, coupled with both the growing interest from the medical and pharmaceutical communities and the lack of a ready natural source, has rendered (+)-discodermolide (**1**, Fig. 1) an alluring target for total synthesis. To date, 12 unique syntheses have been disclosed by 8 different research groups, both in academia and in industry.[41] In addition, a variety of tactics directed at the construction of discodermolide substructures have also appeared.[42] As the body of literature expands, attention has turned toward shorter, more convergent, and generally more practical discodermolide syntheses (i.e., routes that are designed specifically to generate quantities of material sufficient for clinical evaluation).[41h–j,l] Extensive efforts to cultivate the organism responsible for the natural production of discodermolide have thus far not been successful, leaving total synthesis as the sole source of this medicinally relevant natural product.

From the retrosynthetic perspective, all of the total syntheses reported to date disconnect (+)-discodermolide into three major fragments of roughly equivalent complexity, each of which comprise the methyl-hydroxyl-methyl triad of contiguous centers of stereogenicity in the target structure (Fig. 2). It should be noted that several of the early accounts (specifically those of Schreiber, the first-generation Smith approach, and that of Myles) reported the synthesis of the unnatural antipode (−)-discodermolide. The summaries detailed herein, however, will all be depicted in the natural optical series for clarity. Signs of optical rotation for the various intermediates will only be provided for the syntheses in the natural series.

3.1. The Schreiber synthesis of discodermolide

In 1993, Schreiber and co-workers reported the total synthesis of the unnatural antipode (−)-discodermolide, and in turn established the absolute stereochemistry of the natural product.[41a] A full report detailing the synthesis of the naturally occurring enantiomer appeared in 1996. Described here is the synthesis of the natural congener. From the outset, the Schreiber team designed a doubly convergent strategy that exploited the occurrence of the common triad of stereogenic centers (Scheme 1), beginning from the known homoallylic alcohols **2** and **3**,[43] both of which were derived from 3-hydroxy-2-methylpropionate. To begin, alcohol **2** was converted in four straightforward steps to diol **4**. Oxidation to the corresponding keto-aldehyde, followed by vinyl iodide installation under Stork–Zhao conditions,[44] and then diene formation under the conditions of Negishi and co-workers[45] furnished diene **5** in moderate yield.

For the construction of alkynyl iodide fragment **7**, Still–Gennari olefination[46] installed the requisite C(13)–C(14) *Z*-trisubstituted olefin; a six-step sequence entailing homologation to the acetylene[47] and iodination then furnished the desired iodide.

Synthesis of the C(1)–C(6) subunit **10** (Scheme 1) began with ozonolytic cleavage of alkene **3**, Wittig olefination, followed by hemi-acetal formation and in situ intramolecular 1,4-addition of the resulting alkoxide.[48] Two-step formation of the methyl acetal then afforded methyl ester **9**, which was converted in five steps to the final key intermediate, mixed thioacetal **10**.

The Schreiber endgame comprised a Nozaki–Hiyama–Kishi union[49] of alkynyl iodide **7** with aldehyde **10**, followed

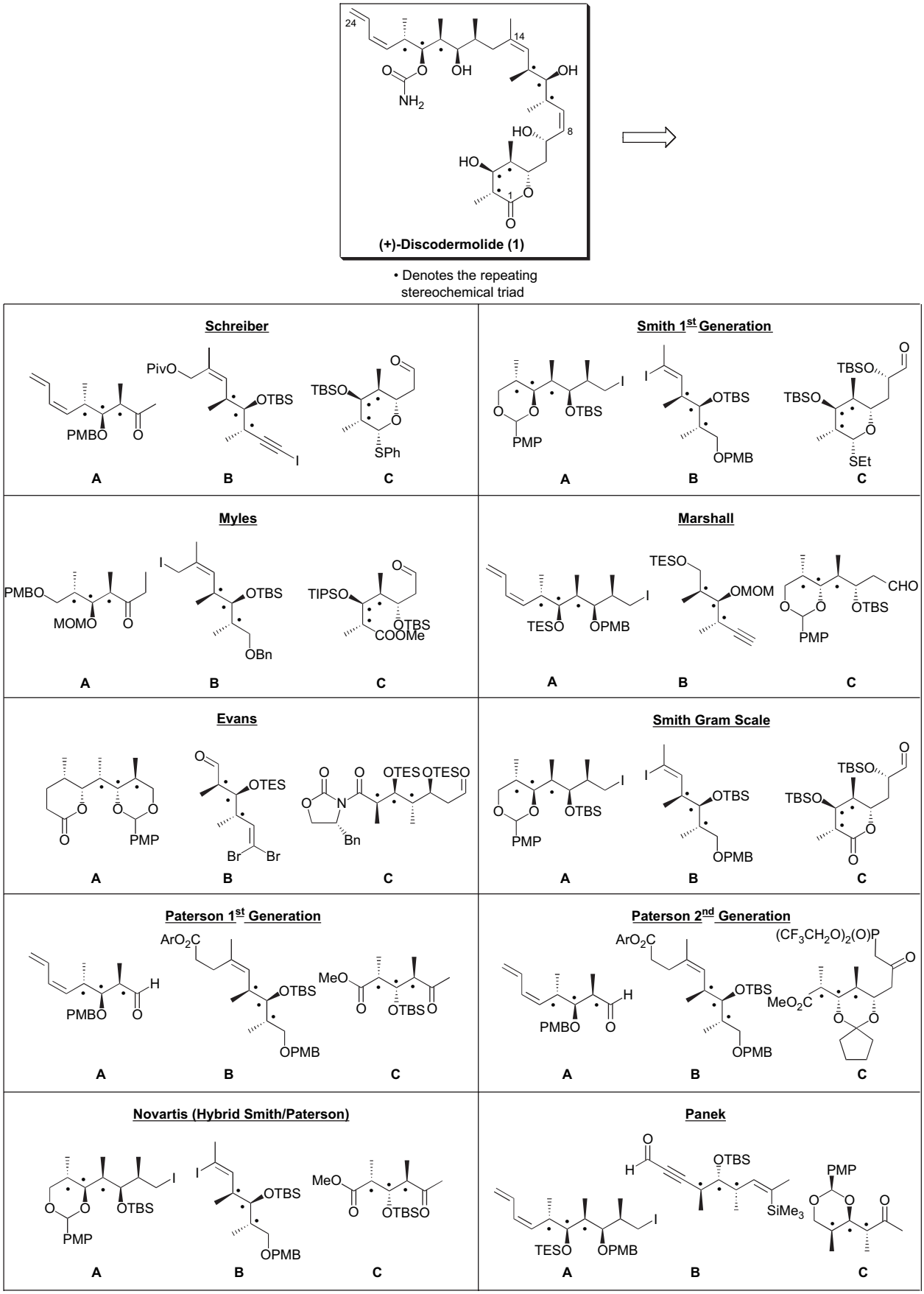

Figure 2. Retrosynthetic analyses of (+)-discodermolide.

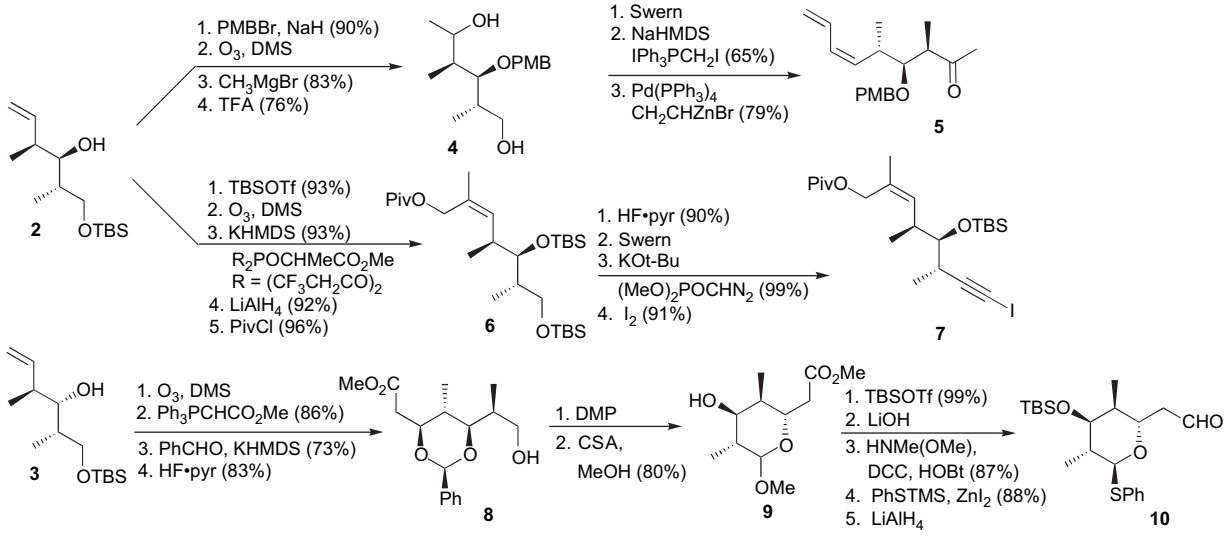

Scheme 1. The Schreiber synthesis of fragments **5**, **7**, and **10**.

by partial hydrogenation of the alkyne to establish the *Z*-configuration at C(8)–C(9); three additional transformations afforded allylic bromide **11** (Scheme 2). Displacement of the allylic bromide with the lithium enolate derived from methyl ketone **5** completed the assembly of the discodermolide backbone and subsequent methylation furnished ketone **12**. A six-step sequence comprising conversion of the thioacetal to the corresponding ketone, carbamate installation,[50] directed reduction of the C(16) lactone, and global deprotection completed the synthetic sequence, providing discodermolide with a longest linear sequence of 24 steps (36 total steps) in an overall yield of 4.3%.

3.2. The first-generation Smith synthesis of discodermolide

The second total synthesis of discodermolide, in this case the (−)-unnatural isomer, was reported in 1995 by Smith and co-workers.[41b] The cornerstone of the triply convergent Smith strategy entailed common precursor **14** (Scheme 3), from which each of the three advanced intermediates **16**, **18**, and **22** would ultimately derive. The common precursor was the product of a highly efficient five-step sequence, beginning from 3-hydroxy-2-methylpropionate, which utilized an Evans *syn* aldol reaction[51] to set the requisite stereochemical arrangement.

Alkyl iodide **16** was generated in six transformations from the common precursor **14** (Scheme 3), including a second Evans aldol[51] to install the requisite stereogenicity at C(16) and C(17). Installation of the critical *Z*-trisubstituted vinyl halide under the conditions of Zhao and co-workers,[52] albeit with modest yield and selectivity, was the central feature of the synthesis of vinyl iodide **18**. A detailed investigation of the mechanism of this troublesome transformation was later reported by Smith and co-workers.[53] Preparation of the third

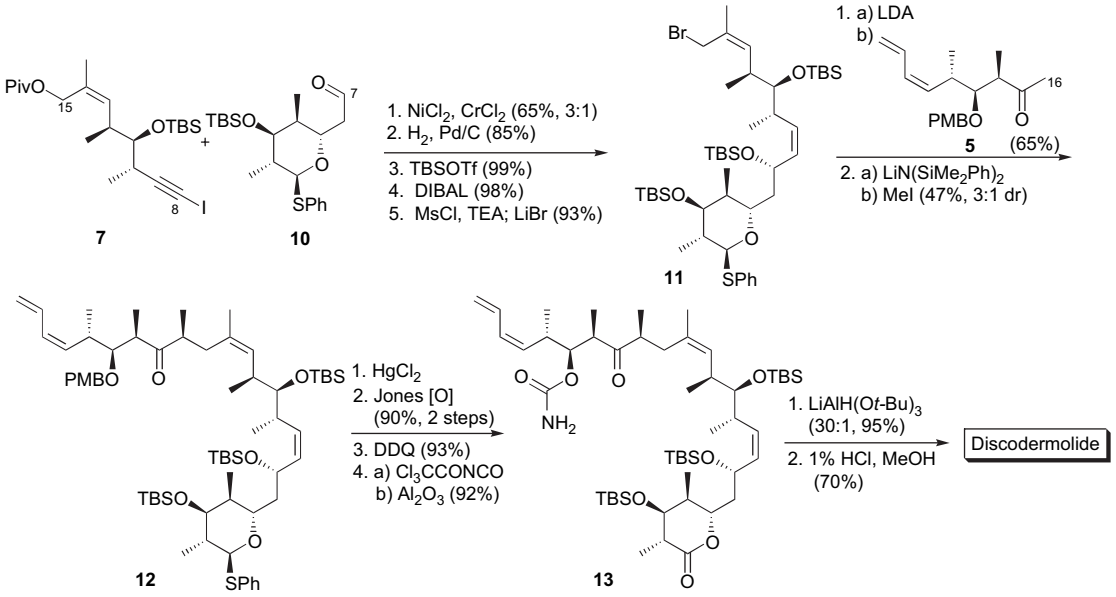

Scheme 2. The Schreiber total synthesis of discodermolide.

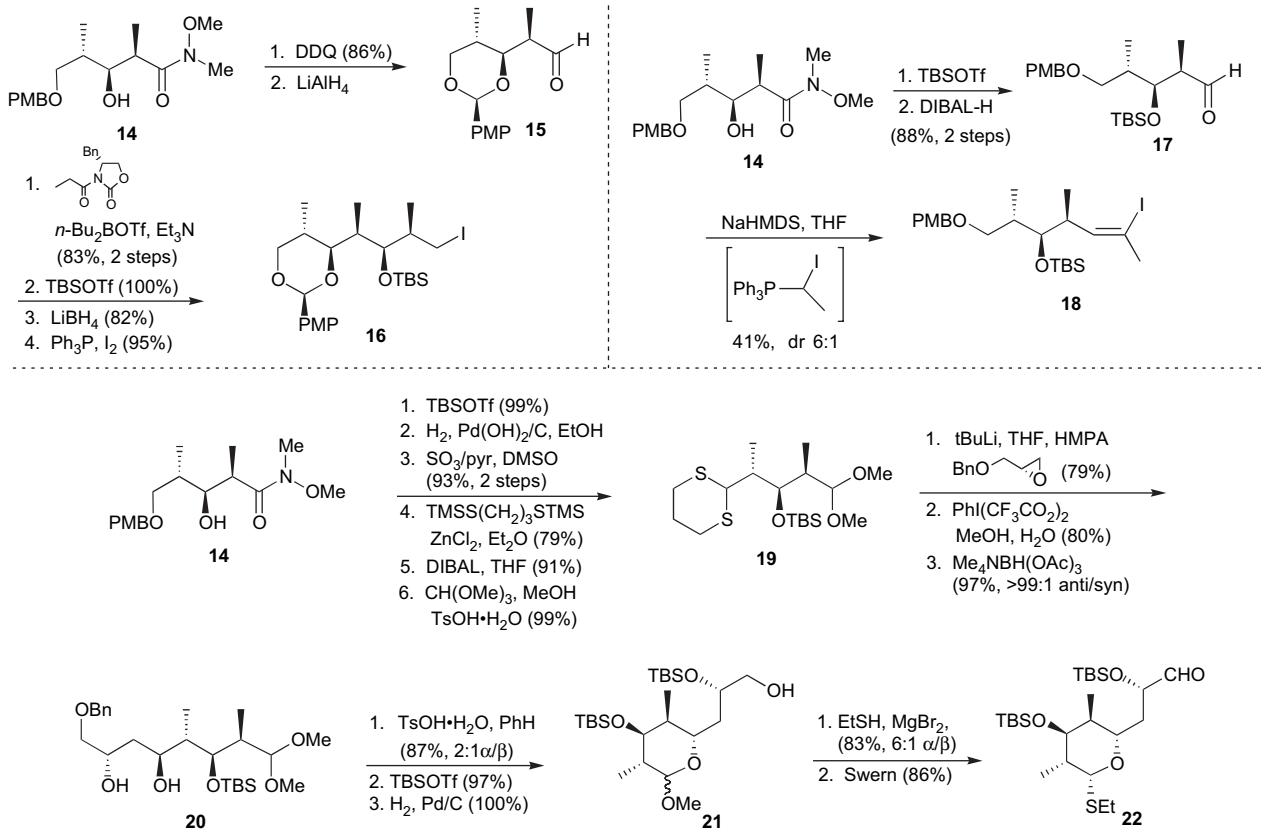

Scheme 3. The Smith first-generation synthesis of fragments **16**, **18**, and **22**.

intermediate, aldehyde **22**, began with a highly efficient six-step sequence from **14** to afford dithiane **19** (Scheme 3). Central to the construction of aldehyde **22** was the addition of the anion derived from dithiane **19** to benzyl glycidyl ether, employing a tactic well-precedented in the Smith group.[54] Seven steps, including installation of the C(7) stereocenter and thioacetal formation, then provided aldehyde **22**, completing a sequence that ultimately required 14 synthetic operations beginning from the common precursor (**14**), placing this fragment squarely on the longest linear route of the Smith first-generation synthesis.

With the three intermediates **16**, **18**, and **22** in hand, attention was turned to their union and subsequent elaboration to

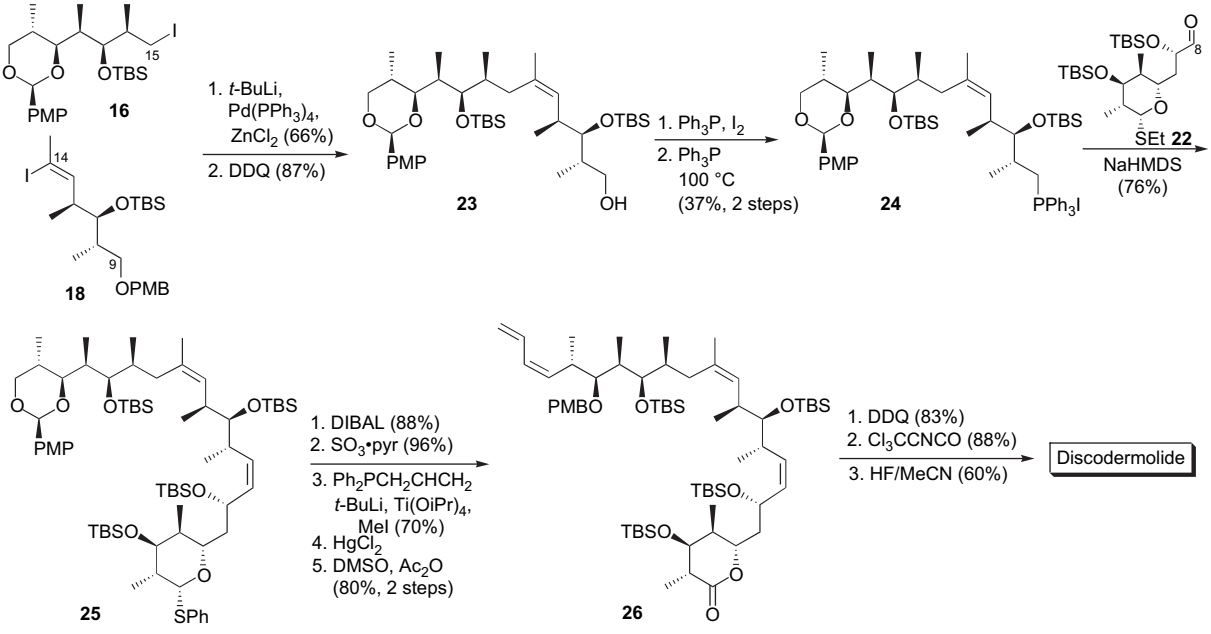

Scheme 4. The Smith first-generation total synthesis of discodermolide.

discodermolide (Scheme 4). Palladium(0)-mediated cross-coupling[45] of vinyl iodide **18** with the organozinc reagent derived from alkyl iodide **16**, followed by oxidative removal of the PMB ether furnished primary alcohol **23**, which was next subjected to what at the time proved to be a difficult two-step conversion to the corresponding phosphonium salt **24**. In particular, a side reaction involving olefin-assisted cyclization of the C(13)–C(14) alkene onto the pendant iodide led to a significant amount of cyclopentane-containing byproducts; at best 37% of the desired salt was achieved. Future iterations of the Smith approach would focus in large part on the optimization of this transformation (see Section 3.6). Wittig union[55] of phosphonium salt **24** with aldehyde **22** proceeded in good yield to furnish acetal **25**. Three-step installation of the diene employing the titanium-mediated conditions reported by Yamamoto and co-workers,[56] first used in the discodermolide area by Heathcock,[42a] completed the construction of the carbon skeleton. What remained was hydrolysis of the thioether, oxidation, carbamate installation,[50] and global deprotection, producing (−)-discodermolide with a longest linear sequence of 29 steps (42 total steps) in an overall yield of 2.0%.

3.3. The Myles synthesis of discodermolide

Myles and co-workers reported their total synthesis of (−)-discodermolide in 1997,[41c] marking the third approach to appear in the literature. A follow-up full account in 2003 recorded the synthesis of the (+)-antipode.[57] The Myles approach to the three major fragments **30**, **32**, and **34** is described in Scheme 5. Most notably, the Myles team employed a titanium-mediated hetero-Diels–Alder[58] reaction of aldehyde **27** with the Danishefsky diene[59] to construct the challenging *Z*-trisubstituted C(13)–C(14) olefin present in allylic iodide **32**. With respect to ethyl ketone **30**, after initially exploring a substrate-controlled approach (**27** to **28**)[60] to induce the stereogenicity found in the C(16)–C(21) subunit, a longer but more selective strategy based on Evans aldol[51] chemistry was employed. The *syn* aldol was subsequently used in tandem with a tin-promoted asymmetric allylation[61] to set the stereogenicity of the final key intermediate, aldehyde **34**. Importantly, fragment **34** bears the correct oxidation state at C(1), which in turn would minimize the late-stage manipulations.

Strategically, the Myles team envisioned discodermolide to arise via a Nozaki–Hiyama–Kishi nickel/chromium-mediated union[49] of a fully elaborated C(8)–C(24) vinyl iodide (**37**) with the C(1)–C(7) aldehyde **34** (Scheme 6). Vinyl iodide **37**, in turn, was constructed beginning with chelate-controlled addition of the enolate of the C(16)–C(21) ketone **30** to an appropriately functionalized allylic iodide (**32**). Schreiber had examined a similar transformation, with C(16) already bearing the methyl substituent, before employing an alternative two-step addition/methylation process. In the Schreiber system,[9c] enolate coupling did not proceed via the expected chelation-controlled transition state, but instead via a transition state conformation governed by allylic ($A^{1,3}$) strain, which led to the undesired C(16)-*R* configuration.

Contrary to the Schreiber results, alkylation of the enolate derived from **30** with allylic iodide **32** in a solvent mixture consisting of hexanes/THF (45:55) proceeded under chelation control to afford the desired C(16) methyl stereoisomer in good yield and with reasonable (6:1) diastereoselectivity (Scheme 6). Further manipulation, including installation of the requisite *cis*-disubstituted vinyl iodide,[44] afforded aldehyde **36**, which would serve as substrate for a Peterson-type olefination,[62] employing the conditions reported by Roush and co-workers[63] to introduce the diene. Acid-mediated deprotection of the C(19) MOM ether followed by carbamate installation[50] completed the synthesis of vinyl iodide **37**. Unfortunately, the subsequent nickel/chromium-mediated union of vinyl iodide **37** with aldehyde **34** proceeded in only modest yield and selectivity, but this route supplied sufficient material to enable global deprotection and completion of (−)-discodermolide. Overall, the Myles total synthesis of discodermolide entailed a longest linear sequence of 25 steps (44 total steps), with an overall yield of 1.5%.

3.4. The Marshall synthesis of (+)-discodermolide

Marshall and co-workers viewed the synthesis of (+)-discodermolide[41d] as an exercise to showcase the utility of their elegant asymmetric allenylmetal-homoaldol tactic[64] to construct polypropionate frameworks. From the retrosynthetic perspective, the strategy incorporates two early disconnections,

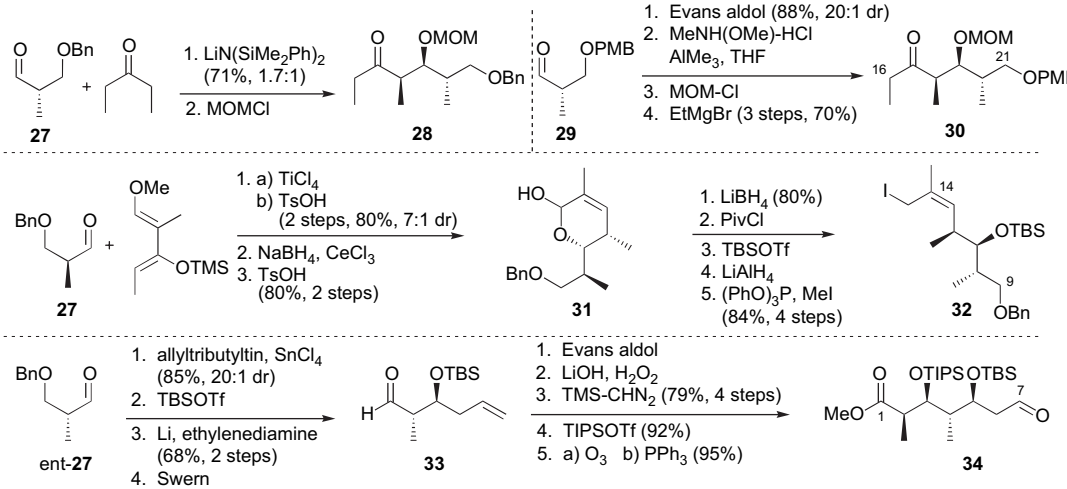

Scheme 5. The Myles synthesis of fragments **30**, **32**, and **34**.

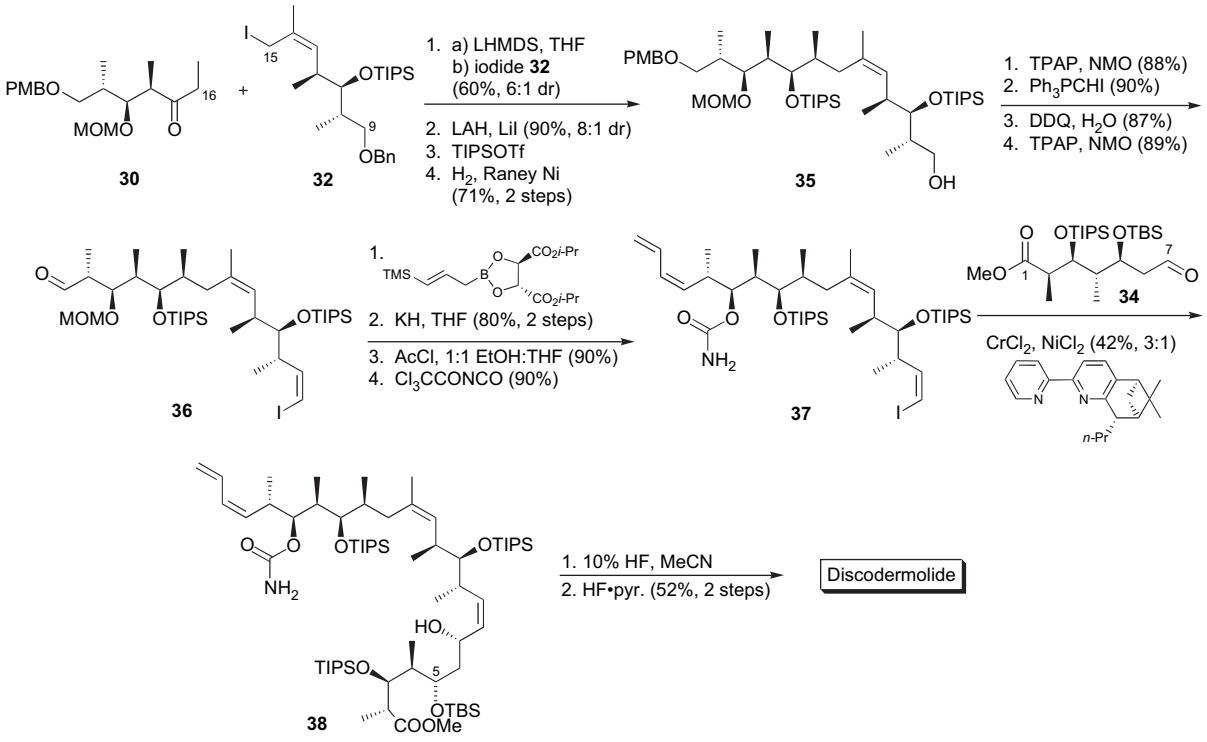

Scheme 6. The Myles total synthesis of discodermolide.

one at the C(14)–C(15) bond, setting the stage for a palladium(0)-catalyzed cross-coupling à la Smith and co-workers (Section 3.2), and the second at the C(7)–C(8) bond, similar to that of both Schreiber (Section 3.1) and Myles (Section 3.3). The novelty of the Marshall approach lies in the utilization of non-racemic allenylmetal reagents for installation of various stereotriad subunits, either in a *syn*/*syn* sense, as in the alkyl iodide fragment (+)-**44**, or in a *syn*/*anti* sense, as in (+)-**48** and (−)-**51** (Scheme 7).

To begin, aldehyde (+)-**39**, produced in three steps from Roche's ester, was subjected to allenyltributylstannane

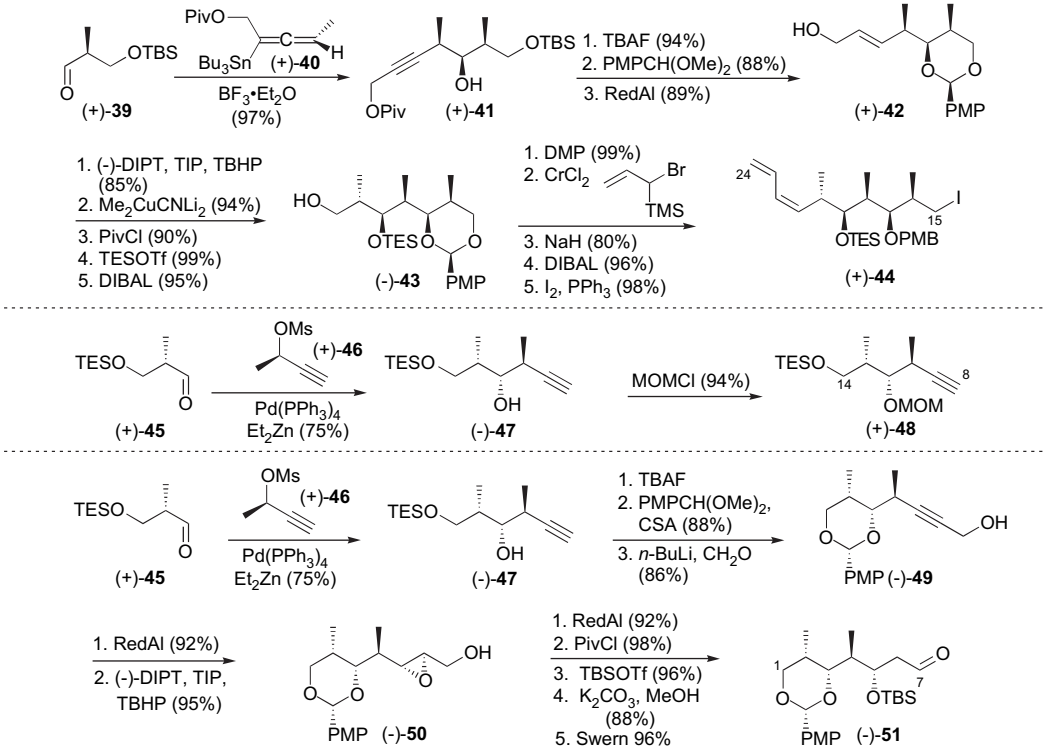

Scheme 7. The Marshall synthesis of fragments (+)-**44**, (+)-**48**, and (−)-**51**.

(+)-**40** in the presence of BF_3-etherate to furnish the *syn*/*syn* isomer (+)-**41** both in excellent yield and with high selectivity. Protecting group manipulation, followed by partial reduction of the alkyne to the corresponding *trans*-olefin, permitted installation of the two remaining stereocenters via an asymmetric epoxidation–methylation[65] sequence. What remained to complete alkyl iodide (+)-**44** was the formation of the pendant *Z*-diene via the Paterson two-step one-pot protocol;[66] the latter entails Nozaki–Hiyama–Kishi addition[49] of α-TMS-allyl bromide to the aldehyde derived from (−)-**43**, followed by Peterson *syn* elimination[62] of the resultant β-hydroxysilane to furnish (+)-**44**. For the C(8)–C(14) fragment (+)-**48**, aldehyde (+)-**45** was treated with the homochiral allenylzinc reagent derived in situ from propargylic mesylate (+)-**46** to furnish alkynyl alcohol (−)-**47**, possessing a *syn*/*anti* methyl-hydroxyl-methyl stereotriad. Protection as a methoxymethyl ether completed the two-step sequence.

The synthesis of C(1)–C(7) aldehyde (−)-**51** also proceeds from alkynyl alcohol (−)-**47** (Scheme 7). Desilylation and acetal formation were followed by hydroxylmethylation of the alkyne to provide alcohol (−)-**49**. Partial alkyne reduction and epoxidation then furnished (−)-**50**, which upon reductive ring opening of the epoxide, followed by a three-step protection of the secondary alcohol and oxidation, completed the synthesis of aldehyde (−)-**51**.

The Marshall endgame (Scheme 8) began with the addition of the alkynyl lithium derived from (+)-**48** to aldehyde (−)-**51**, a transformation that proceeded in 92% yield, with 6:1 diastereoselectivity. Semi-hydrogenation of the resultant alkyne led to the desired C(8)–C(9) *cis*-olefin, at which point four steps, including vinyl iodide installation,[52] set the stage for final coupling. In the event, a Suzuki union[67] of vinyl iodide (−)-**53** with the boronate derived from alkyl iodide (+)-**44** in the presence of catalytic palladium(0) proceeded in good yield to provide the expected tetraene **54**.

Completion of (+)-discodermolide entailed an eight-step sequence involving formation of the C(1) methyl ester, carbamate installation, and global deprotection with concomitant lactonization to afford the natural congener with a longest linear sequence of 30 steps (48 total steps) with an overall yield of 1.3%.

3.5. The Evans synthesis of (+)-discodermolide

In a thesis published in 1999, Halstead, working under the direction of Evans at Harvard, described a fifth total synthesis of discodermolide.[41f] The Evans strategy, not surprisingly, relies heavily on asymmetric aldol methodology for the elaboration of the polypropionate backbone, in conjunction with a novel Claisen condensation to construct the C(13)–C(14) trisubstituted olefin. The C(7)–C(8) disconnection is similar to that employed by Schreiber (Section 3.1) and Myles (Section 3.3).

Halstead and Evans designed their strategy around three major advanced intermediates, lactone (−)-**58**, alkyne (+)-**62**, and aldehyde (+)-**65** (Scheme 9). Synthesis of (−)-**58** began with the tin(II)-mediated *syn* aldol[68] reaction of β-ketoimide (−)-**56** with aldehyde (−)-**55**, which set the stereogenicity of the C(15) and C(16) centers with high diastereoselectivity. Directed reduction of the ketone installed the remaining stereogenic center, which was followed by functional group manipulation and *para*-methoxyphenyl acetal formation to furnish (−)-**58**.

Aldehyde (+)-**62** was produced by a 10-step sequence (Scheme 9) that began with an aldol reaction between the boron enolate of propionyl oxazolidinone (−)-**59** and methacrolein; diastereoselective hydroboration of the resulting olefin with 9-borabicyclo[3,3,1]-nonane then afforded primary alcohol (−)-**61**. Oxidation, Corey–Fuchs reaction,[69] detritylation, and a second oxidation completed the synthesis of the C(8)–C(13) fragment (+)-**62**.

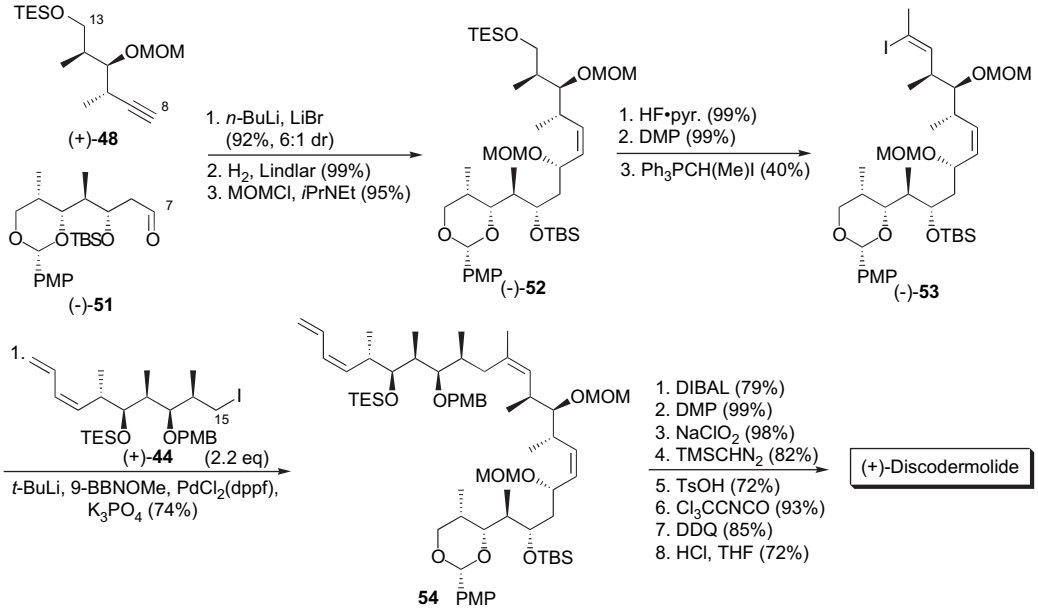

Scheme 8. The Marshall total synthesis of (+)-discodermolide.

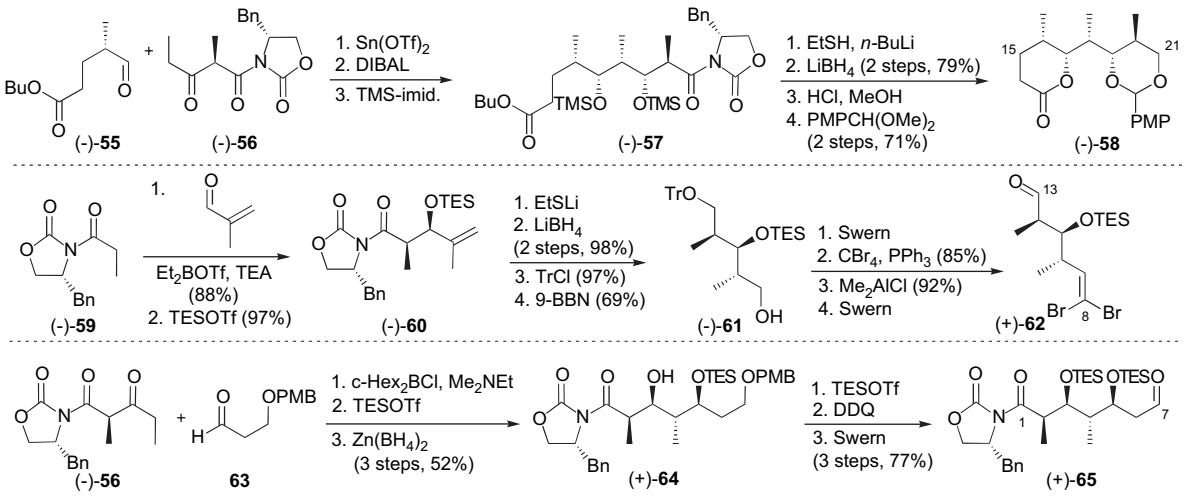

Scheme 9. The Evans synthesis of fragments (−)-**58**, (+)-**62**, and (+)-**65**.

Construction of aldehyde (+)-**65** began with the aldol reaction of the same β-ketoimide (−)-**56** employed for the production of lactone **58**. Here, treatment of aldehyde **63** with the dicyclohexylboron enolate of (−)-**56** furnished the desired *anti* configuration of the nascent stereocenters,[68] in contrast with the tin(II)-mediated conditions used earlier to induce the *syn* aldol product. Protection of the derived hydroxyl as the TES ether and zinc borohydride-promoted *syn* reduction of the ketone then led to (+)-**64**, comprising the complete tetrad of stereogenicity of the C(1)–C(6) region of discodermolide. What remained was the protecting group adjustment and oxidation to complete the synthesis of aldehyde (+)-**65**.

With (−)-**58** and (+)-**62** in hand, a two-step formal aldol condensation was utilized to effect their union, as well as to induce the requisite C(13)–C(14) *Z*-olefin geometry (Scheme 10). A three-step ring opening/deoxygenation protocol was then followed by protecting group adjustment, alkynylation, and iodination to furnish iodide (+)-**68**. Nozaki–Hiyama–Kishi union[49] of (+)-**68** with aldehyde (+)-**65** proceeded in good yield with reasonable diastereoselectivity

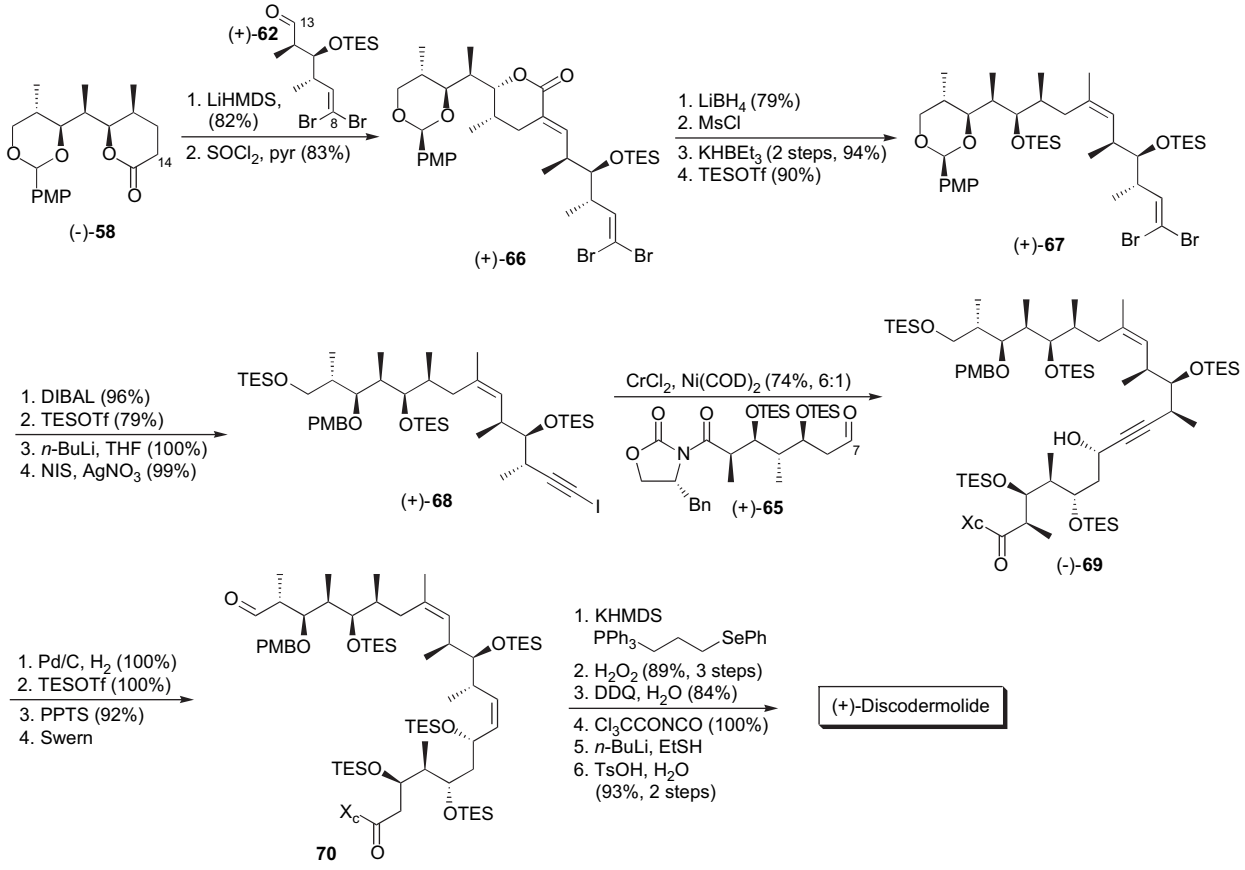

Scheme 10. The Evans total synthesis of (+)-discodermolide.

(ca. 6:1) at the C(7) hydroxyl. This result compared favorably with the 3:1 ratio obtained by Schreiber in an analogous transformation (see Section 3.1). Partial reduction of the C(8)–C(9) alkyne, TES protection of the C(7) hydroxyl, hydrolysis of the C(21) silyl ether, and oxidation then led to aldehyde **70**. Wittig installation of the terminal diene exploiting a γ-selenophosphonium ylide[70] followed by oxidative elimination proceeded smoothly with both high selectivity and excellent yield. What remained was a four-step sequence involving carbamate installation and lactonization to complete the synthesis of (+)-discodermolide, with a longest linear sequence of 31 steps (49 total steps) and an impressive overall yield of 6.4%.

3.6. The Smith gram-scale synthesis of (+)-discodermolide

In order for (+)-discodermolide to become a viable candidate for drug development, quantities of the natural product sufficient to permit pre-clinical evaluation were required. The natural sponge source, which provided only 7 mg of (+)-discodermolide from 434 g of sponge, was clearly not a viable option. Total synthesis, therefore, provided the only feasible means of access. The challenge to produce meaningful quantities of (+)-discodermolide was addressed by Smith and co-workers with the production of 1.043 g of totally synthetic (+)-discodermolide, based on a route that incorporated several practical improvements vis-à-vis the earlier triply convergent, first-generation approach (see Section 3.2).[41e] The 1-g synthesis marked a turning point in the development of (+)-discodermolide as a potential chemotherapeutic agent, as the material produced and the synthetic route employed for the production were subsequently licensed to Novartis Pharmaceuticals. Phase I clinical trials began just 3 years later.

While the Smith first-generation synthesis (Section 3.2) of the unnatural antipode (−)-discodermolide could be readily modified to produce the natural congener, the route was far from optimal. A critical analysis of the weak points of the earlier approach was undertaken prior to initiating the preparative-scale synthesis. Two key areas required readdressing. First, the linear sequence was simply too long and had to be reduced, ideally with a corresponding increase in overall convergence. With this idea in mind, an improved second-generation plan was developed that retained the efficient triply convergent nature of the first-generation approach (Scheme 11). Second, formation of an advanced intermediate phosphonium salt [such as **24**, Scheme 4 or (+)-**71**, Scheme 11] from the corresponding primary alcohol required optimization.

Facile production of large quantities of common precursor (−)-**14** was central to this endeavor. A notable improvement to the five-step route to (−)-**14** (Scheme 12) derived from the discovery that aldol adduct (+)-**78**, which contains the norephedrine-based oxazolidinone moiety, was a crystalline solid,[71] while the corresponding first-generation intermediate, phenylalaninol-derived adduct (−)-**76**, proved to be an oil. Recognition of this fact allowed (+)-**78** to be isolated directly from the reaction mixture by crystallization. As a result, chromatographic purification was not required for the first four steps of the sequence.

With an efficient and practical route to (−)-**14** in hand, the early stages of the first-generation approach, comprising the synthesis of alkyl iodide (+)-**16** and vinyl iodide (+)-**18** from (−)-**14**, proved to be readily scalable, and thus required little modification. The first major point of departure from the first-generation strategy entailed synthesis of the C(1)–C(8) lactone fragment (−)-**72**. Here, a strategic opportunity to carry the intact δ-lactone moiety unprotected into the endgame sequence was envisioned, which in turn would lead to fewer late-stage manipulations. In the end, a seven-step route from (−)-**14**, comprising a chelation-controlled Mukaiyama aldol[72] reaction to set the C(5) stereogenicity, followed by a diastereoselective K-Selectride reduction of the resultant C(7) ketone (Scheme 12), were ultimately employed to furnish the advanced lactone aldehyde (−)-**72**.

With the three fragments in hand, union of vinyl iodide (+)-**18** with the mixed organozinc reagent derived from alkyl iodide (+)-**16** under modified Negishi[45] conditions proceeded smoothly to afford the trisubstituted olefin (+)-**80** (Scheme 13). Further manipulation then furnished aldehyde (+)-**81**, which would serve as the substrate for the installation of the C(21)–C(24) terminal diene.[56] Deprotection of the C(9) trityl ether set the stage for exploration of the problematic two-step iodination/Wittig salt construction. The initial solution to this problem was the use of ultra-high pressure,

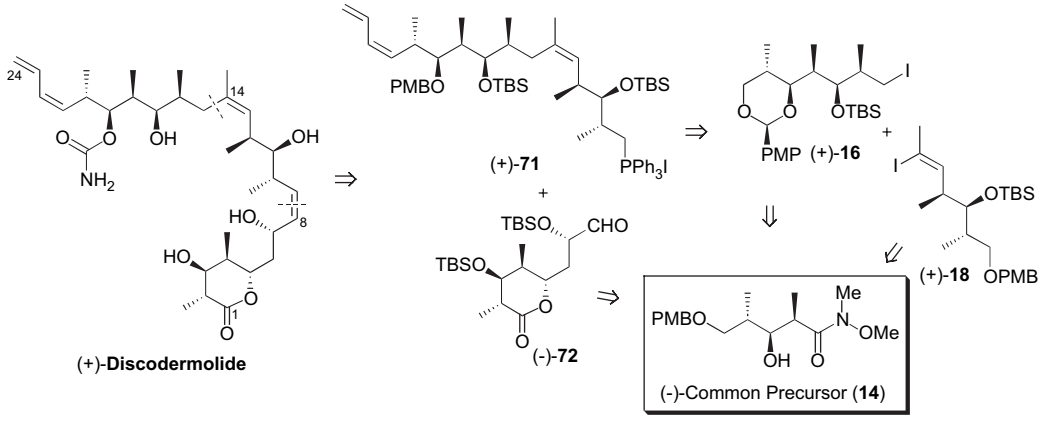

Scheme 11. Smith gram-scale discodermolide retrosynthesis.

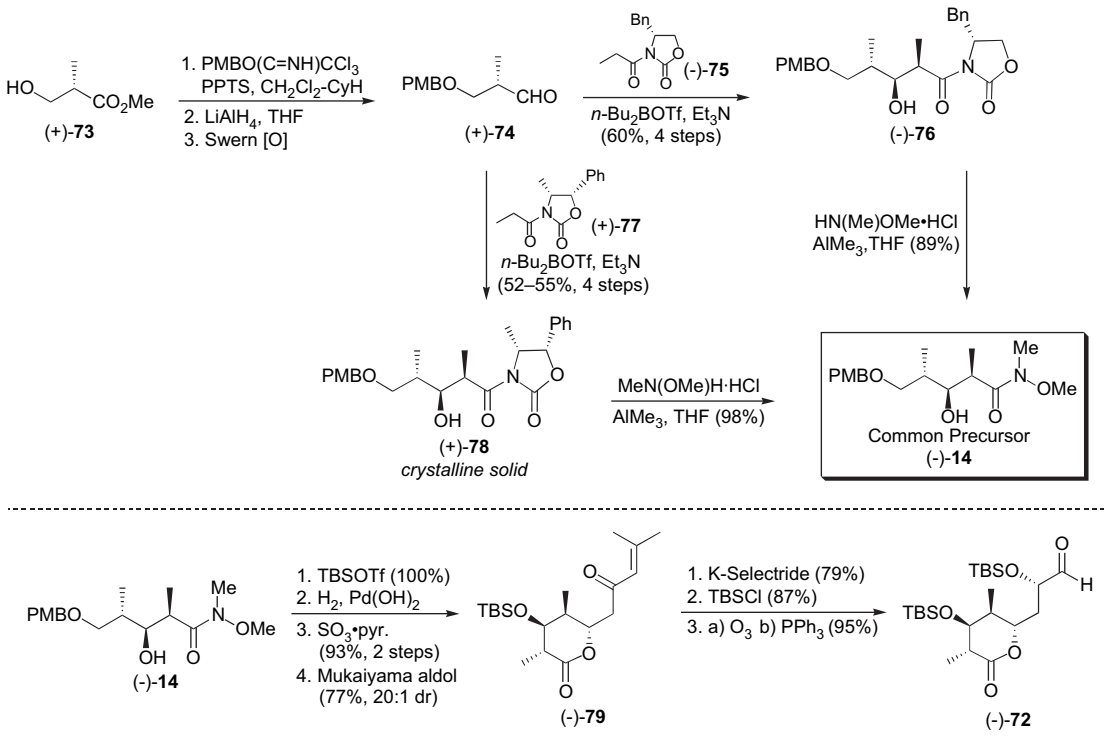

Scheme 12. The Smith gram-scale synthesis of (−)-**14** and (−)-**72**.

a tactic that was pioneered by Dauben and co-workers to accelerate the alkylation of phosphines.[73] In the event, treatment of a highly concentrated benzene solution of the C(9) primary iodide with 10 equiv PPh_3 at 12.8 kbar for 7–10 days afforded the desired phosphonium salt (+)-**71** in 79% yield, with only 20% of the undesired cyclopentane byproducts. Continuing, union[55] of the Wittig ylide derived from (+)-**71** with the fully functionalized C(1)–C(8) lactone aldehyde (−)-**72** proceeded in good yield, thus completing the construction of the discodermolide carbon skeleton. What remained was a three-step sequence involving deprotection of the C(19) PMB ether, carbamate installation, and global deprotection.

While the ultra-high pressure tactic provided sufficient phosphonium salt [(+)-**71**] for the production of over 1 g of discodermolide, a more practical method for the generation of phosphonium salt (+)-**71** would remain the subject of intense investigation in the Smith laboratory. Two years after the one-gram synthesis of (+)-discodermolide, a third-generation effort that simply replaced the bulky TBS ether protecting group at C(11) of the precursor iodide with a less sterically encumbering group, as in MOM ether (+)-**84** (Scheme 14), was disclosed by Smith and co-workers. This tactic proved to bias the system to produce the desired phosphonium salt, at ambient pressure, at the expense of the undesired cyclopentanes.[41h] Smith and co-workers later

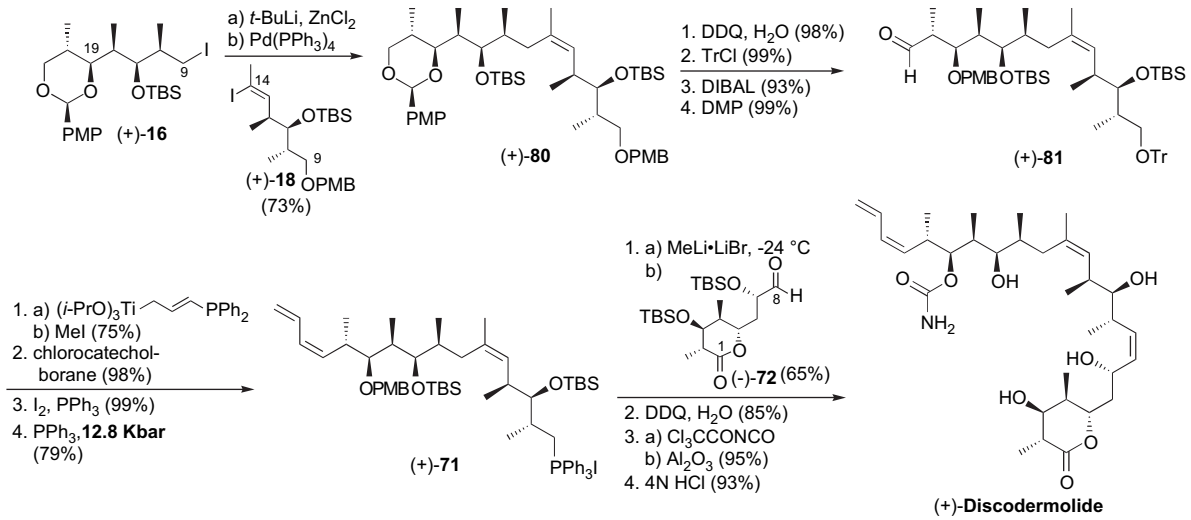

Scheme 13. The Smith gram-scale total synthesis of (+)-discodermolide.

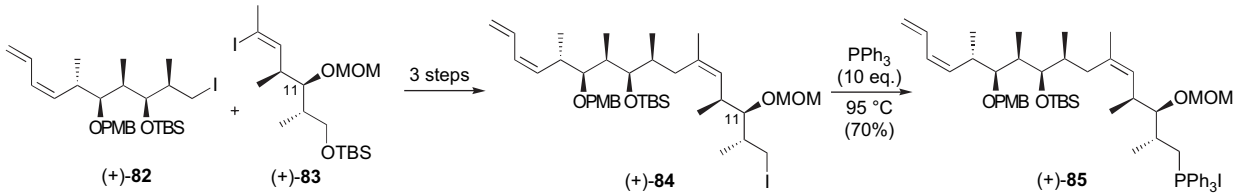

Scheme 14. Third-generation improvements to the Smith gram-scale synthesis.

found that alkyl iodide (+)-**82**, which possesses the terminal diene, and vinyl iodide (+)-**83**, in which the requisite protecting group exchange had already been effected, served as viable coupling partners in the context of the sequence described above (Scheme 13).[411] This modification served to increase the overall convergence of the gram-scale route to (+)-discodermolide.

Taken together, the improvements described above ultimately afforded (+)-discodermolide with a longest linear sequence of 21 steps (35 total steps) and a much improved overall yield of 6.0%.

3.7. The fourth-generation Smith synthesis of (+)-discodermolide

The final iteration of the Smith synthesis of (+)-discodermolide was reported in 2005.[411] The highlight of the fourth-generation approach was the construction and sequential bidirectional union of the vinyl iodide/phosphonium salt (−)-**88** (Scheme 15). Due to the relatively deactivated nature of the trisubstituted vinyl iodide, phosphonium salt (−)-**88** could be readily generated in two steps from alcohol (−)-**86**, with no evidence of concomitant cyclopentane formation that plagued several earlier syntheses. Wittig union with (−)-**89** followed by Suzuki coupling with alkyl iodide (+)-**82** efficiently furnished tetraene (+)-**91**. To complete the endeavor, debenzylation, carbamate installation, and global deprotection then afforded totally synthetic (+)-discodermolide (**1**) with an overall yield of 9.0% and with a longest linear sequence of 17 steps (36 total steps). Importantly, this synthesis entails the shortest linear sequence reported to date.

3.8. The first-generation Paterson synthesis of (+)-discodermolide

In 2000, Paterson and co-workers at the University of Cambridge (UK) reported their initial efforts regarding a preparative approach toward (+)-discodermolide.[41g] Retrosynthetically, the Paterson first-generation strategy (Fig. 2) was based on two key aldol-type disconnections, employing aldehyde (+)-**95**, ester (+)-**100**, and methyl ketone (−)-**103** (Scheme 16). Production of each subunit began with boron-mediated *anti*-aldol reactions as the stereoselective transformation, a tactic well-precedented in the Paterson laboratory.[74]

Employing a novel chelation-controlled aldol reaction for the construction of the C(16)–C(17) bond, the enolate of aryl ester (+)-**100** was treated with aldehyde (+)-**95** to furnish the desired *anti*-aldol adduct (+)-**104**, both with complete Felkin–Anh[75] selectivity and in good overall yield (Scheme 17). Reductive removal of the aryl ester moiety was followed by an eight-step sequence including carbamate installation and then a Still–Gennari Horner–Wadsworth–Emmons reaction[46] to induce the requisite cis geometry of the C(8)–C(9) olefin. Reagent-controlled aldol union of (+)-diisopinocampheylborane enolate derived from the C(1)–C(6) methyl ketone (−)-**103** with aldehyde (+)-**106**

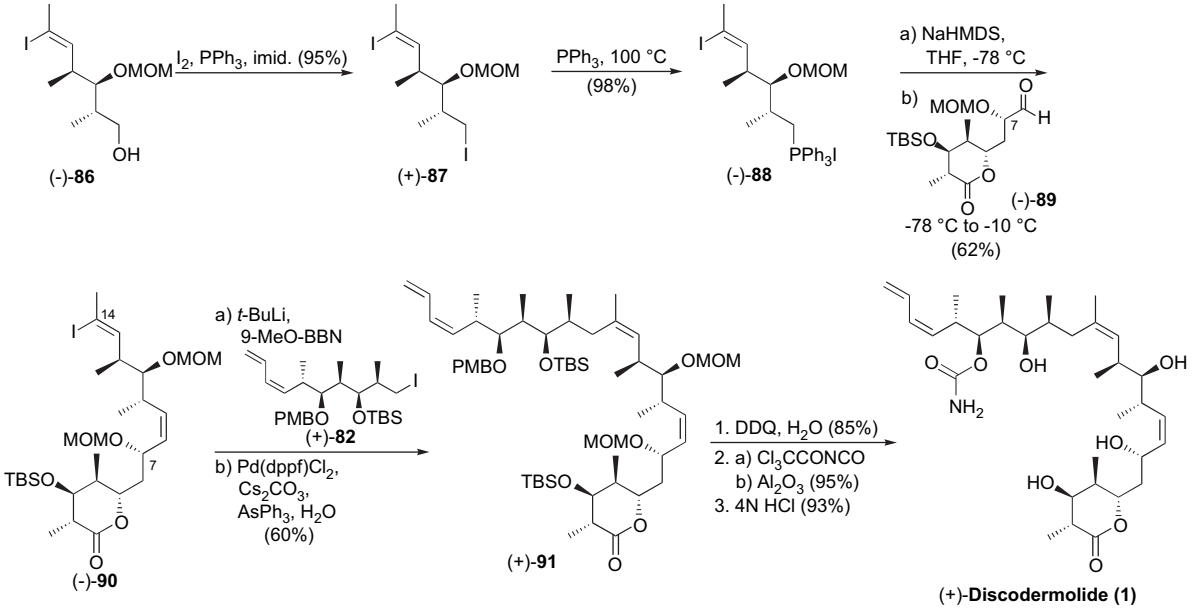

Scheme 15. Smith fourth-generation synthesis of (+)-discodermolide.

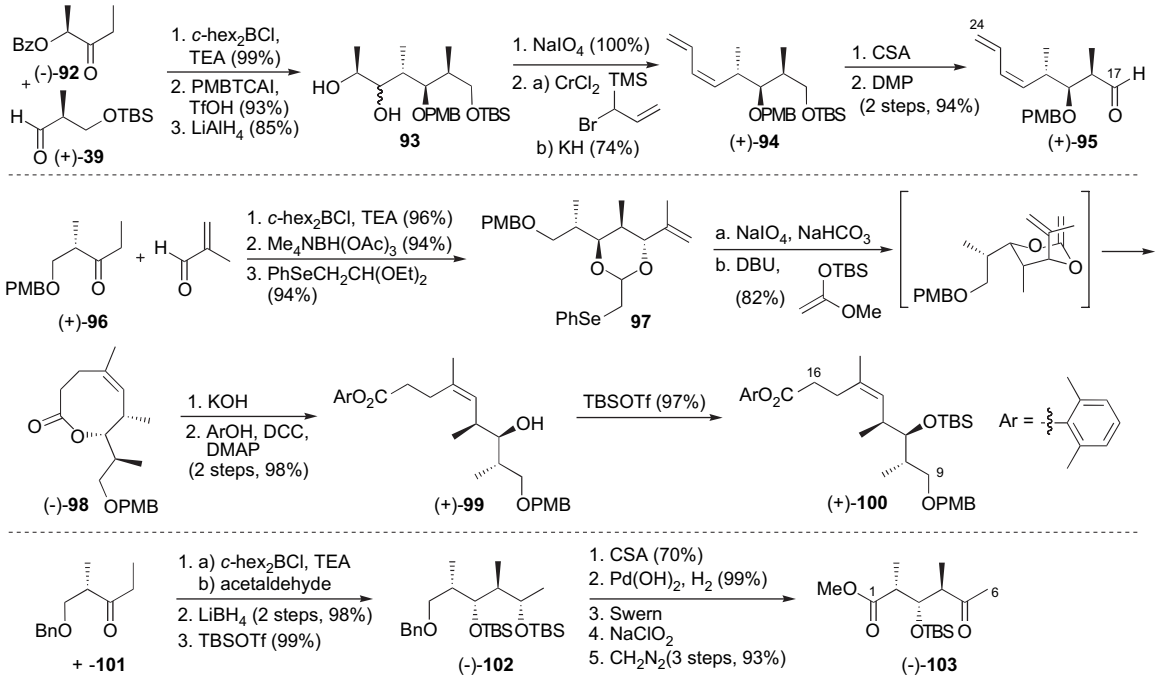

Scheme 16. The Paterson first-generation synthesis of (+)-**95**, (+)-**100**, and (−)-**103**.

then led to the desired carbon skeleton, simultaneously setting the stereogenicity at C(7). Directed reduction of ketone (+)-**107**, followed by global deprotection with concomitant lactonization, completed the Paterson first-generation synthesis of (+)-discodermolide, which required 23 steps as the longest linear sequence (42 total steps) and proceeded with a remarkable overall yield of 10.3%.

3.9. The second- and third-generation Paterson syntheses of (+)-discodermolide

Three years later, in 2003, Paterson and co-workers communicated a revised approach to the synthesis of (+)-discodermolide based solely on substrate-derived stereocontrol.[41i] A full report[76] of this second-generation route was published shortly thereafter. While the retrosynthetic strategy was largely analogous to their first-generation approach (Section 3.7), a few key changes were made. Specifically, the stereoselective incorporation of the C(1)–C(5) subunit **103** was accomplished via a dicyclohexylboron-mediated *anti*-aldol, which replaced the reagent-controlled transformation employed in the first-generation synthesis. Additionally, construction of the C(13)–C(14) trisubstituted olefin was achieved via a Still–Gennari modified Horner–Wadsworth–Emmons reaction.[46]

The syntheses of each of the three major second-generation Paterson intermediates (+)-**95**, (+)-**112**, and (−)-**114** are detailed in Scheme 18. Note that the key stereoselective transformation in each case is the same dicyclohexylboron-mediated *anti*-aldol reaction that was exploited to great success in the first-generation Paterson synthesis.

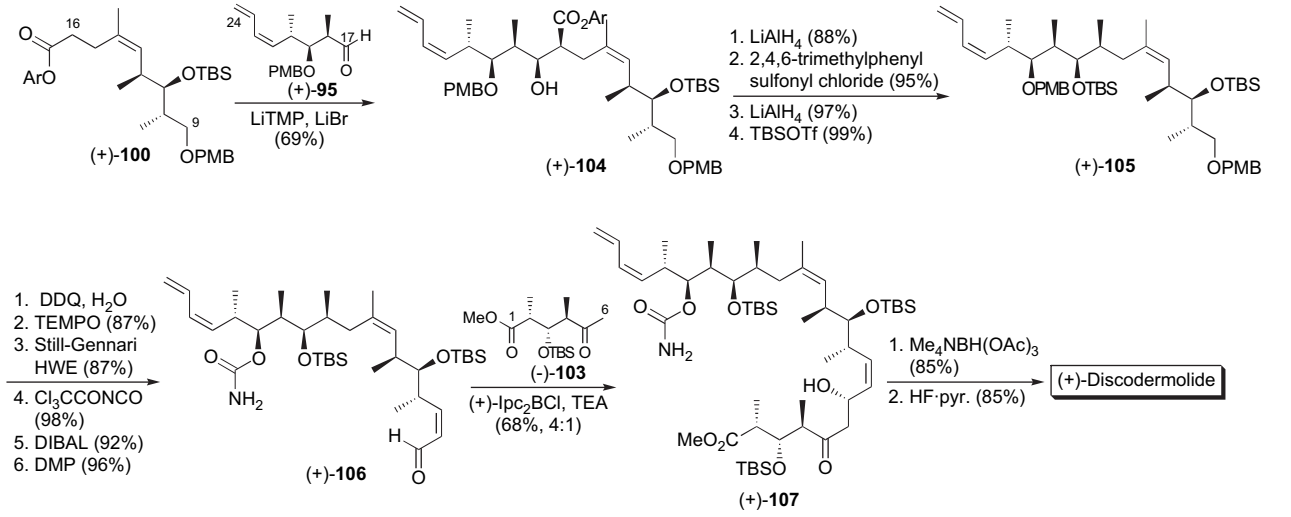

Scheme 17. The Paterson first-generation total synthesis of (+)-discodermolide.

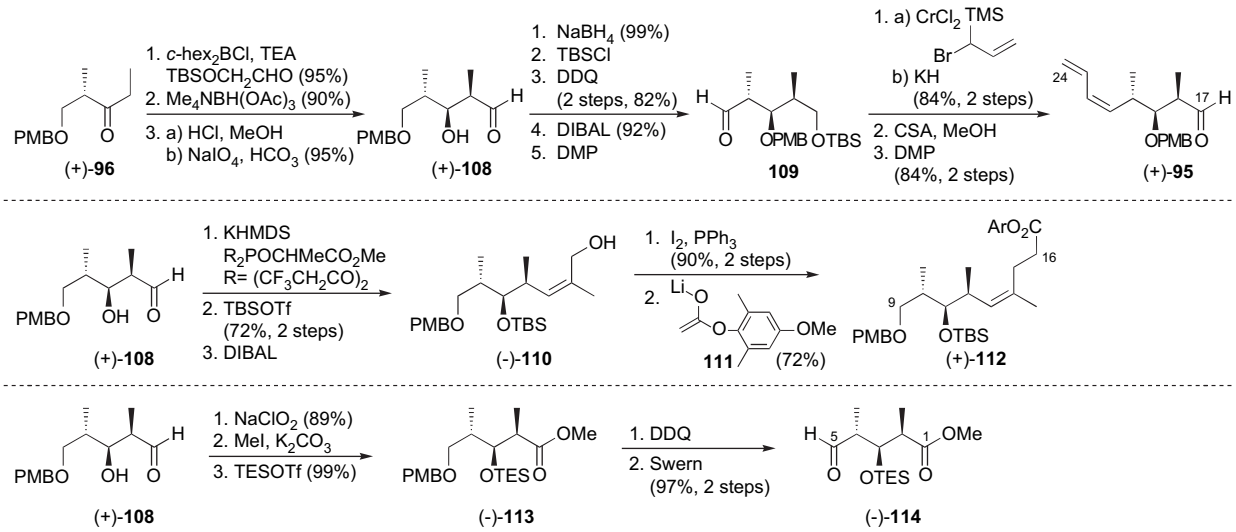

Scheme 18. The Paterson second-generation synthesis of (+)-**95**, (+)-**112**, and (−)-**114**.

The choice of an aromatic ester proved to be critical for the construction and utility of the C(9)–C(16) fragment (+)-**112**. In the earlier Paterson approach, when the aromatic substituent was 2,6-dimethylphenyl, the aldol reaction of the enolate derived from aryl ester (+)-**100** with aldehyde (+)-**95** proceeded with 97% diastereoselectivity and in good chemical yield (cf. Scheme 17). The first-generation 2,6-dimethylphenyl ester (+)-**100**, in turn, was the product of esterification of the corresponding carboxylic acid (Scheme 16). Access to the requisite 2,6-dimethylphenyl ester (+)-**100** via the second-generation approach, however, entailed alkylation of the aryl ester enolate with an allylic iodide, which at best proceeded in 38% yield (results not shown). Accordingly, a series of aryl substituents were evaluated; ultimately, 2,6-dimethyl-4-methoxyphenyl substituent, as in **111**, afforded the best results both in the alkylation reaction [Scheme 18, (−)-**110**→(+)-**112**] and in the subsequent aldol union (Scheme 19, **95**+**112**). Continuing with the synthesis, a three-step reductive removal of the aryl ester moiety, followed by silylation of the secondary alcohol furnished bis-PMB ether (+)-**105** (Scheme 19). Debenzylation and TEMPO oxidation then provided an intermediate aldehyde, which upon Still–Gennari reaction[46] installed the *Z*-disubstituted C(8)–C(9) olefin. After introduction of the C(19) carbamate, the stage was set for the final fragment union.

In the event (Scheme 19), treatment of aldehyde (−)-**114** with the dicyclohexylboron enolate of methyl ketone (+)-**116** proceeded in high yield and with good diastereoselectivity. Paterson proposes that the geometry of the nascent C(5) stereocenter is controlled by 1,6-stereoinduction, based on a transition state conformation governed by minimization of A(1,3) strain at C(10). To complete the synthesis, lactonization, stereoselective reduction of the C(7) ketone, and global desilylation then furnished (+)-discodermolide, with a longest linear sequence of 24 steps (35 total steps) and an overall yield of 7.8%.

Subsequently (2004), Paterson and co-workers reported a third-generation endgame,[41m] in which a late-stage Still–Gennari-type olefination[46] replaced the stepwise method used previously to incorporate the C(1)–C(8) subunit, thus increasing the overall convergence. Accordingly, C(1)–C(8) phosphonate ester (−)-**118** (Scheme 20) was designed and constructed. A selective *anti*-aldol reaction of the

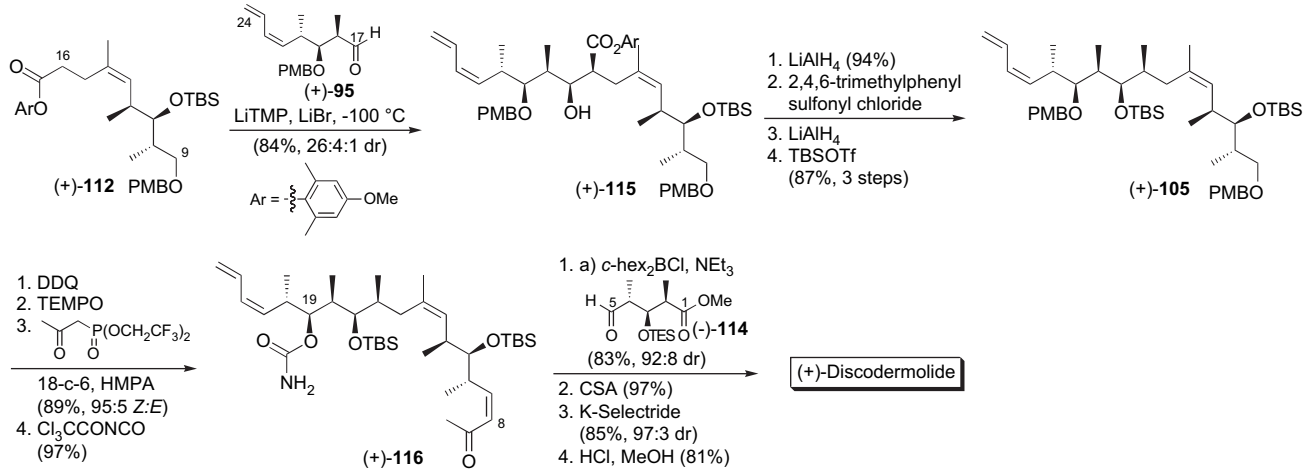

Scheme 19. The Paterson second-generation total synthesis of (+)-discodermolide.

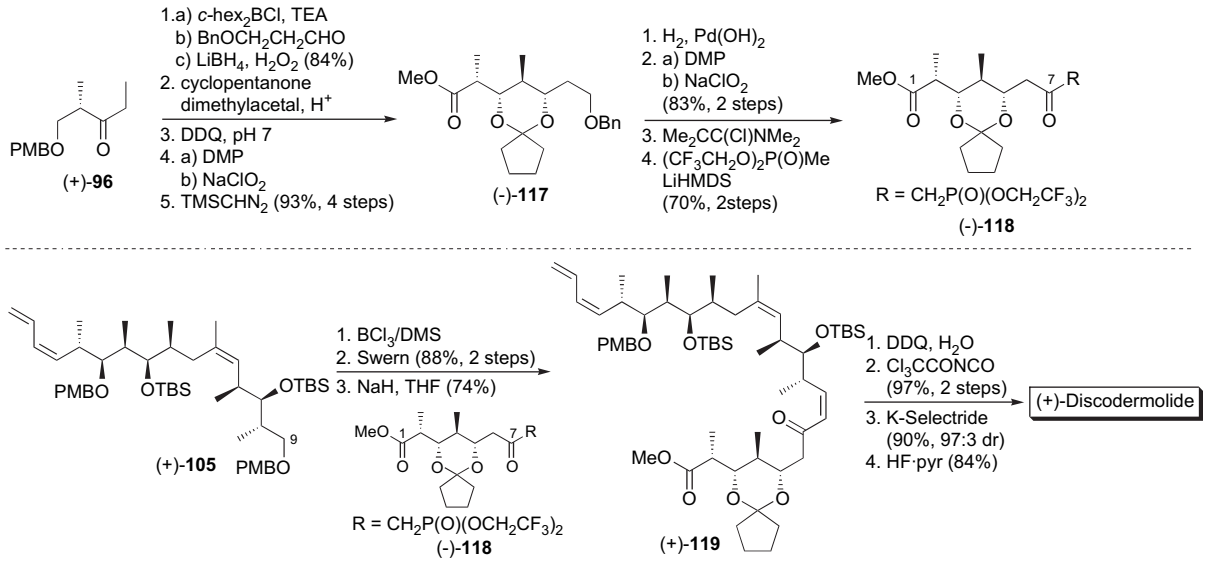

Scheme 20. The Paterson third-generation synthesis of (+)-discodermolide.

dicyclohexylboron enolate derived from ethyl ketone (+)-**96** with 2-benzyloxypropanal and in situ reduction of the intermediate aldolate installed the stereotetrad in high yield and with excellent diastereoselectivity (97:3 dr). Further manipulation furnished phosphonate ester (−)-**118**.

The endgame of the Paterson third-generation synthesis begins with bis-PMB ether (+)-**105** (Scheme 20), an intermediate found in both previous Paterson routes. Horner–Wadsworth–Emmons reaction under the conditions of Still and Gennari[46] effected the desired olefination to furnish tetraene (+)-**119** with a cis/trans selectivity of 10:1 in 74% isolated yield after separation of the minor isomer. Carbamate installation, K-Selectride-mediated reduction of the C(7) ketone, and acid-promoted desilylation then furnished (+)-discodermolide, this time with a longest linear sequence of 21 steps (37 total steps) and with an impressive overall yield of 11.1%, the highest reported to date.

3.10. The Novartis 60-g total synthesis of (+)-discodermolide

In early 2004, the work of Smith and Paterson directed at a practical large-scale synthesis of (+)-discodermolide was validated by a disclosure from Novartis Pharmaceuticals, which detailed the production of *60 g* of the natural product[41j] utilizing a hybrid of the Smith gram-scale approach[41e] (Section 3.6) and the Paterson first-generation endgame[41g] (Section 3.7). The material thus produced proved to be sufficient to permit Phase I clinical trials to evaluate the efficacy of (+)-discodermolide as an in vivo chemotherapeutic for adult patients presenting with advanced solid malignancies.

During the planning stages, the Novartis team carefully analyzed each of the existing synthetic routes (vide supra), evaluating parameters including the length of the sequence, overall chemical yield, potential for scalability, and cost of goods. From an economic perspective, the Smith gram-scale triply convergent strategy was particularly attractive, given the ready availability of the requisite common precursor (−)-**14**. At the time Novartis initiated their synthetic efforts, however, the Smith sequence had one major drawback, the ultra-high pressure reaction required for efficient formation of phosphonium salt (+)-**71** (Scheme 13). To circumvent this transformation, the Novartis strategy ultimately constructed the C(9)–C(24) subunit exactly á la Smith[41e] (Scheme 13) and then segued into the Paterson endgame,[41g] albeit requiring the addition of two steps to the linear sequence (Scheme 21). Pleasingly, the Smith routes to amide (−)-**14**, alkyl iodide (+)-**16**, and vinyl iodide (+)-**18** (Scheme 3, Scheme 12) proved to be readily amenable for production scale, with a few exceptions. The Paterson-type C(1)–C(6) subunit **120** was derived from the Smith common precursor (−)-**14**, via a route developed at Novartis.[41j] Due to workup-related issues and safety concerns, pyrophoric aluminum reagents were replaced with more benign substitutes, a change that necessitated a two-step transamidation protocol for the formation of Weinreb amide (−)-**14**. Additionally, the use of the Swern oxidation was precluded due to the stench produced by methyl sulfide; TEMPO and bleach based oxidants were employed instead.

To effect the first key coupling, that of alkyl iodide (+)-**16** with vinyl iodide (+)-**18** (Scheme 21), the Novartis process group initially examined zinc-mediated palladium(0)-catalyzed cross-coupling under the modified Negishi conditions used successfully by our group.[41e] However, while this process did generate the desired product in 62% yield (not shown), the reaction product proved to be quite difficult to purify on scale. Attention, therefore, turned to a boron-mediated Suzuki-type[67] cross-coupling, similar to that used by Marshall (Section 3.4) for the construction of the C(14)–C(15) bond. This resulted in a much cleaner reaction mixture, with the desired trisubstituted olefin (+)-**80** isolated in a reproducible yield of 73%.

At this point, transition to the Paterson endgame began with the construction of (+)-**105** (cf. Scheme 17). To this end, diene installation was achieved in three steps.[66] Still–Gennari modified Horner–Wadsworth–Emmons reaction[46] and introduction of the C(19) carbamate then furnished

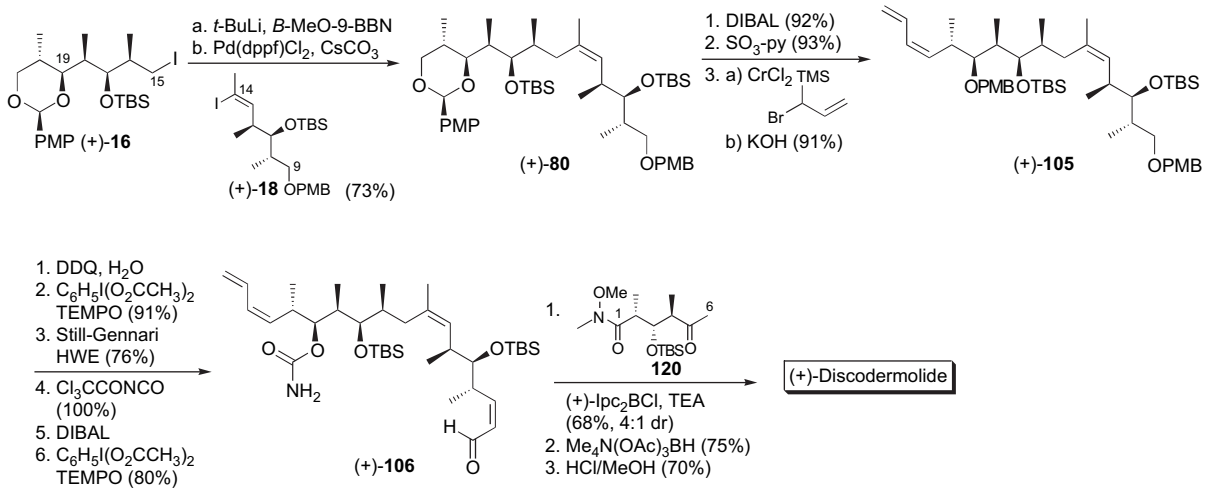

Scheme 21. The Novartis 60-g total synthesis of (+)-discodermolide.

aldehyde (+)-**106**. A total of nine synthetic transformations were required for the Smith to Paterson transition. This set the stage for what the Novartis researchers described as "the most challenging phase of the whole campaign", attachment of the C(1)–C(6) subunit **120**. The Paterson first-generation synthesis called for a final union employing the reagent-controlled aldol addition of the (+)-diisopinocampheylboron enolate of a C(1)–C(6) ketone with aldehyde (+)-**106** (Scheme 17). In a similar fashion, the Novartis team would construct the C(6)–C(7) bond using methyl ketone **120** (Scheme 21) as the enolate coupling partner. In the event, this transformation required 6.6 equiv of the **120**-derived enolate relative to (+)-**106** and furnished at best 60% yield of the desired C(7) epimer, together with 15% of the undesired isomer. Unfortunately, this reaction also proved to be quite capricious. On several occasions none of the desired adduct was observed; instead multiple products derived from an initial isomerization of the C(8)–C(9) olefin of (+)-**106** arose. While the mechanism for this isomerization remains undetermined, this problem was solved by replacing solid (+)-*B*-chlorodiisopinocampheylborane (DIP-Cl) with a commercially available 70% solution in hexane. On production scale, the instability of the aldol adduct/boron complex to the original workup conditions also proved to be detrimental to the overall efficiency of the reaction. This puzzle was eventually solved simply by subjecting the crude reaction mixture directly to reverse-phase silica gel chromatography. Ultimately, the large-scale boron-mediated aldol union proceeded with a reproducible yield of 65%, albeit with a diastereoselectivity of only 4:1. Equally disappointing, the transformation still required greater than a 6-fold excess of the C(1)–C(6) component **120**

What remained was the directed reduction of the C(5) ketone and global deprotection to afford (+)-discodermolide with a longest linear sequence of 26 steps (33 total steps) and an overall yield of 0.65%. While far from optimal, the Novartis–Smith–Paterson hybrid sequence was exploited for the production of over 60 g of the natural product. This amazing feat required the efforts of 43 chemists over a period of 20 months. The material thus generated proved to be sufficient for evaluation of (+)-discodermolide in early-stage human clinical trials.

3.11. The Panek total synthesis of (+)-discodermolide

The most recent total synthesis of (+)-discodermolide comes from the research group of Panek,[41k] whose approach to the polypropionate framework is built largely upon the stereoselective crotylsilane-based C–C bond construction protocol developed in the Panek Laboratory.[77] Here, control of the stereochemical relationships, both absolute and relative, depends upon the choice of the crotylsilane reagents and Lewis acids used for the particular transformation. Accordingly, retrosynthetic disconnections of the C(6)–C(7) and C(14)–C(15) σ-bonds led to alkyl iodide (+)-**125**, aldehyde (−)-**127**, and methyl ketone (−)-**129**, which in turn would be generated via treatment of crotylsilanes (+)-**121**, (−)-*ent*-**121**, and (−)-**128**, respectively, with an appropriately functionalized Roche ester-derived aldehyde (+)-**27** (Scheme 22).

Synthesis of the Panek C(15)–C(24) subunit (+)-**125** began with a highly diastereoselective Felkin-controlled addition[75] of crotylsilane (+)-**121** to aldehyde (+)-**122**, followed by acidic workup (Scheme 22). Protection of the resulting diol as the di-*tert*-butylsilylene acetal and ozonolytic olefin cleavage furnished aldehyde (+)-**123**, which in turn was subjected to a second stereoselective crotylation event, this time utilizing silane (−)-*ent*-**121**. Six transformations including installation of the diene employing the boron-mediated procedure of Tsai and Matteson[78] then furnished alkyl iodide (+)-**125**.

In a similar fashion, crotylation of benzyl aldehyde (+)-**27** with silane (−)-*ent*-**121** began the synthesis of the C(7)–C(14) subunit (−)-**127**. A four-step conversion to TMS-alkyne (−)-**126**, followed by hydrozirconation,[79] iodination, and palladium(0)-mediated methylation, completed the construction of the C(13)–C(14) trisubstituted olefin, wherein the *Z*-vinylsilane functionality would serve as a masked vinyl iodide.[80] Working next at the opposite terminus of the fragment, debenzylation and oxidation were followed by a second Corey–Fuchs homologation,[69] this time with subsequent formylation to afford the C(7)–C(14) aldehyde (−)-**127**. Production of C(1)–C(6) fragment (−)-**129** began with a highly selective Felkin-controlled[75] crotylation of aldehyde (+)-**122** (Scheme 22). In this case, the use of silane (−)-**128**, which bears an additional methyl group, ultimately

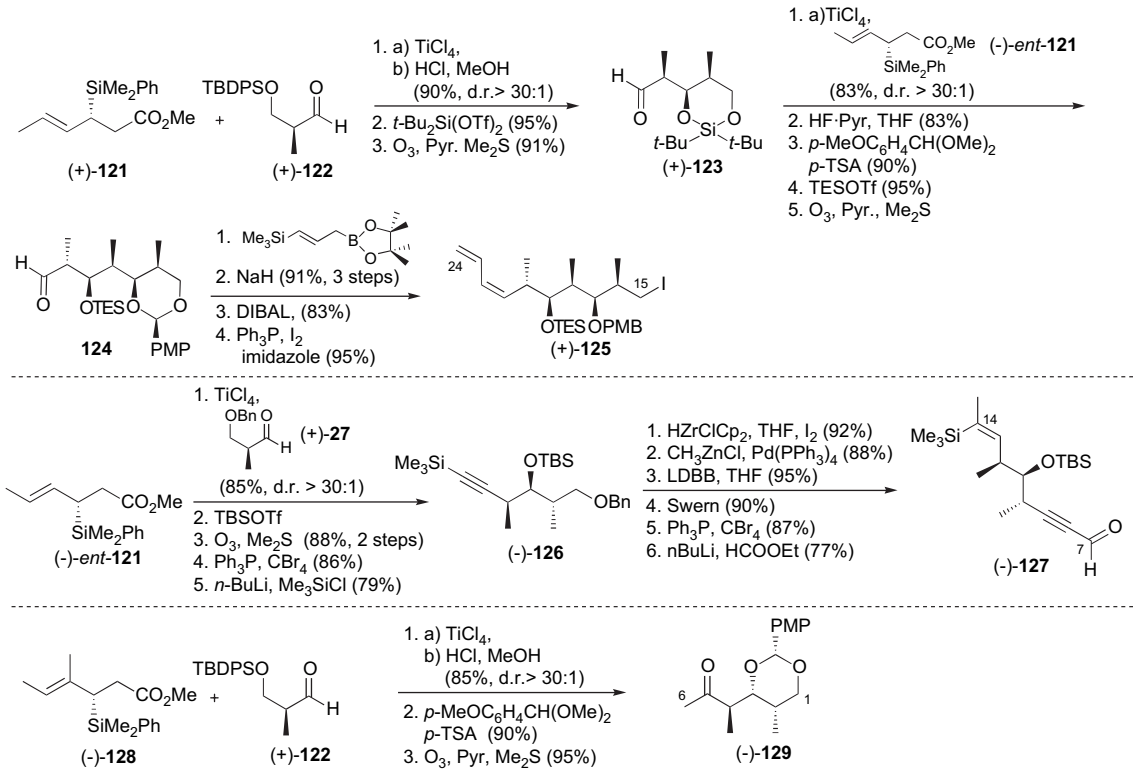

Scheme 22. The Panek synthesis of (+)-**125**, (−)-**127**, and (−)-**129**.

afforded the desired methyl ketone (−)-**129** after acetalization and oxidative olefin cleavage.

In the Panek approach, construction of the C(6)–C(7) bond was effected via a dialkylboron-mediated substrate-controlled acetate aldol reaction between methyl ketone (−)-**129** and aldehyde (−)-**127** (Scheme 23). Precedent had demonstrated that the desired 1,5-*anti* sense of stereoinduction should pertain.[81,82] Indeed, a variety of dialkylboron triflate reagents and solvent conditions led to high levels of diastereoselectivity favoring the desired 1,5-*anti* isomer (−)-**130**, with the best case proving to be that exploiting dibutylboron triflate as the boron component. With the C(5) stereogenicity in place, Evans–Tishchenko *anti*-selective reduction[83] of β-hydroxy ketone (−)-**131** induced the requisite C(7)-*S* configuration. Upon basic hydrolysis of the resulting β-hydroxybutyrate and silica gel chromatography, Panek and co-workers noted an unexpected acetal migration, which they turned to their advantage via a two-step oxidation/methylation sequence involving the newly liberated primary alcohol to furnish the corresponding methyl ester (−)-**131**. Protection of the C(7) hydroxyl as a MOM ether, partial reduction of the alkyne, and iododesilylation[84] then set the stage for the next major fragment union in the form of a palladium(0)-catalyzed cross-coupling as Smith (Sections 3.2 and 3.6) and Marshall (Section 3.4) had employed. Initial attempts to effect the desired C–C bond formation with the C(11) hydroxyl protected as a TBS ether, however, met with failure, under both boron- and zinc-mediated conditions (not shown). After considerable experimentation, replacement of the C(11) TBS ether with a MOM ether, as in (+)-**132**, provided a viable reaction partner for the requisite cross-coupling (Scheme 23).

In the event, treatment of vinyl iodide (+)-**132** with the boronate derived from alkyl iodide (+)-**125** in the presence of catalytic $PdCl_2$(dppf) and thallium ethoxide[67] led to the construction of the discodermolide carbon skeleton. A four-step sequence requiring installation of the C(19) carbamate[50] and global deprotection completed the synthesis, which comprised a longest linear sequence of 27 steps (42 total steps) and an overall yield of 2.1%.

4. Design, synthesis, and biological evaluation of analogues of (+)-discodermolide

4.1. Introduction

The potential chemotherapeutic application of (+)-discodermolide has inspired a number of research programs directed toward the design, synthesis, and evaluation of analogues.[81,9b,c,85–88] The goals of such efforts typically fall into three major categories: (1) identification of the minimum structural elements required for potent tumor cell growth suppression; (2) development of an understanding of the structure–activity relationship, ideally one that would enable the rational design of additional more potent congeners; and (3) structural simplification to lessen the production cost, thus facilitating pharmaceutical development. Highlights of various analogue programs are presented in the sections to follow.

4.2. Schreiber analogues of (+)-discodermolide

In 1994, Schreiber and co-workers reported the biological evaluation of the two antipodes of discodermolide.[9b]

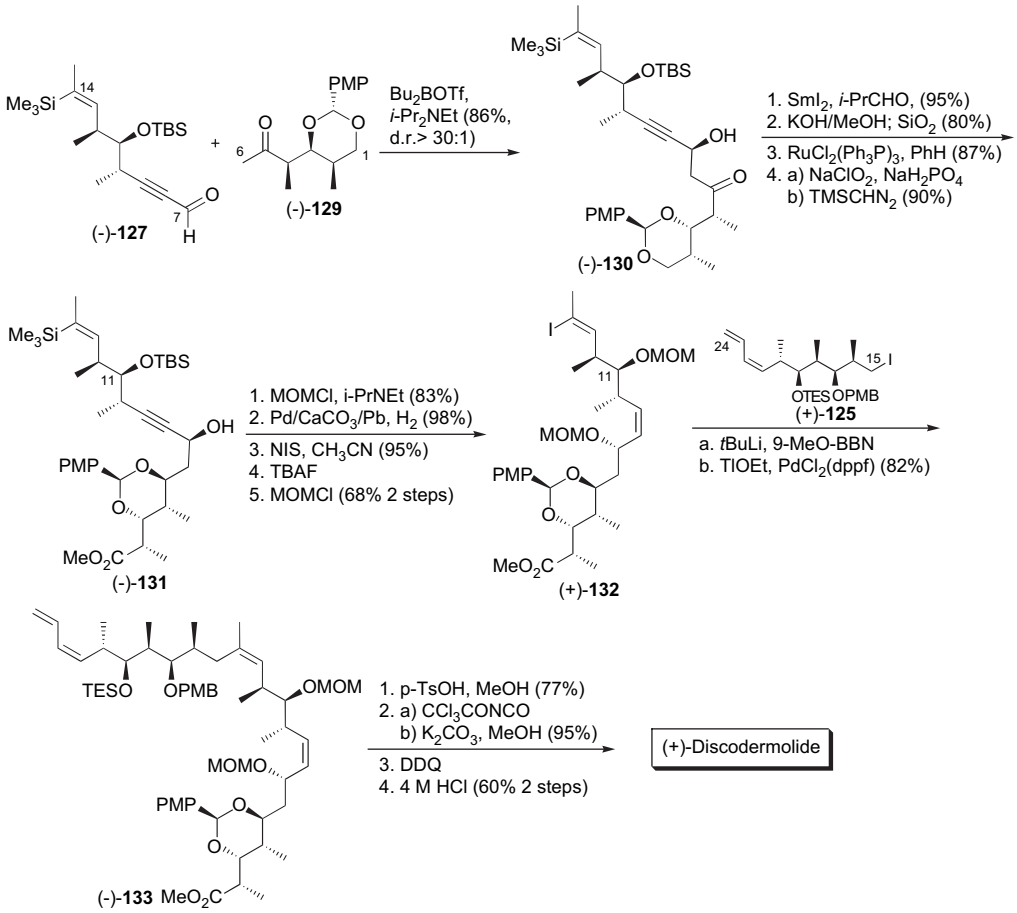

Scheme 23. The Panek total synthesis of (+)-discodermolide.

Surprisingly, both the natural (**1**) and the unnatural (−) enantiomers (Fig. 3, **134**) inhibited cell proliferation, with IC_{50} values of 6 and 72 nM, respectively, in the MG63 human osteoblast cell line. The mechanism of inhibition for the two agents was distinguished via flow cytometric analysis, which demonstrated that cells treated with the natural (+)-discodermolide were arrested at the G_2/M phase of the cell cycle, while (−)-discodermolide-treated cells were arrested in S phase. Subsequent experiments employing radiolabeled discodermolides showed that the natural (+) congener exhibited specific binding to a then-unidentified receptor, while no specific binding was noted for (−)-discodermolide, even at micromolar concentrations. Additionally, the unnatural (−)-antipode did not compete for (+)-discodermolide binding, further suggesting that the two agents interact with distinct cellular targets. Several months later, in early 1996, concurrent reports from Schreiber and co-workers[25] and the ter Haar laboratory[24] identified microtubules as the cellular receptor for (+)-discodermolide.

In the course of these investigations, Schreiber and co-workers devised and synthesized a number of structurally varied analogues,[9c] with the aim of further elucidating the interaction between (+)-discodermolide and microtubules. The Schreiber team found that substantial truncation of the carbon skeleton was severely detrimental (Fig. 3); removal of either the C(1)–C(7) subunit, as in **135**, or the C(16)–C(24) subunit, as in **136**, resulted in compounds that exhibited no cell growth inhibitory activity. Subtle simplification was, however, tolerated, as the 16-normethyl congener (+)-**137** retained low-nanomolar potency, while epimerization of the C(16) stereogenic center (as in **138**) led to diminished activity. Likewise, some modification was acceptable at C(17), as demonstrated by the acetyl congener **139**. Conversely, epimerization of C(17), as in **140**, resulted in complete loss of cell growth inhibition.

Examining next the C(1)–C(6) subunit, neither the lactone nor even the lactone oxidation state was found to be required for effective cell growth inhibition. Indeed, thiophenyl acetals (+)-**141** and (+)-**142** (Fig. 4) retained nearly identical potency to the natural product (+)-discodermolide (**1**). The 16-normethyl thiophenyl acetal counterpart (+)-**143** was also highly active. In their search for an appropriate scaffold upon which to develop a discodermolide-like affinity binding probe, Schreiber and co-workers attached a long-chain substituent in a manner that did not significantly interfere with the ligand–receptor interaction. To this end, three compounds were developed (**144**–**146**), which revealed the effects of extension at C(24), C(17), and C(16), respectively. Appendages at the C(24) or C(17) position resulted in only a moderate decrease in cytotoxicity, however, extension of the C(16) methyl was not tolerated.

The Schreiber analogues began to illustrate the complex structure–activity relationships of (+)-discodermolide with tubulin. First, the stereogenicity of C(16) and C(17) proved to be of great importance, but the C(16) methyl substituent

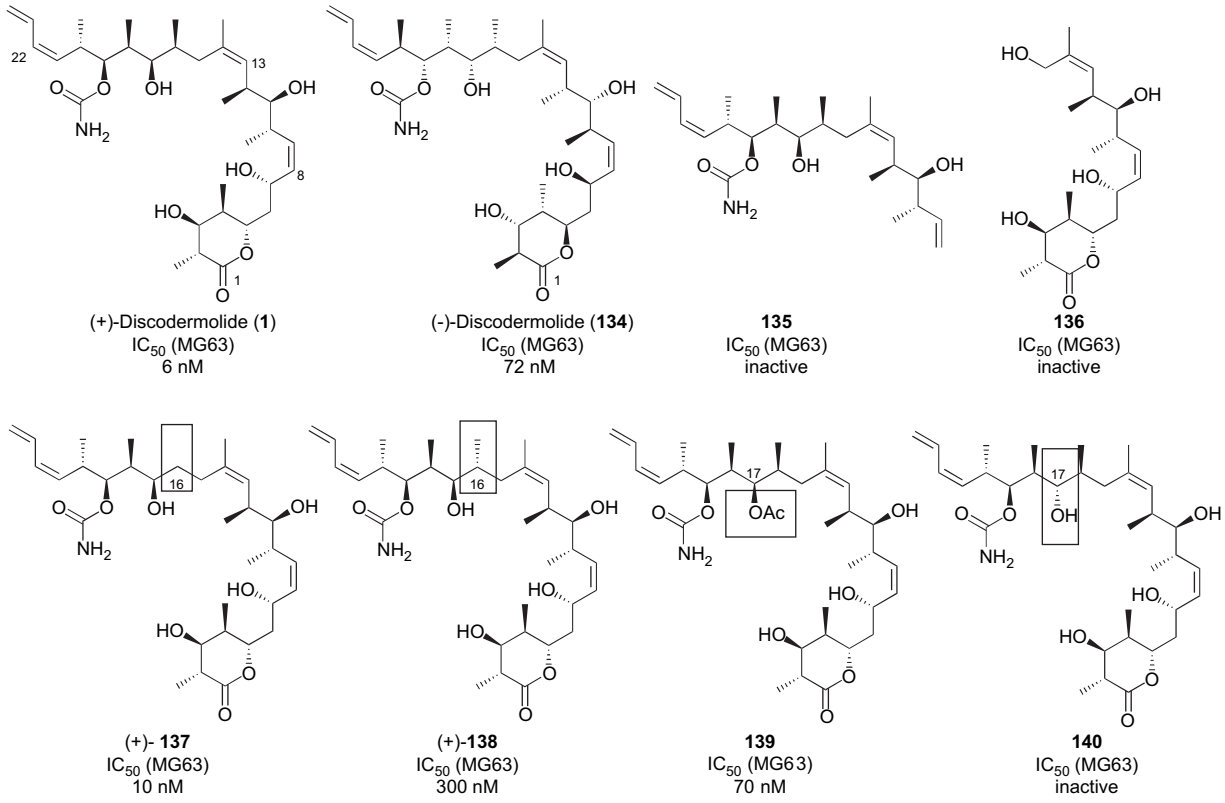

Figure 3. (+)-Discodermolide, (−)-discodermolide, and other Schreiber analogues.

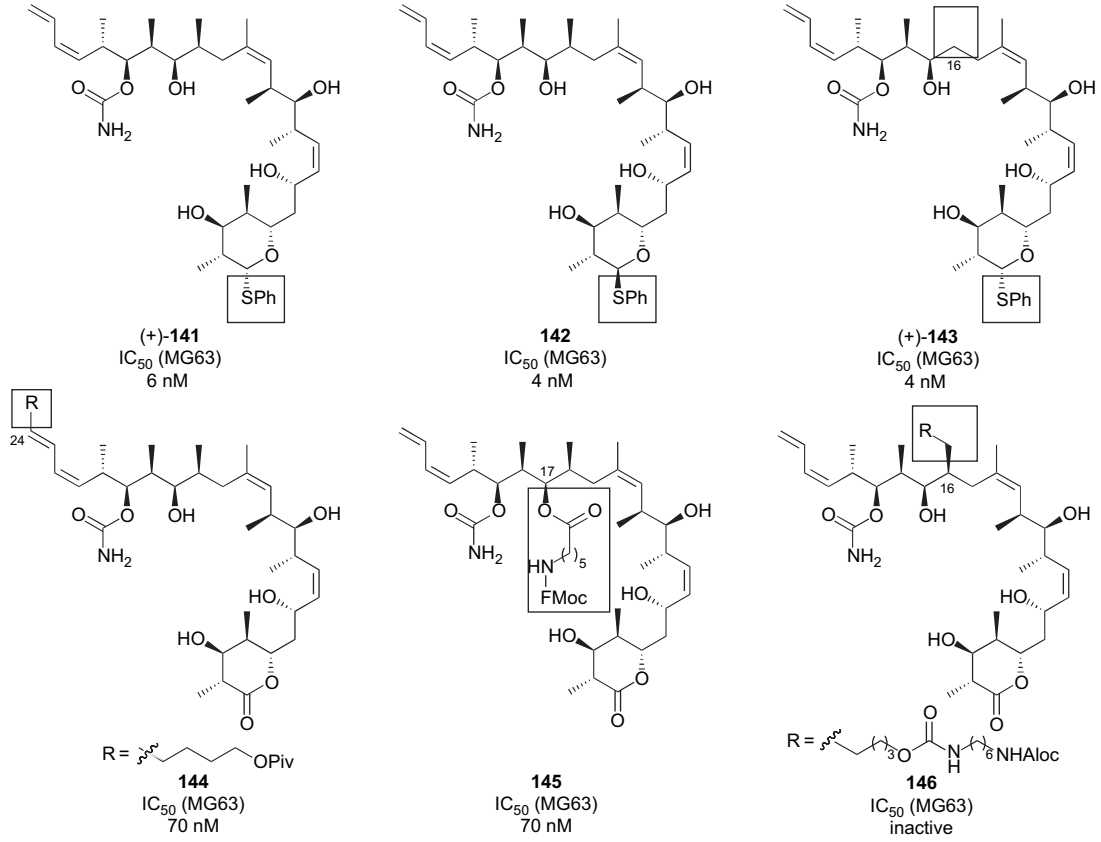

Figure 4. Schreiber analogues of (+)-discodermolide.

could be removed with little impact. Second, Schreiber demonstrated that either the lactone region could be modified or the terminal diene could be extended, without severely diminishing activity. These observations laid the groundwork for the development of future analogues of (+)-discodermolide, most notably by the research groups of Smith, Paterson, and Curran, and also by researchers at the Harbor Branch Oceanographic Institute, Novartis Pharmaceuticals, and Kosan Biosciences, Inc.

4.3. Harbor Branch Oceanographic Institute—semi-synthetic analogues and new naturally occurring derivatives

As the group responsible for the isolation of the natural product,[8] Gunasekera and co-workers at Harbor Branch were in a unique position to use naturally occurring (+)-discodermolide as a starting point for the development of semi-synthetic analogues (Fig. 5). Their initial efforts focused on the preparation of acetylated congeners (**147**–**152**),[85a,b] while a later report disclosed a series of saturated congeners (**153**–**156**) resulting from platinum oxide promoted hydrogenation of (+)-discodermolide.[85d] In vitro cell growth proliferation assay against several cancer cell lines revealed considerable structure–activity relationship vis-à-vis the four pendant hydroxyl groups, as well as the various olefins embedded in the discodermolide backbone.

For example, acetylation of either the C(3) hydroxyl, the C(7) hydroxyl, or both concurrently, as in (+)-**147**, (+)-**148**, and (+)-**149**, respectively, imparts an increase in cytotoxicity relative to the parent (+)-discodermolide (Table 1).[89] Conversely, incorporation of acetyl substituents at either the C(11) hydroxyl, as in (+)-**150** or (+)-**151**, or at the C(17) hydroxyl, as in (+)-**152**, led to a dramatic reduction in potency. With respect to the saturated variants, fully saturated congener (−)-**153** was completely inactive against the cell lines tested, while monoene (−)-**154**, which retains only the C(13)–C(14) trisubstituted olefin of (+)-discodermolide, exhibited modest nanomolar cytotoxicity in all but one cell line

Table 1. Cytotoxicity for analogues **147**–**156**[89]

	IC_{50} (nM)					
	P388	A549	HCT116	MIP-101	1A9	1A9-PTX22
(+)-**1**	35	25	7	10	10	6
(+)-**147**	12.6	4	0.2	14	4	1
(+)-**148**	3.9	0.2	0.1	3	3	0.2
(+)-**149**	0.74	1	0.2	10	20	2
(+)-**150**	103	330	30	520	40	330
(+)-**151**	166	830	620	5200	490	2800
(+)-**152**	1149	1000	1000	5500	3300	3300
(−)-**153**	>8292	>8292	n/t	n/t	n/t	n/t
(−)-**154**	33.8	30	20	1100	2	50
155	10	4	150	800	30	50
(−)-**156**	309	20	50	510	40	150

(Table 1). An improvement in activity was realized in the A549, P388, and MIP-100 cell lines upon reincorporation of the C(8)–C(9) *cis*-olefin, as in **155**, but activity in the remaining cell lines suffered. Diminished potency was also noted upon removal of the C(7) hydroxyl from monoene (−)-**154** to give (−)-**156**.

The Harbor Branch team also prepared a series of α,β-unsaturated discodermolide derivatives, employing the acetylated congeners as a starting point (Fig. 6, Table 2).[85d] The most potent compound isolated during these studies was the same (+)-2,3-anhydrodiscodermolide **157** that had been observed previously by Smith and co-workers as a low level byproduct in their global deprotection (see Section 4.7.1). Also produced were α,β-unsaturated analogues **158**–**161**, which comprise varying patterns of acetylation. In this series, incorporation of the acetyl moiety at C(11) [as in (+)-**158**] diminished the activity somewhat, and acetylation at C(17) [as in (+)-**159**] completely abolished activity, following the same trend noted in the saturated lactone series (Section 4.3). Not surprisingly, (+)-**160** and (+)-**161** were essentially inactive as well. In a separate set of experiments, two truncated derivatives of discodermolide (**162** and **163**) were also generated, but these compounds likewise displayed no cell growth inhibition.

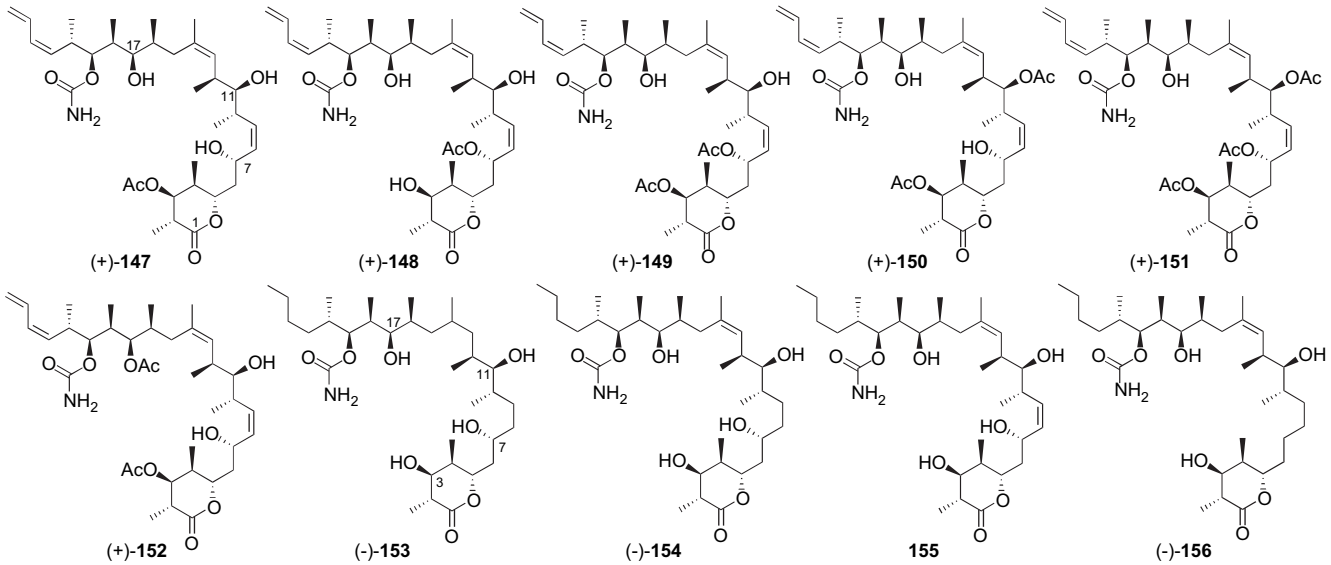

Figure 5. Harbor Branch semi-synthetic analogues.

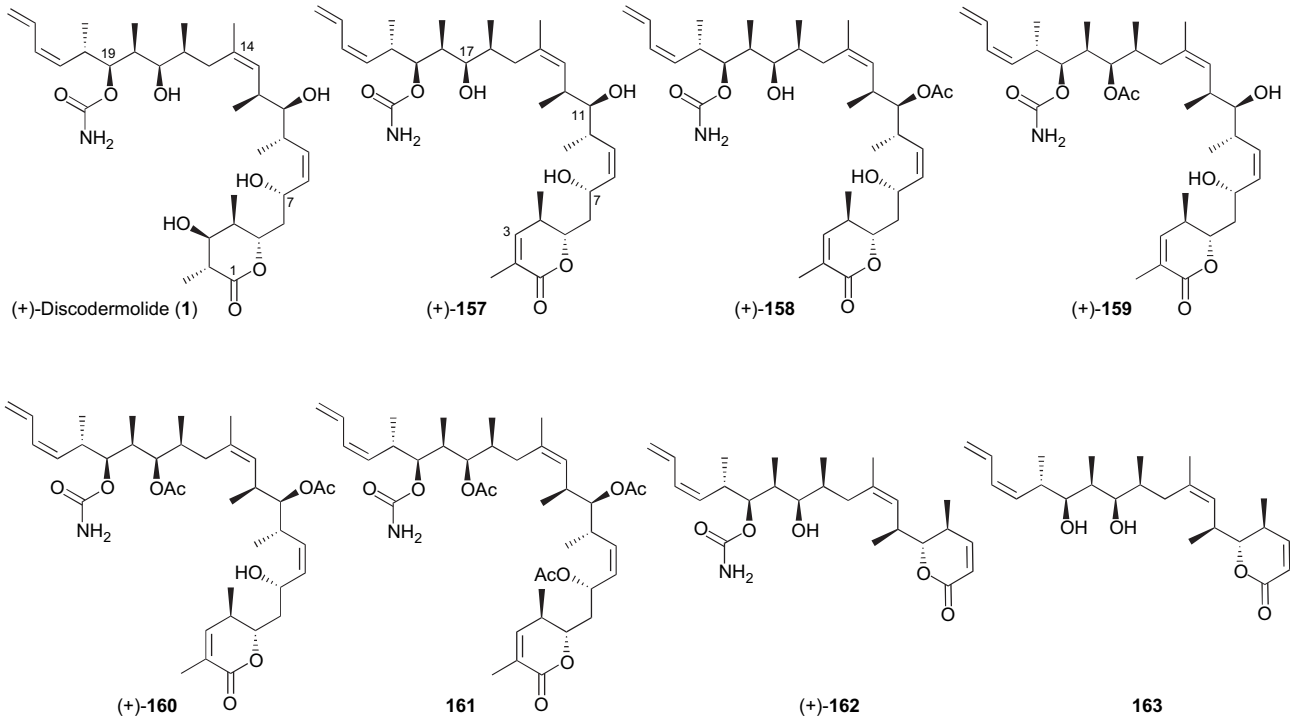

Figure 6. Harbor Branch semi-synthetic analogues.

Table 2. Cytotoxicity for analogues **157–163**

	IC_{50} (nM)					
	P388	A549	HCT116	MIP-101	1A9	1A9-PTX22
(+)-**1**	35	25	7	10	10	6
(+)-**157**	33.6	2	0.3	30	10	10
(+)-**158**	519	2800	2500	4500	3600	3200
(+)-**159**	>8103	>8103	n/t	n/t	n/t	n/t
(+)-**160**	>7587	4900	6100	10,000	20,000	5300
161	7076	14,000	14,000	19,000	>18,000	14,000
(+)-**162**	3686	6774	n/t	n/t	n/t	n/t
163	>12,787	>12,787	n/t	n/t	n/t	n/t

Some 12 years after the isolation of (+)-discodermolide from the marine sponge *D. dissoluta*,[8] researchers at Harbor Branch reported the isolation and structural elucidation of several new naturally occurring discodermolide congeners from sponge samples of the *Discodermia* genus (**164–168**, Fig. 7).[85c] Evaluation of the newly discovered congeners (Table 3) revealed that epimerization or removal of the C(2) methyl substituent [(+)-**164** and (+)-**165**] moderately diminished the activity. Additionally, the linear discodermolide methyl ester (+)-**166** and the *C*(19)-descarbamoyl analogue (+)-**167** retained only modest potency relative to (+)-discodermolide, while the cyclic analogue (+)-**168** was inactive.

4.4. Paterson analogues of (+)-discodermolide

Shortly after the completion of their first-generation total synthesis of (+)-discodermolide,[41g] Paterson and co-workers disclosed the synthesis of three stereoisomers (**169–171**) and two truncated analogues (**172** and **173**) of the natural product (Fig. 8).[81] A follow-up report detailed the production of three additional discodermolide congeners (**174–176**).[86] All of these compounds were produced by exploiting intermediates and/or side products generated during their discodermolide syntheses. To date, biological activity has been reported for only four of the eight compounds (Table 4).[89] Here, potency was reduced, on average, by over an order of magnitude for C(5) epimer (+)-**169** and C(7) epimer (+)-**170**, while deletion of the C(15)–C(24) subunit completely abolished activity. Remarkably, triol (+)-**173**, in which the entire C(1)–C(7) portion has been replaced by a hydroxymethyl substituent, exhibits antiproliferative activity comparable to the C(5) and C(7) epimeric congeners **169** and **170**. This result contrasts with the Schreiber observation, wherein a very similar truncated congener **135** (Fig. 3), missing only the hydroxymethyl substituent, was completely inactive.

4.5. Novartis analogues of (+)-discodermolide

In support of their discodermolide program, which ultimately resulted in the advancement of the natural product into Phase I clinical trials, researchers at Novartis Pharmaceuticals also designed, synthesized, and evaluated a number of synthetic analogues. During this program, variation was incorporated at each of the three major subunits of discodermolide [specifically, the C(1)–C(7), C(8)–C(14), and C(15)–C(24) regions]. The compounds and the data to result from this effort were first reported in 2002 meeting of the American Association for Cancer Research,[90] and also in a series of patents published in 2002 and 2003.[91]

With respect to the C(1)–C(7) lactone subunit, the Novartis group found that the completely unsubstituted lactone congener **177** (Fig. 9, Table 5) displayed cell growth inhibitory activity rivaling that of the natural product, and the sodium salt of discodermolide seco-acid **178** retained the modest potency. Replacement of the C(1)–C(7) moiety with a variety of other substituents, as in carbamate **179**, phenyl ether

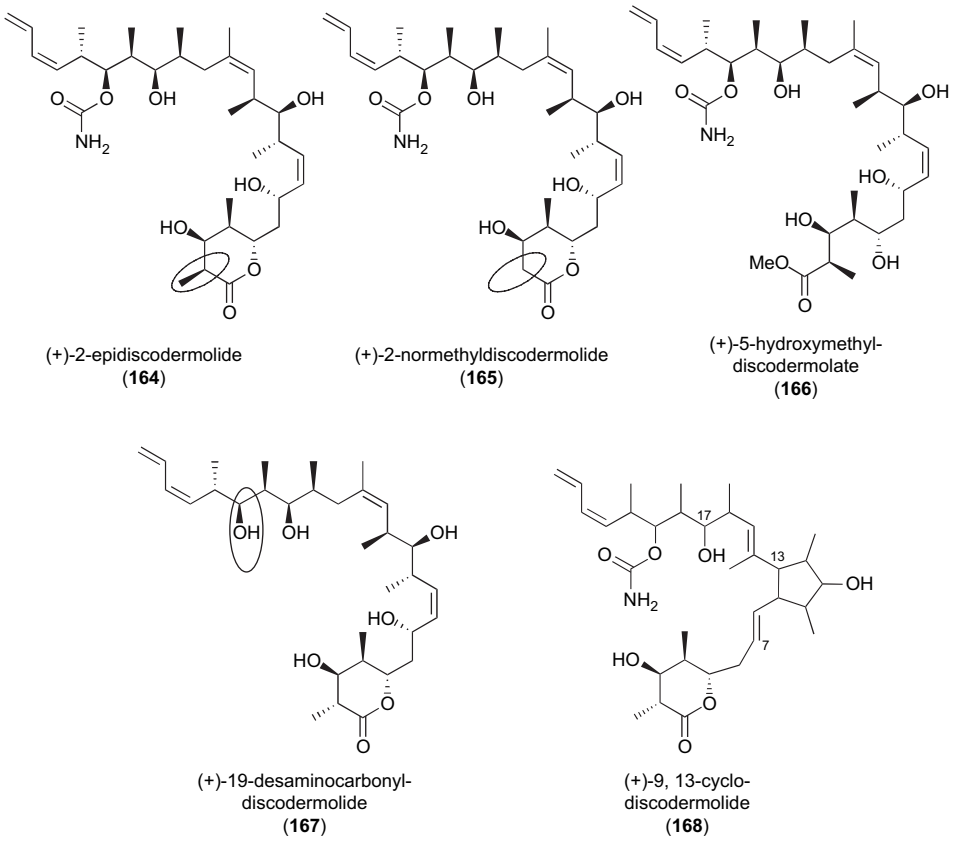

Figure 7. Harbor Branch naturally occurring discodermolide congeners.

180, or amides **181** and **182**, while not completely debilitating, did result in lessened activity. Lactone **183** and truncated congener **184** were essentially inactive.

The next set of analogues from the Novartis team explored the effect of saturation, truncation, or replacement of the C(21)–C(24) terminal diene (**185**–**190**, Fig. 10). On the whole, these modifications were well-tolerated (Table 6), an observation that was also noted by Schreiber (Section 4.2), Harbor Branch (Section 4.3), and Smith (Section 4.7.2) in similar systems. Dihydro congeners **185**–**187** were particularly potent, exhibiting single-digit nanomolar activity in four of the five tested cell lines. Triene **188**, which lacks carbons C(23) and C(24), displayed good to excellent antiproliferative activity across the panel. Replacement of the diene with either a phenyl or a benzyl ether, as in **189** and **190**, respectively, had a major lowering effect on potency only in the MIP-101 cell line. Two final compounds described by Novartis incorporated modification of the critical central region of (+)-discodermolide. Originally reported by Smith and co-workers (see Section 4.7.2), 14-normethyldiscodermolide **191** retains low-nanomolar potency in four of the five cell lines tested at Novartis. On the other hand, compound **192**, in which the *N*-methyl amide was intended to mimic the C(13)–C(15) substructure of the natural product, displayed sub-micromolar activity only in the A549 cell line.

A final series of compounds to be described by the Novartis group were evaluated and reported in collaboration with Harbor Branch.[85e] During the final step of the Novartis campaign to produce 60 g of (+)-discodermolide, an HCl-mediated global desilylation, several additional compounds in trace quantities were subsequently purified and characterized by Gunasekera and co-workers. Of the six derivatives isolated (Fig. 11, Table 7), five (**193**–**197**) can be seen to have arisen from an acid-promoted C(13)–C(9) olefin-assisted cyclization with concomitant displacement of the allylic C(7) hydroxyl group. The multitude of products formed suggests the intermediacy of a tertiary carbocation, which either undergoes E1-type elimination [as in (−)-**193** and (+)-**194**] or alternately is trapped by water to afford **195**–**197**. The sixth compound, (+)-**198**, resulted from direct displacement of the C(7) hydroxyl by the C(11) substituent.

Upon evaluation, the bicyclic discodermolide congeners were all less potent than the natural product (+)-**1**. However, one compound retained modest cell growth inhibitory activity, specifically (+)-**194**, which bears an *exo*-methylene at C(14).

Table 3. Cytotoxicity for analogues **164**–**168**[89]

	IC_{50} (nM)					
	P388	A549	HCT116	MIP-101	1A9	1A9-PTX22
(+)-**1**	35	25	7	10	10	6
(+)-**164**	134	30	40	70	30	40
(+)-**165**	172	60	30	190	260	210
(+)-**166**	66	60	6	40	40	20
(+)-**167**	128	5	4	60	10	30
(+)-**168**	5043	4487	n/t	n/t	n/t	n/t

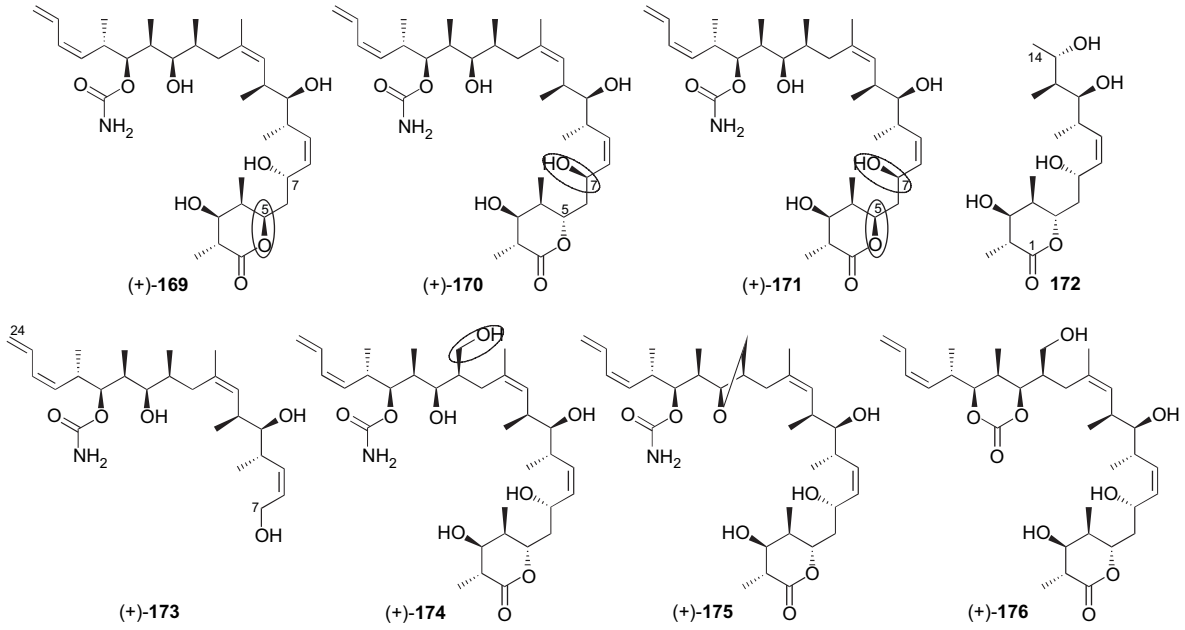

Figure 8. Paterson analogues of (+)-discodermolide.

4.6. Curran/Day analogues of (+)-discodermolide

In a joint research program at the University of Pittsburgh, Curran (Chemistry Department) and Day (Pharmacy) engaged in the design and synthesis of simplified discodermolide analogues.[88] The simplest compounds produced, which possessed the general structure defined by skeleton **199** (Fig. 12), exhibited at best minimal cell growth inhibitory potency (on the order of double digit micromolar). Many of these compounds did, however, retain properties unique to (+)-discodermolide, such as the ability to hypernucleate tubulin polymerization at low temperature.[88d] The most potent antiproliferatives to result from the Curran/Day work (Fig. 12, Table 8), although still only in the low micromolar regime, were those that retained a C(1)–C(6) cyclic subunit and the C(21)–C(24) terminal diene,[88d] such as (+)-**200a**, (+)-**200b**, and (+)-**201c**.

Table 4. Cytotoxicity for analogues **169**, **170**, **172**, and **173**[89]

	IC_{50} (nM)				
	A549	HCT116	MIP-101	1A9	1A9-PTX22
(+)-**1**	25	7	10	10	6
(+)-**169**	150	100	1000	100	300
(+)-**170**	500	100	1000	200	300
(+)-**172**	8700	12,000	58,000	49,000	11,000
(+)-**173**	130	400	1300	70	70

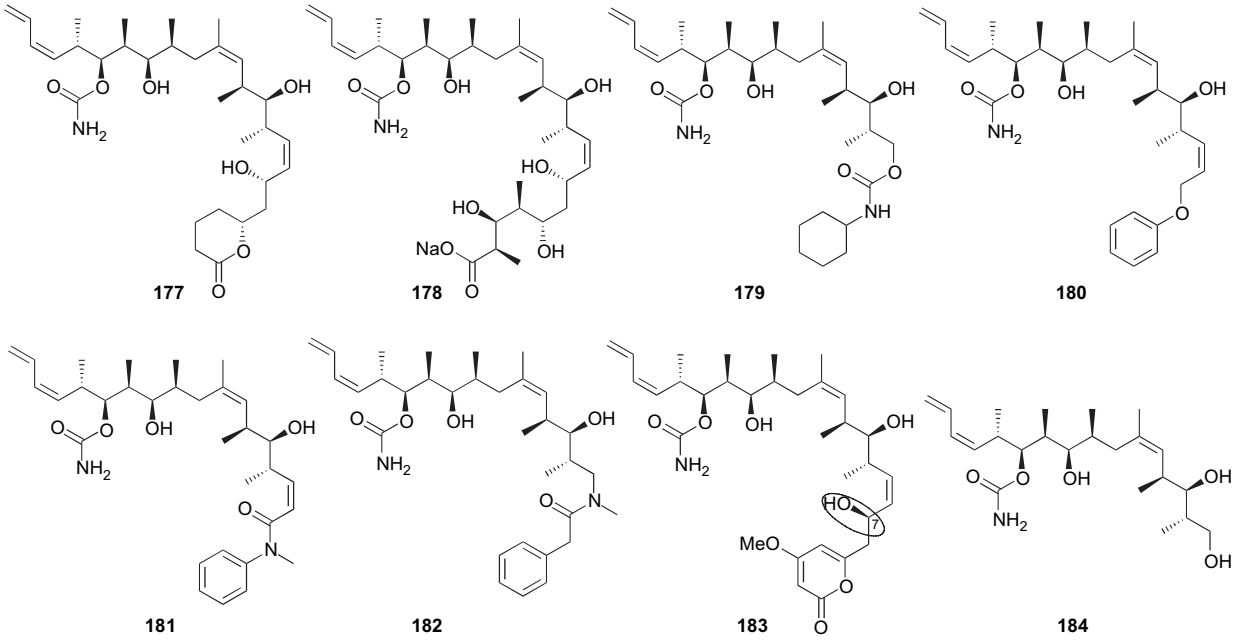

Figure 9. Novartis analogues of (+)-discodermolide.

Table 5. Cytotoxicity for analogues **177–184**

	IC_{50} (nM)				
	A549	HCT116	MIP-101	1A9	1A9-PTX22
(+)-**1**	25	7	10	10	6
177	n/t	7	60	6	7
178	n/t	50	300	100	200
179	n/t	400	3200	500	400
180	n/t	200	400	300	100
181	n/t	800	3200	500	400
182	n/t	300	600	n/t	80
183	3200	600	6500	300	400
184	1000	4000	6000	1000	2000

Table 6. Cytotoxicity for analogues **185–192**

	IC_{50} (nM)				
	A549	HCT116	MIP-101	1A9	1A9-PTX22
(+)-**1**	25	7	10	10	6
185	10	4	7	3	4
186	4	2	25	1	4
187	5	1	130	3	6
188	120	40	300	50	60
189	60	40	3600	20	100
190	300	200	3800	30	180
191	50	30	200	20	50
192	410	13,000	20,000	4000	6000

4.7. Smith and Smith/Kosan analogues of (+)-discodermolide

Following the successful effort to produce 1 g of totally synthetic (+)-discodermolide, the discodermolide program at Penn broadened to include the production of structurally related analogues. This venture was significantly strengthened by a trio of very productive collaborations, both academic and industrial. Horwitz and co-workers at the Albert Einstein School of Medicine contributed much of the cytotoxicity data that are presented in this section. Moreover, the Horwitz group continues to actively pursue elucidation of the discodermolide binding domain of β-tubulin. In 2002, Smith and co-workers also initiated a productive partnership with Myles at Kosan Biosciences, which resulted in many of the analogues and most of the biological data described in this section. Finally, a collaboration with Vogelstein at The Johns Hopkins University (Howard Hughes Medical Institute) permitted in vivo evaluation of (+)-discodermolide and several analogues both as stand-alone chemotherapeutics and as the chemical component of the treatment paradigm known as combination bacteriolytic therapy (COBALT).

The design of the initial set of analogues[87a] was guided largely by the knowledge gained during the gram-scale effort; the first compounds created were drawn directly from minor byproducts isolated during the latter stages of that endeavor, while many of the later analogues would address the synthetic difficulties encountered therein. Additionally, several (+)-discodermolide congeners were created simply to probe the structure–activity relationship. Tactically, the Smith/Kosan groups addressed the discodermolide skeleton at four key points: (1) the C(1)–C(6) lactone, (2) the C(14) methyl substituent, (3) the C(19) carbamate moiety, and (4) the terminal diene subunit.

4.7.1. Smith and Smith/Kosan lactone-replacement analogues. The first analogue to be isolated arose as a minor byproduct of global desilylation[87a] during the final stage of the Smith gram-scale discodermolide synthesis. While the deprotection proceeded reliably and in high yield (>90%), the scale of those reactions permitted the isolation of significant quantities of a secondary product. Single-crystal X-ray analysis revealed this compound to be α,β-unsaturated lactone (+)-**157** (Fig. 13), the result of an acid-mediated dehydration event. Interestingly, despite the simplified structure, subsequent biological evaluation against a number of human cancer cell lines established that 2,3-anhydrodiscodermolide (+)-**157** was generally a more potent inhibitor of cell growth than (+)-discodermolide (Table 9). Smith

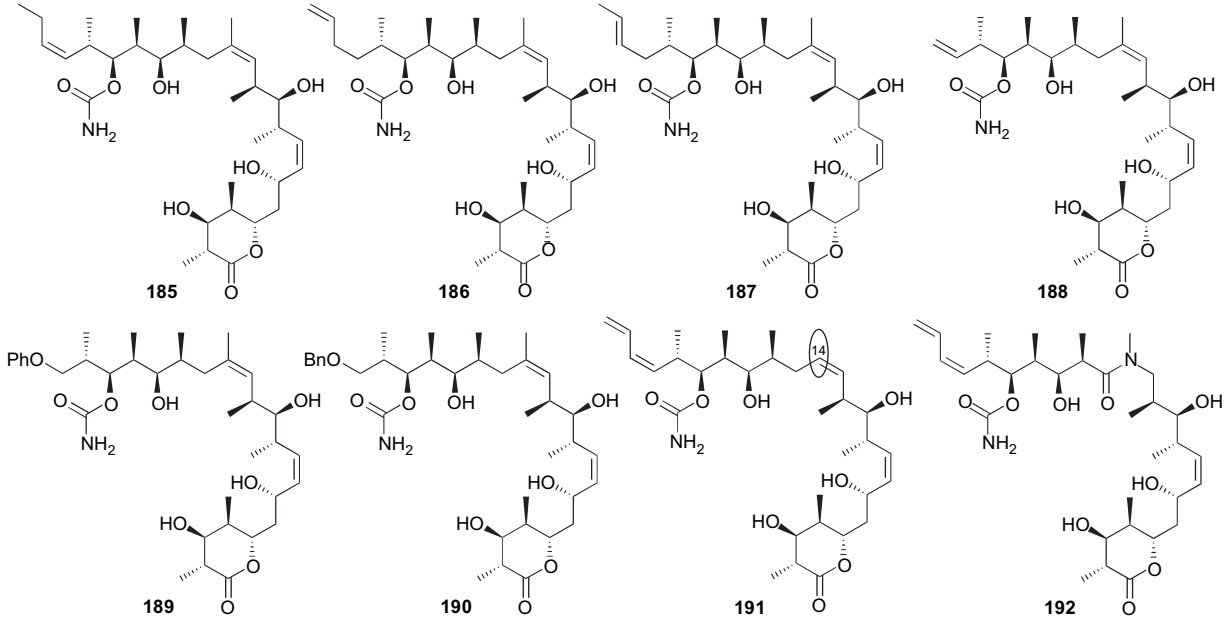

Figure 10. Novartis analogues of (+)-discodermolide.

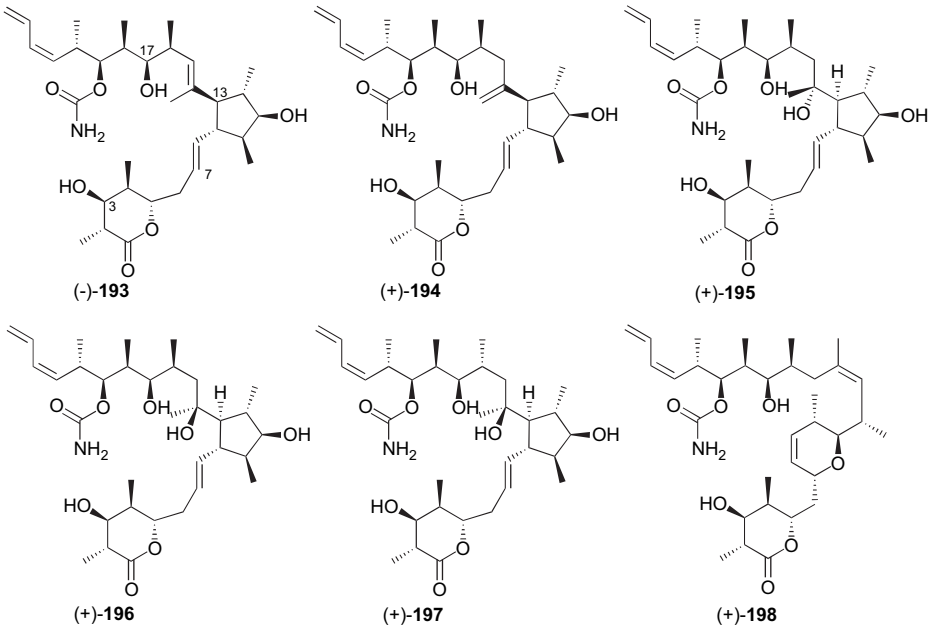

Figure 11. Novartis/Harbor Branch synthetic analogues.

Table 7. Cytotoxicity for analogues **193–198**

	IC_{50} (nM)					
	P388	A549	MCF-7	NCI/ADR	PANC-1	VERO
(+)-**1**	33	15	2.4	17	49	30,000
(−)-**193**	2130	6640	2100	>5000	6570	21,900
(+)-**194**	190	100	130	3400	330	690
(+)-**195**	2420	840	2360	>5000	3030	4300
(+)-**196**	2090	2640	1730	>5000	>5000	16,600
(+)-**197**	7650	>5000	7350	>5000	>5000	11,400
(+)-**198**	1000	1460	1800	4400	3130	3650

and co-workers, therefore, embarked on a systematic investigation of the structure–activity relationship of the lactone region.[87e] The results indicated that the lactone moiety could indeed be further simplified, while retaining considerable potency (Table 9); both (+)-2-normethyl-2,3-anhydrodiscodermolide (**203**) and (+)-2,4-normethyl-2,3-anhydrodiscodermolide (**204**) show activity comparable to (+)-**157**, and thus superior to (+)-discodermolide (**1**). The α,β-unsaturation also proved to be unnecessary, as (+)-2-normethyl-3-deoxydiscodermolide **205** possessed cell growth inhibitory activity on par with the unsaturated congeners, while the unsubstituted, saturated lactone congener (+)-**206** (also prepared by Novartis) was less potent only in the NCI/ADR cell line. Removal of the C(7) hydroxyl group, as in (+)-**207** and (+)-**208**, was moderately detrimental to cytotoxicity.

An interesting discovery was the potency of (+)-4,5-*epi*-2,3-anhydrodiscodermolide **209**. This observation led to the hypothesis that only the lactone carbonyl is involved in a critical interaction, and that the function of the ring substituents is simply to direct the orientation of the carbonyl. In other words, the 4,5-*epi* congener (+)-**209** was able to competently preserve the lactone position and thus retain potent bioactivity. Under the notion that the conformationally more rigid five-membered ring might provide a more effective scaffold, three γ-lactone discodermolide congeners were synthesized and evaluated by our colleagues at Kosan (Fig. 13). Upon evaluation, butyrolactone **210**, which bears the C(5) and C(7) stereogenicity (using discodermolide numbering) found in the natural product, exhibited cell growth inhibitory

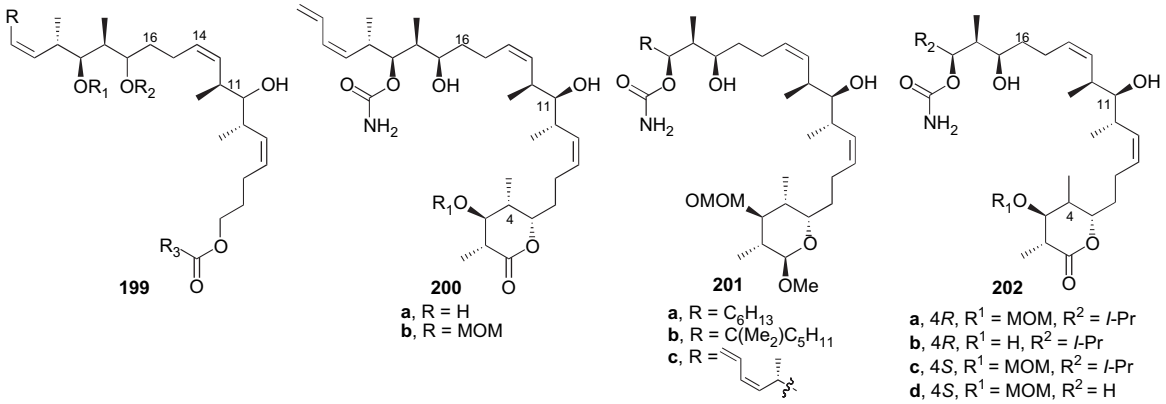

Figure 12. Curran/Day simplified analogues.

Table 8. Biological activity for analogues **200–202**

	GI_{50} (μM)				
	MDA-MB231	PC-3	2008	MT assembly (%)	^{3}H-paclitaxel displace (%)
(+)-**1**	0.016	0.067	0.72	>100	64
(+)-**200a**	2.1	7.5	5.2	11	21
(+)-**200b**	0.87	1.8	0.65	27	57
(−)-**201a**	24	>50	29	6	9
(−)-**201b**	23	38	42	9	15
(+)-**201c**	3.4	15	4.7	11	19
(+)-**202a**	>50	>50	>50	7	10
(+)-**202b**	>50	>50	>50	13	10
(+)-**202c**	46	>50	>50	<5	3
(+)-**202d**	30	>50	>50	<5	13

Table 9. Cytotoxicity for analogues **157** and **203–211**

	IC_{50} (nM)			
	MCF-7	NCI/ADR	A549	CCRF-CEM
(+)-**1**	28	240	22	16
(+)-**157**	5.6	463	8.6	3.0
(+)-**203**	2.1	95	3.7	2.7
(+)-**204**	3.2	630	7.9	3.8
(+)-**205**	2.7	150	6.0	1.5
(+)-**206**	8.4	>1000	36	2.9
(+)-**207**	23	330	160	6.3
(+)-**208**	63	878	47	n/t
(+)-**209**	4.6	350	7.8	4.0
210	2.9	350	4.9	2.3
211	390	>10,000	2000	310

activity superior to discodermolide in the drug-sensitive cell lines, while maintaining potency against the multi-drug-resistant cell line (Table 9). In contrast, 5,7-bis-epimer **211** was significantly less potent.

Smith and co-workers speculated that the lactone region could perhaps be simplified further while preserving significant cell growth inhibitory activity. To explore this idea, several discodermolide congeners in which the entire C(1)–C(7) subunit has been replaced with arylethyl substituents (Fig. 14) were designed and synthesized.[87b] Pleasingly, despite the removal of *five* stereogenic centers, the majority of these analogues displayed sub-micromolar activity against the drug-sensitive cell lines; moreover, several retain activity in the resistant line (Table 10). The simple phenol derivative, (+)-**213**, proved to be the most potent of the aryl lactone-replacement congeners, exhibiting antiproliferative potency not far removed from that of (+)-discodermolide. Taken together, these observations could have a significant impact on both the cost and the ease of synthesizing a discodermolide derivative as a pharmaceutical.

Seeking to retain the synthetic simplicity of the aryl analogues shown in Figure 14, Smith and co-workers returned to the hypothesis that, with respect to the C(1)–C(7) subunit, it is the placement and orientation of the C(1) carbonyl that drive potency. With this in mind, a series of coumarin and lactam-derived compounds (**225–230**)[87g] were designed and synthesized to probe further the geometric requirements for antiproliferative activity. Again, the placement of the lactone carbonyl proved to be critical, with the 7-substituted coumarin (+)-**225** and the 23,24-dihydro counterpart (+)-**226** exhibiting cell growth inhibitory activity equivalent to (+)-discodermolide (**1**) in all three cell lines tested, while 6-coumarin (+)-**227** was significantly less potent (Fig. 15, Table 11). *Notably, analogues (+)-**225** and (+)-**226** represent the structurally simplest congeners reported to date that retain the low-nanomolar antiproliferative activity exhibited by (+)-discodermolide.* On the other hand, the three lactam analogues proved to be somewhat diminished in potency relative to the coumarins, although lactam (−)-**228**, which bears a free NH, is more active than the two *N*-substituted congeners (+)-**229** and (+)-**230**.

4.7.2. Smith 14-normethyl analogues of (+)-discodermolide. The C(13)–C(14) *Z*-trisubstituted olefin embedded in the parent (+)-discodermolide represented a significant synthetic challenge. Indeed, the efficient installation of

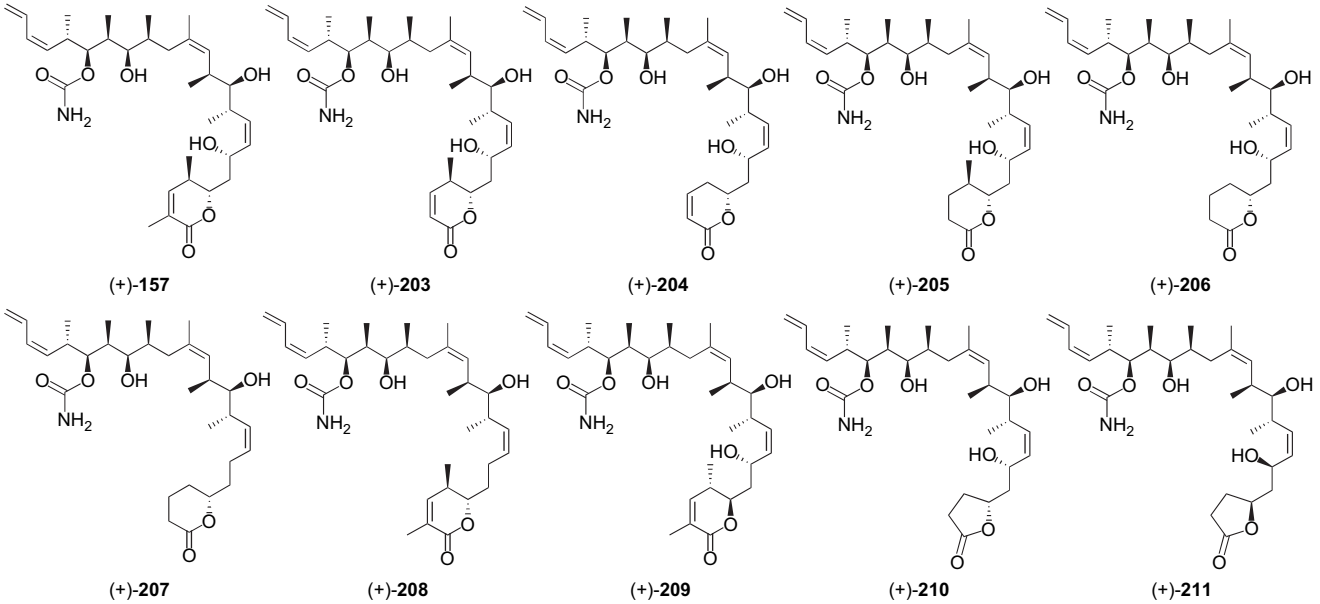

Figure 13. Smith and Smith/Kosan lactone-replacement analogues of (+)-discodermolide.

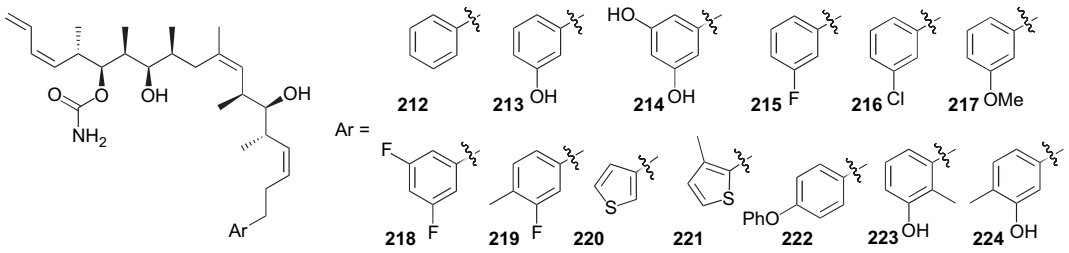

Figure 14. Smith aryl lactone-replacement analogues.

Table 10. Cytotoxicity for analogues **212–224**

	IC_{50} (nM)			
	MCF-7	NCI/ADR	A549	SKOV-3
(+)-**1**	28	240	22	21
(+)-**212**	480	560	510	350
(+)-**213**	130	390	190	40
(+)-**214**	160	>1000	310	45
215	370	500	650	400
216	400	650	580	380
217	330	500	600	370
218	600	2000	1000	360
219	1000	4000	4000	1000
220	850	4000	4000	440
221	370	620	790	370
222	4000	10,000	10,000	10,000
223	490	1000	910	270
224	770	4000	4000	410

this structural motif was (and remains) among the most challenging aspects of the total synthesis. Deletion of the C(14) methyl group, generating a *Z*-disubstituted olefin, served to simplify the structure, and, more importantly, to simplify the chemistry required for construction. Adding to the merit of this strategy, Schreiber and co-workers had noted that deletion of the nearby C(16) methyl group had no negative impact on activity (see Section 4.2). Gratifyingly, totally synthetic (+)-14-normethyldiscodermolide[87a] (**191**, Fig. 16) retained potent cell growth inhibition in three of the four cell lines tested (Table 12). Unlike (+)-discodermolide (**1**), however, the 14-normethyl congener (+)-**191** is essentially inactive at sub-micromolar levels in the multi-drug-resistant NCI/ADR line. This deficiency notwithstanding the relative ease of synthesis and the potent cytotoxicity of (+)-**191** made the 14-normethyl scaffold an attractive starting point for the design of a number of analogues.

This investigation began with the production of simplified lactone-replacement analogues (**231–235**, Fig. 16),[87c]

Table 11. Cytotoxicity for analogues **225–230**

	IC_{50} (nM)		
	SKOV3	MCF-7	NCI/ADR
(+)-**1**	25	26	260
(+)-**225**	44	12	190
(+)-**226**	35	15	230
(+)-**227**	1800	1600	3300
(+)-**228**	790	430	840
(+)-**229**	2400	1600	3200
(+)-**230**	2900	3000	4000

mimicking the modifications made in the 14-methyl series. Interestingly, while dehydration of the lactone of (+)-discodermolide (**1**) to form (+)-**157** (Fig. 13, Table 9) led to a more potent compound in the three drug-sensitive cell lines, identical modification of the 14-normethyl scaffold, as in (+)-**231**, results in a significant *decrease* in tumor cell growth inhibition (Table 12). Further simplification by removal of the C(2) methyl group [(+)-**232**] restores potency to the levels displayed by the parent (+)-14-normethyldiscodermolide (**191**) in the MCF-7 and SKOV-3 lines, while activity in the A549 cell line is relatively depressed. An even more striking contrast between the discodermolide and the 14-normethyl scaffolds appears when the hydroxyphenylethylene unit replaces the lactone. While the 14-methylated congener of this compound [(+)-**213**, Figure 14, Table 10] displays considerable potency, no cytotoxicity is observed with the 14-normethyl variant (+)-**233** at levels up to 5 μM. Replacement of the phenol with an aniline moiety, as in (+)-**234**, likewise leads to an inactive congener, as does substitution of the lactone with a pyridone ring [(+)-**234**].

Smith and co-workers next sought to explore the effect of saturation and truncation of the C(21)–C(24) terminal diene of (+)-14-normethyldiscodermolide (**191**).[87a,c] To this end, a series of four analogues were prepared (**236–239**, Fig. 17). In vitro evaluation of the tumor cell growth

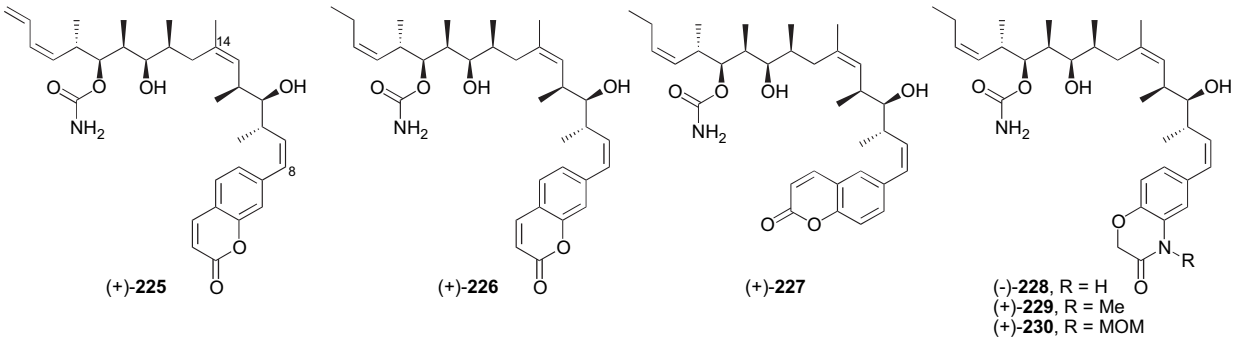

Figure 15. Smith coumarin-derived lactone-replacement analogues.

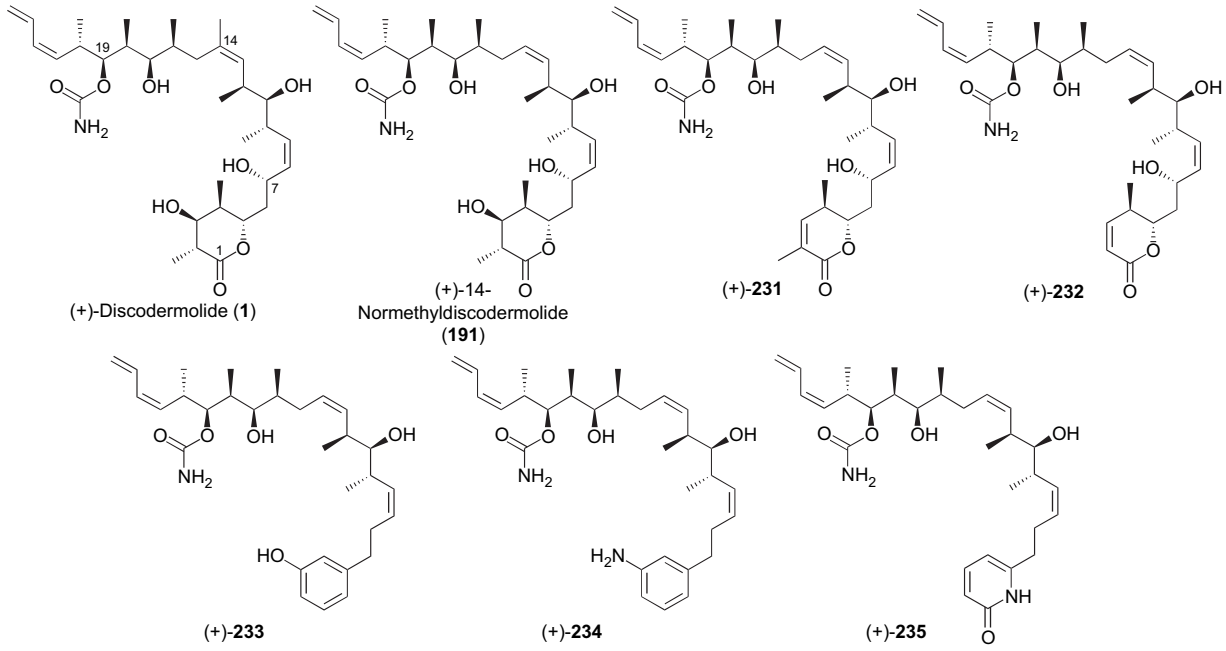

Figure 16. Smith 14-normethyl lactone-replacement analogues.

Table 12. Cytotoxicity for analogues **231–235**

	IC_{50} (nM)			
	MCF-7	NCI/ADR	A549	SKOV-3
(+)-**1**	28	240	22	21
(+)-**191**	46	8200	50	35
(+)-**157**	5.6	463	8.6	3.4
(+)-**231**	185	>1000	536	82
(+)-**232**	45	>1000	300	50
(+)-**233**	>5000	>5000	>5000	>5000
(+)-**234**	>1000	>1000	>1000	790
(+)-**235**	>1000	>1000	>1000	>1000

inhibitory activity of this series again demonstrated the impotency of the 14-normethyl variants of (+)-discodermolide (**1**) in the multi-drug-resistant NCI/ADR cell line, as all four congeners proved to be essentially inactive at sub-micromolar levels (Table 13). In fact, the most truncated analogues, (+)-**236** and (+)-**237**, display no appreciable cytotoxicity in any of the cell lines tested. Against MCF-7 and SKOV-3 cells, reincorporation of C(23) in the form of triene (+)-**238** restored moderate cytotoxicity, while (+)-**239**, which retains the full carbon skeleton of (+)-14-normethyldiscodermolide, but with a saturated terminus, displayed potency rivaling that of the natural product. Similar results were noted by Novartis

Table 13. Cytotoxicity for analogues **236–239**

	IC_{50} (nM)			
	MCF-7	NCI/ADR	A549	SKOV-3
(+)-**1**	28	240	22	21
(+)-**191**	46	8200	50	35
(+)-**236**	>1000	>1000	>1000	>1000
(+)-**237**	>1000	>1000	>1000	>1000
(+)-**238**	72	>1000	570	130
(+)-**239**	28	>1000	100	20

in systems with the C(14) methyl intact (Section 4.5). Taken together, these results clearly exhibit a trend of decreasing activity as the C(24) terminus is truncated, while isosteric replacement of the terminal olefin with a saturated counterpart preserves cell growth inhibitory activity.

4.7.3. Smith and Smith/Kosan carbamate analogues. In an effort to find modifications that might improve either the activity or the physicochemical properties of discodermolide, the influence of substitution at the C(19) carbamate was explored next. The most extensive series of carbamate-substitution congeners was generated employing the synthetically simplified 14-normethyl scaffold (Fig. 18).[87a,d] The cell growth inhibitory activity data gathered during this study

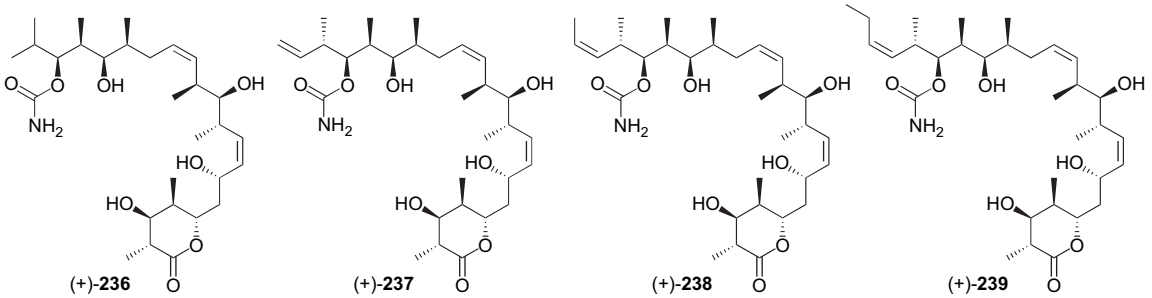

Figure 17. Smith diene-replacement analogues of (+)-14-normethyldiscodermolide.

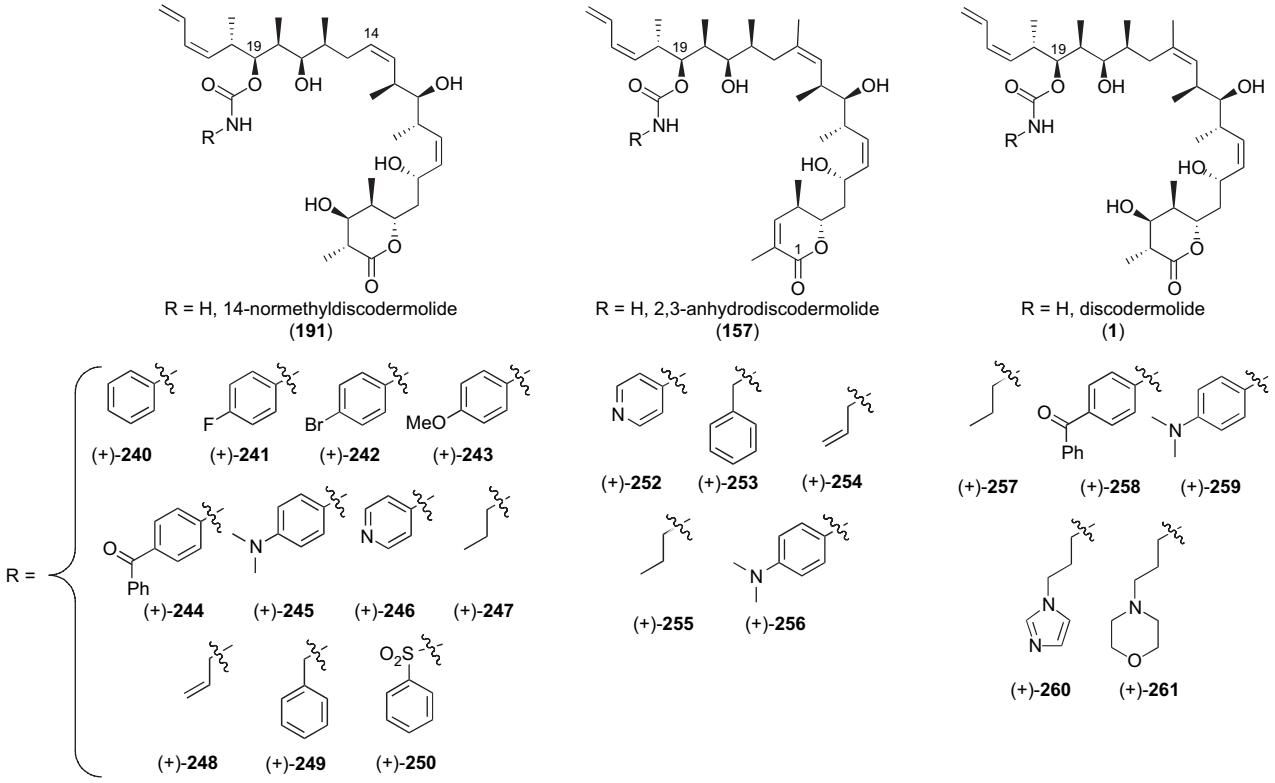

Figure 18. Smith carbamate-substitution analogues of (+)-discodermolide.

(Table 14) demonstrated that appending the carbamate in the 14-normethyl series (**240**–**250**), by and large, had little effect on cytotoxic potency across the panel of cell lines tested, with dimethylaniline congener (+)-**245** exhibiting the best activity. A significant loss in potency was noted with phenylsulfone congener (+)-**250**, while complete removal of the carbamate, leaving a free hydroxyl group at C(19) [(+)-**251**, not depicted), likewise lowered the activity. Curiously, carbamate substitutions applied to the 2,3-anhydro scaffold, as in **252**–**255** (Fig. 18), were detrimental to potency.[87a,d] The dimethylaniline congener (+)-**256**, however, exhibited activity comparable to that of 2,3-anhydrodiscodermolide **157**. Moving to the parent discodermolide skeleton, the dimethylaniline substituent, as in (+)-**259**, again proved to be the most promising addition to the carbamate.[87d] However, the dimethylaniline moiety is known to be labile in vivo, primarily due to the action of cytochrome P450. Thus, the less labile imidazole (+)-**260** and morpholine (+)-**261** were designed and synthesized; unfortunately, the resulting cytotoxicity did not equal that shown by (+)-**259**.

Table 14. Cytotoxicity for analogues **240**–**261**

	IC_{50} (nM)			
	MCF-7	NCI/ADR	A549	SKOV-3
(+)-**1**	28	240	22	21
(+)-**191**	46	8200	50	35
(+)-**157**	5.6	463	8.6	3.4
(+)-**240**	48	>1000	135	47
(+)-**241**	42	>1000	125	47
(+)-**242**	84	>1000	247	90
(+)-**243**	23	>1000	89	23
(+)-**244**	23	>1000	67	36
(+)-**245**	6.2	2000	27	12
(+)-**246**	27	>1000	110	38
(+)-**247**	22	>1000	73	20
(+)-**248**	17	4000	55	10
(+)-**249**	27	4000	51	30
(+)-**250**	>1000	>1000	>1000	>1000
(+)-**251**	365	>1000	>1000	200
(+)-**252**	120	>1000	400	250
(+)-**253**	290	>1000	410	380
(+)-**254**	630	>1000	2000	790
(+)-**255**	660	>1000	2000	610
(+)-**256**	5.6	260	9.4	7.6
(+)-**257**	27	>1000	54	34
(+)-**258**	8.4	>1000	10	8
(+)-**259**	1.9	450	5.1	1.8
(+)-**260**	33	>1000	58	31
(+)-**261**	10	>1000	30	14

4.7.4. (+)-Discodermolide and analogues as in vivo chemotherapeutics. In collaboration with the Vogelstein group at The Johns Hopkins University (Howard Hughes Medical Institute), (+)-discodermolide (**1**) and three of the most interesting analogues [(+)-**191**, (+)-**157**, and (+)-**203**, Figure 19] generated by the Smith group were evaluated for antitumor efficacy in an in vivo mouse model, specifically employing HCT-116 colon carcinoma xenografts. Each of these agents served to slow the growth of the treated tumors upon a single administration of the drug. The most potent of these agents, 2,3-anhydrodiscodermolide (+)-**157**, completely halted tumor growth for a full 20 days. Importantly, little general toxicity was observed during these studies.

Based on these single-agent studies, 2,3-anhydrodiscodermolide (+)-**157** was next employed as the chemical component of the Vogelstein therapeutic paradigm COBALT (*co*mbination *bac*terio*l*ytic *t*herapy), which has proven to be remarkably effective in human xenograft mouse models

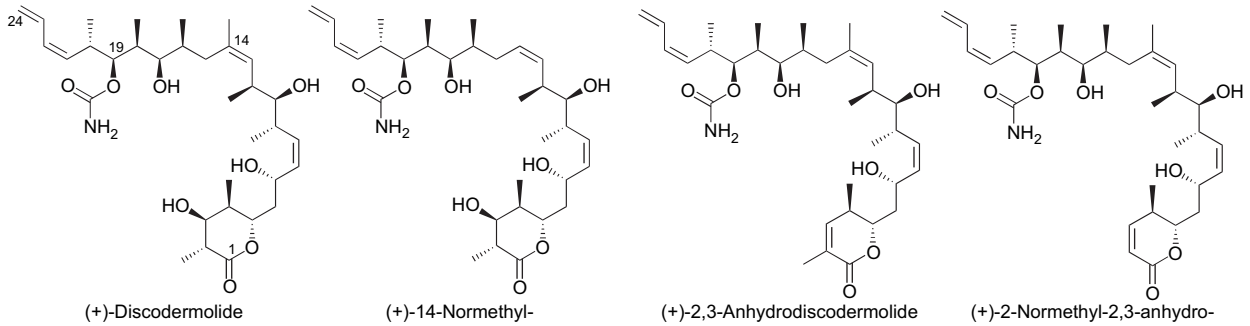

Figure 19. Compounds evaluated as in vivo tumor suppression agents.

for the treatment of fast-growing, poorly vascularized, solid tumors.[92,93] This treatment protocol entailed administration of a combination of (+)-**157** and the genetically modified, non-toxic anaerobic bacteria *Clostridium novyi-NT*, in this case to mice bearing HCT-116 xenograft tumors. Remarkably, the treated tumors exhibited massive hemorrhagic necrosis within 1 day following treatment.[87f] These lesions gradually scarred over and healed during the next 3 weeks; ultimately, complete tumor regression was observed, after only a single administration of the combination therapy.

5. Summary and outlook

As the library of discodermolide analogues grows, so too does our understanding of the structure–activity relationship of this most interesting antitumor agent. For example, the data currently available suggest that the conformational restrictions imparted by the *Z*-olefins at C(8)–C(9) and, particularly, C(13)–C(14) are critical to maintain potent cell growth inhibitory activity. Likewise, the perturbation caused by manipulation of the C(11) and/or C(17) hydroxyl groups, either in terms of stereogenicity or in terms of functionality, proved to be quite detrimental to activity, a result that is not surprising given the role that these substituents play in governing the conformation of (+)-discodermolide through nonbonded interactions.[28,29] Conversely, some discodermolide substructures could indeed withstand significant modification or group deletion. For example, the C(19) carbamate and the C(23)–C(24) olefin could be completely removed while maintaining potency; saturation of the terminal diene was also acceptable. Alternatively either the carbamate or the diene could be appended with a variety of substituents with little impact on inhibitory potency. Removal of the C(14) or C(16) methyl groups also had little effect on activity in most of the cell lines evaluated. Perhaps most notably, the data reveal that the C(1)–C(7) region could be considerably simplified, while retaining extremely potent cell growth inhibitory activity. The latter modifications, while providing useful structure–activity information, also serve to ease somewhat the synthetic difficulty associated with production of highly active discodermolide-related compounds.

A number of curious structure–activity effects were noted in analogues incorporating multiple modifications that independently had little impact on cytotoxicity. For example, while removal of the C(19) carbamate, truncation of the diene and simplification of the C(1)–C(7) lactone all have little or no detrimental effect on cytotoxicity when the C(14) methyl group is intact, identical changes to the 14-normethyl scaffold render the resulting discodermolide congeners completely devoid of activity at the sub-micromolar level. Likewise, the 2,3-anhydro skeleton seems to be quite sensitive to substitution at the carbamate, while the 14-normethyl and the parent discodermolide systems tolerate changes to this region.

With respect to the underlying biology, a number of factors account for the potent cytotoxicity exhibited by (+)-discodermolide. The most striking is the unparalleled degree of tubulin hypernucleation promoted by this agent, even at low temperatures and in the absence of helper proteins. Discodermolide is also not a substrate for *P*-glycoprotein, and thus retains activity against paclitaxel-resistant and multi-drug-resistant cell lines. For reasons not yet fully understood, discodermolide and paclitaxel actually form a synergistic drug combination, wherein each is much more potent in the presence of low concentrations of the other than would be predicted from the individual IC_{50} values. Furthermore, it is now known that discodermolide possesses a second mode of cytotoxicity, specifically the induction of an accelerated senescence phenotype, which is not observed with paclitaxel or other members of this class of microtubule-stabilizing agents. Separately, the potential utility of microtubule-stabilizing natural products, including (+)-discodermolide, as neuroprotective agents is only beginning to be explored.

From the synthetic perspective, methods for the production of (+)-discodermolide have become increasingly shorter and more efficient. Indeed, the production of 60 g of the natural product by Novartis showcased the increasing potential of total synthesis to provide clinically relevant quantities of complex natural products. In a broader sense, the Novartis work is simply the continuation of an accelerating trend in pharmaceutical development; over 60% of the small-molecule drugs introduced to the market between 1981 and 2002 either were, or were derived from, naturally occurring compounds.[94] Furthermore, our investigation of nature's reserve of interesting, medicinally useful

compounds has barely scratched the surface. Going forward, it is likely that many potentially useful lead compounds will be identified that possess synthetically demanding architectures. Thus, future therapeutic breakthroughs will depend, at least in part, on the ability of synthetic chemists to rise to the challenge.

Acknowledgements

The discodermolide synthetic program in the Smith Laboratory was supported by the National Institutes of Health (National Cancer Institute and Institute of General Medical Sciences) through grants CA-19033 and GM-29028, by the U.S. Army through grant DAMD17-00-1-0404, and by Kosan Biosciences, Inc.

References and notes

1. Mann, J. *Nat. Rev. Cancer* **2002**, *2*, 143–148.
2. (a) Schiff, P. B.; Fant, J.; Horwitz, S. B. *Nature* **1979**, *277*, 665–667; (b) Schiff, P. B.; Horwitz, S. B. *Proc. Natl. Acad. Sci. U.S.A.* **1980**, *77*, 1561–1565; (c) Parness, J.; Horwitz, S. B. *J. Cell Biol.* **1981**, *91*, 479–487; (d) Horwitz, S. B.; Parness, J.; Schiff, P. B.; Manfredi, J. J. *Cold Spring Harbor Symp. Quant. Biol.* **1982**, *46*, 219–226.
3. Gerth, K.; Bedorf, N.; Hofle, G.; Irschik, H.; Reichenbach, H. *J. Antibiot.* **1996**, *49*, 560–563.
4. (a) Bollag, D. M.; McQueney, P. A.; Zhu, J.; Hensens, O.; Koupal, L.; Liesch, J.; Goetz, M.; Lazarides, E.; Woods, C. M. *Cancer Res.* **1995**, *55*, 2325–2333; (b) Su, D.-S.; Balog, A.; Meng, D.; Bertinato, P.; Danishefsky, S. J.; Zheng, Y.-H.; Chou, T.-C.; He, L.; Horwitz, S. B. *Angew. Chem., Int. Ed.* **1997**, *36*, 2093–2096; (c) Chou, T.-C.; Zhang, X.-G.; Balog, A.; Su, D.-S.; Meng, D.; Savin, K.; Bertino, J. R.; Danishefsky, S. J. *Proc. Natl. Acad. Sci. U.S.A.* **1998**, *95*, 9642–9647.
5. (a) Rivkin, A.; Yoshimura, F.; Gabarda, A. E.; Cho, Y. S.; Chou, T.-C.; Dong, H.; Danishefsky, S. J. *J. Am. Chem. Soc.* **2004**, *126*, 10913–10922; (b) Rivkin, A.; Chou, T.-C.; Danishefsky, S. J. *Angew. Chem., Int. Ed.* **2005**, *44*, 2838–2850.
6. Source: <http://www.kosan.com>.
7. Source: <http://www.clinicaltrials.gov>.
8. Gunasekera, S. P.; Gunasekera, M.; Longley, R. E.; Schulte, G. K. *J. Org. Chem.* **1990**, *55*, 4912–4915; Correction: *J. Org. Chem.* **1991**, *56*, 1346.
9. (a) Nerenberg, J. B.; Hung, D. T.; Somers, P. K.; Schreiber, S. L. *J. Am. Chem. Soc.* **1993**, *115*, 12621–12622; (b) Hung, D. T.; Nerenberg, J. B.; Schreiber, S. L. *Chem. Biol.* **1994**, *1*, 67–71; (c) Hung, D. T.; Nerenberg, J. B.; Schreiber, S. L. *J. Am. Chem. Soc.* **1996**, *118*, 11054–11080.
10. (a) Longley, R. E.; Caddigan, D.; Harmony, D.; Gunasekera, M.; Gunasekera, S. *Transplantation* **1991**, *52*, 650–656; (b) Longley, R. E.; Caddigan, D.; Harmony, D.; Gunasekera, M.; Gunasekera, S. *Transplantation* **1991**, *52*, 656–661.
11. Klein, L.; Freeze, B. S.; Smith, A. B., III; Horwitz, S. B. *Cell Cycle* **2005**, *4*, 501–507.
12. (a) Martello, L. A.; McDaid, H. M.; Regl, D. L.; Yang, C.-P. H.; Meng, D.; Pettus, T. R. R.; Kaufman, M. D.; Arimoto, H.; Danishefsky, S. J.; Smith, A. B., III; Horwitz, S. B. *Clin. Cancer Res.* **2000**, *6*, 1978–1987; (b) Honore, S.; Kamath, K.; Braguer, D.; Horwitz, S. B.; Wilson, L.; Briand, C.; Jordan, M. A. *Cancer Res.* **2004**, *64*, 4957–4964.
13. Lindel, T.; Jensen, P. R.; Fenical, W.; Long, B. H.; Casazza, A. M.; Carboni, J.; Fairchild, C. R. *J. Am. Chem. Soc.* **1997**, *119*, 8744–8745.
14. Hamel, E.; Sackett, D. L.; Vourloumis, D.; Nicolaou, K. C. *Biochemistry* **1999**, *38*, 5490–5498.
15. Mooberry, S. L.; Tien, G.; Hernandez, A. H.; Plubrukarn, A.; Davidson, B. S. *Cancer Res.* **1999**, *59*, 653–660.
16. Wright, A. E.; Cummins, J. L.; Pomponi, S. A.; Longley, R. E.; Isbrucker, R. A. WO 2,001,062,239, 2001.
17. Hood, K. A.; West, L. M.; Rouwe, B.; Northcote, P. T.; Berridge, M. V.; Wakefield, S. J.; Miller, J. H. *Cancer Res.* **2002**, *62*, 3356–3360.
18. Sato, B.; Nakajima, H.; Miyauchi, M.; Muramatsu, H.; Ito, K.; Takase, S.; Terano, H. WO 9,632,402, 1996.
19. Muramatsu, H.; Miyauchi, M.; Sato, B.; Yoshimura, S.; Takase, S.; Terano, H.; Oku, T. *Tennen Yuki Kagobutsu Toronkai Koen Yoshishu* **1998**, *40*, 487–492.
20. Hemscheidt, T. K.; Mooberry, S. L. WO 2,000,071,563, 2000.
21. Jacobs, R. S.; Wilson, L.; Madari, H. WO 2,002,062,293, 2002.
22. Buey, R. M.; Barasoain, I.; Jackson, E.; Meyer, A.; Giannakakou, P.; Paterson, I.; Mooberry, S.; Andreu, J. M.; Diaz, J. F. *Chem. Biol.* **2005**, *12*, 1269–1279.
23. Longley, R. E.; Gunasekera, S. P.; Faherty, D.; McLane, J.; Dumont, F. *Ann. N.Y. Acad. Sci.* **1993**, *696*, 94–107.
24. ter Haar, E.; Kowalski, R. J.; Hamel, E.; Lin, C. M.; Longley, R. E.; Gunasekera, S. P.; Rosenkranz, H. S.; Day, B. W. *Biochemistry* **1996**, *35*, 243–250.
25. Hung, D. T.; Chen, J.; Schreiber, S. L. *Chem. Biol.* **1996**, *3*, 287–293.
26. Xia, S.; Kenesky, C. S.; Rucker, P. V.; Smith, A. B., III; Orr, G. A.; Horwitz, S. B. *Biochemistry* **2006**, *45*, 11762–11775.
27. Smith, A. B., III; Rucker, P. V.; Brouard, I.; Freeze, B. S.; Xia, S.; Horwitz, S. B. *Org. Lett.* **2005**, *7*, 5199–5202.
28. Martello, L. A.; LaMarche, M. J.; He, L.; Beauchamp, T. J.; Smith, A. B., III; Horwitz, S. B. *Chem. Biol.* **2001**, *8*, 843–855.
29. (a) Monteagudo, E.; Cicero, D. O.; Cornett, B.; Myles, D. C.; Snyder, J. P. *J. Am. Chem. Soc.* **2001**, *123*, 6929–6930; (b) Smith, A. B.; LaMarche, M. J.; Falcone-Hindley, M. *Org. Lett.* **2001**, *3*, 695–698.
30. Kowalski, R. J.; Giannakakou, P.; Gunasekera, S. P.; Longley, R. E.; Day, B. W.; Hamel, E. *Mol. Pharmacol.* **1997**, *52*, 613–622.
31. Chou, T.-C.; Talalay, P. *Adv. Enzyme Regul.* **1984**, *22*, 27–55.
32. Huang, G. S.; Lopez-Barcons, L.; Freeze, B. S.; Smith, A. B., III; Goldberg, G. L.; Horwitz, S. B.; McDaid, H. M. *Clin. Cancer Res.* **2006**, *12*, 298–304.
33. Dimri, G.; Lee, X.; Basile, G.; Acosta, M.; Scott, G.; Roskelley, C.; Medrano, E.; Linskens, M.; Rubelj, I.; Pereira-Smith, O.; Peacocke, M.; Campisi, J. *Proc. Natl. Acad. Sci. U.S.A.* **1995**, *92*, 9363–9367.
34. For a recent review, see: Forman, M. S.; Trojanowski, J. Q.; Lee, V. M.-Y. *Nat. Med.* **2004**, *10*, 1055–1063.
35. Zhang, B.; Maiti, A.; Shively, S.; Lakhani, F.; McDonald-Jones, G.; Bruce, J.; Lee, E. B.; Xie, S. X.; Joyce, S.; Li, C.; Toleikis, P. M.; Lee, V. M.-Y.; Trojanowski, J. Q. *Proc. Natl. Acad. Sci. U.S.A.* **2005**, *102*, 227–231.
36. <http://www.lclark.edu/~reiness/neurobiology/Lectures/Axonal%20Transport.pdf>.
37. Busciglio, J.; Lorenzo, A.; Yeh, J.; Yankner, B. A. *Neuron* **1995**, *14*, 879–888.
38. Goedert, M. *Neuroscientist* **1997**, *3*, 131–141.
39. Ishihara, T.; Hong, M.; Zhang, B.; Nakagawa, Y.; Lee, M. K.; Trojanowski, J. Q.; Lee, V.-M. *Neuron* **1999**, *24*, 751–762.

40. (a) Michaelis, M. L.; Ranciat, N.; Chen, Y.; Bechtel, M.; Ragan, R.; Hepperle, M.; Liu, Y.; Georg, G. *J. Neurochem.* **1998**, *70*, 1623–1627; (b) Michaelis, M. L.; Ansar, S.; Chen, Y.; Reiff, E. R.; Seyb, K. I.; Himes, R. H.; Audus, K. L.; Georg, G. I. *J. Pharmacol. Exp. Ther.* **2005**, *312*, 659–666.
41. (a) See Ref. 9a; (b) Smith, A. B., III; Qiu, Y.; Jones, D. R.; Kobayashi, K. *J. Am. Chem. Soc.* **1995**, *117*, 12011–12012; (c) Harried, S. S.; Yang, G.; Strawn, M. A.; Myles, D. C. *J. Org. Chem.* **1997**, *62*, 6098–6099; (d) Marshall, J. A.; Johns, B. A. *J. Org. Chem.* **1998**, *63*, 7885–7892; (e) Smith, A. B., III; Kaufman, M. D.; Beauchamp, T. J.; LaMarche, M. J.; Arimoto, H. *Org. Lett.* **1999**, *1*, 1823–1826; (f) Halstead, D. P. Ph.D. Thesis, Harvard University, Cambridge, MA, 1999. (g) Paterson, I.; Florence, G. J.; Gerlach, K.; Scott, J. *Angew. Chem., Int. Ed.* **2000**, *39*, 377–380; (h) Smith, A. B.; Freeze, B. S.; Brouard, I.; Hirose, T. *Org. Lett.* **2003**, *5*, 4405–4408; (i) Paterson, I.; Delgado, O.; Florence, G. J.; Lyothier, I.; Scott, J. P.; Sereinig, N. *Org. Lett.* **2003**, *5*, 35–38; (j) Mickel, S. J.; Niederer, D.; Daeffler, R.; Osmani, A.; Kuesters, E.; Schmid, E.; Schaer, K.; Gamboni, R.; Chen, W.; Loeser, E.; Kinder, F. R., Jr.; Konigsberger, K.; Prasad, K.; Ramsey, T. M.; Repic, O.; Wang, R.-M.; Florence, G.; Lyothier, I.; Paterson, I. *Org. Process Res. Dev.* **2004**, *8*, 122–130 and references cited therein; (k) Arefolov, A.; Panek, J. S. *J. Am. Chem. Soc.* **2005**, *127*, 5596–5603; (l) Smith, A. B., III; Freeze, B. S.; Xian, M.; Hirose, T. *Org. Lett.* **2005**, *7*, 1825–1828; (m) Paterson, I.; Lyothier, I. *Org. Lett.* **2004**, *6*, 4933–4936.
42. (a) Clark, D. L.; Heathcock, C. H. *J. Org. Chem.* **1993**, *58*, 5878–5879; (b) Evans, P. L.; Golec, J. M. C.; Gillespie, R. J. *Tetrahedron Lett.* **1993**, *34*, 8163–8166; (c) Golec, J. M. C.; Gillespie, R. J. *Tetrahedron Lett.* **1993**, *34*, 8167–8168; (d) Golec, J. M. C.; Jones, S. D. *Tetrahedron Lett.* **1993**, *34*, 8159–8162; (e) Miyazawa, M.; Oonuma, S.; Maruyama, K.; Miyashita, M. *Chem. Lett.* **1997**, 1193–1194; (f) Miyazawa, M.; Oonuma, S.; Maruyama, K.; Miyashita, M. *Chem. Lett.* **1997**, 1191–1192; (g) Filla, S. A.; Song, J. J.; Chen, L.; Masamune, S. *Tetrahedron Lett.* **1999**, *40*, 5449–5453; (h) Misske, A. M.; Hoffmann, H. M. R. *Tetrahedron* **1999**, *55*, 4315–4324; (i) Arjona, O.; Menchaca, R.; Plumet, J. *Tetrahedron* **2001**, *57*, 6751–6755; (j) BouzBouz, S.; Cossy, J. *Org. Lett.* **2001**, *3*, 3995–3998; (k) Chakraborty, T. K.; Laxman, P. *J. Indian Chem. Soc.* **2001**, *78*, 543–545; (l) Day, B. W.; Kangani, C. O.; Avor, K. S. *Tetrahedron: Asymmetry* **2002**, *13*, 1161–1165; (m) Shahid, K. A.; Mursheda, J.; Okazaki, M.; Shuto, Y.; Goto, F.; Kiyooka, S.-i. *Tetrahedron Lett.* **2002**, *43*, 6377–6381; (n) Shahid, K. A.; Li, Y.-N.; Okazaki, M.; Shuto, Y.; Goto, F.; Kiyooka, S.-i. *Tetrahedron Lett.* **2002**, *43*, 6373–6376; (o) Yadav, J. S.; Abraham, S.; Reddy, M. M.; Sabitha, G.; Sankar, A. R.; Kunwar, A. C. *Tetrahedron Lett.* **2002**, *43*, 3453; (p) BouzBouz, S.; Cossy, J. *Org. Lett.* **2003**, *5*, 3029–3031; (q) Choy, N.; Shin, Y.; Nguyen, P. Q.; Curran, D. P.; Balachandran, R.; Madiraju, C.; Day, B. W. *J. Med. Chem.* **2003**, *46*, 2846–2864; (r) Kiyooka, S.-i.; Shahid, K. A.; Goto, F.; Okazaki, M.; Shuto, Y. *J. Org. Chem.* **2003**, *68*, 7967–7978; (s) Shahid, K. A.; Mursheda, J.; Okazaki, M.; Shuto, Y.; Goto, F.; Kiyooka, S.-i. *Tetrahedron Lett.* **2003**, *44*, 1519–1520; (t) Yakura, T.; Kitano, T.; Ikeda, M.; Uenishi, J. i. *Heterocycles* **2003**, *59*, 347–358; (u) Bazan-Tejeda, B.; Georgy, M.; Campagne, J.-M. *Synlett* **2004**, 720–722; (v) BouzBouz, S.; Cossy, J. *Synlett* **2004**, 2034–2036; (w) Loiseleur, O.; Koch, G.; Wagner, T. *Org. Process Res. Dev.* **2004**, *8*, 597–602; (x) Parker, K. A.; Katsoulis, I. A. *Org. Lett.* **2004**, *6*, 1413–1416; (y) Ramachandran, P. V.; Prabhudas, B.; Chandra, J. S.; Reddy, M. V. R. *J. Org. Chem.* **2004**, *69*, 6294–6304.
43. Roush, W. R.; Palkowitz, A. D.; Ando, K. *J. Am. Chem. Soc.* **1990**, *112*, 6348–6359.
44. Stork, G.; Zhao, K. *Tetrahedron Lett.* **1989**, *30*, 2173–2175.
45. Negishi, E.; Valente, L. F.; Kobayashi, M. *J. Am. Chem. Soc.* **1980**, *102*, 3298–3299.
46. Still, W. C.; Gennari, C. *Tetrahedron Lett.* **1983**, *24*, 4405–4408.
47. Gilbert, J. C.; Weerasooriya, U. *J. Org. Chem.* **1979**, *44*, 4997–4998.
48. Evans, D. A.; Gauchet-Prunet, J. A. *J. Org. Chem.* **1993**, *58*, 2446–2453.
49. (a) Hiyama, T.; Okude, Y.; Kimura, K.; Nozaki, H. *Bull. Chem. Soc. Jpn.* **1982**, *55*, 561–568; (b) Takai, K.; Kuroda, T.; Nakatsukasa, S.; Oshima, K.; Nozaki, H. *Tetrahedron Lett.* **1985**, *26*, 5585–5588; (c) Takai, K.; Tagashira, M.; Kuroda, T.; Oshima, K.; Utimoto, K.; Nozaki, H. *J. Am. Chem. Soc.* **1986**, *108*, 6048–6050; (d) Jin, H.; Uenishi, J.; Christ, W. J.; Kishi, Y. *J. Am. Chem. Soc.* **1986**, *108*, 5644–5646; (e) Aicher, T. D.; Kishi, Y. *Tetrahedron Lett.* **1987**, *28*, 3463–3466.
50. Kocovsky, P. *Tetrahedron Lett.* **1986**, *27*, 5521–5524.
51. Gage, J. R.; Evans, D. A. *Org. Synth.* **1990**, *68*, 77–82.
52. Chen, J.; Wang, T.; Zhao, K. *Tetrahedron Lett.* **1994**, *35*, 2827–2828.
53. Arimoto, H.; Kaufman, M. D.; Kobayashi, K.; Qiu, Y.; Smith, A. B., III. *Synlett* **1998**, 765–767.
54. Smith, A. B., III; Adams, C. M. *Acc. Chem. Res.* **2004**, *37*, 365–377.
55. Wittig, G.; Schollkopf, U. *Chem. Ber.* **1954**, *87*, 1318–1330.
56. Ikeda, Y.; Ukai, J.; Ikeda, N.; Yamamoto, H. *Tetrahedron* **1987**, *43*, 723–730.
57. Harried, S. S.; Lee, C. P.; Yang, G.; Lee, T. I. H.; Myles, D. C. *J. Org. Chem.* **2003**, *68*, 6646–6660.
58. Springer, J. B.; DeBoard, J.; Corcoran, R. C. *Tetrahedron Lett.* **1995**, *36*, 8733–8736.
59. Danishefsky, S. J.; Pearson, W. H.; Harvey, D. F.; Maring, C. J.; Springer, J. P. *J. Am. Chem. Soc.* **1985**, *107*, 1256–1268.
60. (a) Yang, G.; Myles, D. C. *Tetrahedron Lett.* **1994**, *35*, 2503–2504; (b) Yang, G.; Myles, D. C. *Tetrahedron Lett.* **1994**, *35*, 1313–1316.
61. (a) Linderman, R. J.; Cusack, K. P.; Jaber, M. R. *Tetrahedron Lett.* **1996**, *37*, 6649–6652; (b) White, J. D.; Nylund, C. S.; Green, N. J. *Tetrahedron Lett.* **1997**, *38*, 7329–7332.
62. Peterson, D. J. *J. Org. Chem.* **1968**, *33*, 780–784.
63. Roush, W. R.; Grover, P. T. *Tetrahedron* **1992**, *48*, 1981–1998.
64. (a) Marshall, J. A.; Perkins, J. F.; Wolf, M. A. *J. Org. Chem.* **1995**, *60*, 5556–5559; (b) Marshall, J. A.; Lu, Z.-H.; Johns, B. A. *J. Org. Chem.* **1998**, *63*, 817–823.
65. Gao, Y.; Klunder, J. M.; Hanson, R. M.; Masamune, H.; Ko, S. Y.; Sharpless, K. B. *J. Am. Chem. Soc.* **1987**, *109*, 5765–5780.
66. (a) Paterson, I.; Schlapbach, A. *Synlett* **1995**, 498–500; (b) Hodgson, D. M.; Wells, C. *Tetrahedron Lett.* **1992**, *33*, 4761–4762.
67. Miyaura, N.; Suzuki, A. *Chem. Rev.* **1995**, *95*, 2457–2483.
68. (a) Evans, D. A.; Kim, A. S.; Metternich, R.; Novack, V. J. *J. Am. Chem. Soc.* **1998**, *120*, 5921–5942; (b) Evans, D. A.; Kim, A. S. *J. Am. Chem. Soc.* **1996**, *118*, 11323–11324; (c) Evans, D. A.; Ratz, A. M.; Huff, B. E.; Sheppard, G. S. *J. Am. Chem. Soc.* **1995**, *117*, 3448–3467; (d) Evans, D. A.; Ng, H. P.; Reieger, D. L. *J. Am. Chem. Soc.* **1993**, *115*,

11446–11459; (e) Evans, D. A.; Gage, J. R.; Leighton, J. L. *J. Am. Chem. Soc.* **1992**, *114*, 9434–9453.
69. Corey, E. J.; Fuchs, P. L. *Tetrahedron Lett.* **1972**, *13*, 3769–3772.
70. Nicolaou, K. C.; Reddy, M. M.; Skokotas, G.; Sato, F.; Xiao, X.-Y.; Hwang, C.-K. *J. Am. Chem. Soc.* **1993**, *115*, 3558–3575.
71. Walkup, R. D.; Kane, R. R.; Boatman, P. D., Jr.; Cunningham, R. T. *Tetrahedron Lett.* **1990**, *31*, 7587–7609.
72. Mukaiyama, T.; Narasaka, K.; Banno, K. *Chem. Lett.* **1973**, 1011–1014.
73. Dauben, W. G.; Gerdes, J. M.; Bunce, R. A. *J. Org. Chem.* **1984**, *49*, 4293–4295.
74. Cowden, C. J.; Paterson, I. *Org. React. (N.Y.)* **1997**, *51*, 1–200.
75. (a) Cherest, M.; Felkin, H.; Prudent, N. *Tetrahedron Lett.* **1968**, 2199–2204; (b) Anh, N. T.; Eisenstein, O. *Nouv. J. Chim.* **1977**, *1*, 61–70.
76. Paterson, I.; Delgado, O.; Florence, G. J.; Lyothier, I.; O'Brien, M.; Scott, J. P.; Sereinig, N. *J. Org. Chem.* **2005**, *70*, 150–160.
77. Masse, C. E.; Panek, J. S. *Chem. Rev.* **1995**, *95*, 1293–1316.
78. Tsai, D. J. S.; Matteson, D. S. *Tetrahedron Lett.* **1981**, *29*, 2751–2752.
79. Hart, D. W.; Schwartz, J. *J. Am. Chem. Soc.* **1974**, *96*, 8115–8516.
80. Blumenkopf, T. A.; Overman, L. E. *Chem. Rev.* **1986**, *86*, 857–874.
81. (a) Paterson, I.; Gibson, K. R.; Oballa, R. M. *Tetrahedron Lett.* **1996**, *37*, 8585–8588; (b) Paterson, I.; Florence, G. J.; Gerlach, K.; Scott, J. P.; Sereinig, N. *J. Am. Chem. Soc.* **2001**, *123*, 9535–9544.
82. (a) Evans, D. A.; Trotter, B. W.; Coleman, P. J.; Cote, B.; Dias, L. C.; Rajapakse, H. A.; Tyler, A. N. *Tetrahedron* **1999**, *55*, 8671–8726; (b) Evans, D. A.; Coleman, P. J.; Cote, B. *J. Org. Chem.* **1997**, *62*, 788–789.
83. Evans, D. A.; Hoveyda, A. H. *J. Am. Chem. Soc.* **1990**, *112*, 6447–6449.
84. Stamos, D. P.; Taylor, A. G.; Kishi, Y. *Tetrahedron Lett.* **1996**, *37*, 8647–8650.
85. (a) Gunasekera, S. P.; Longley, R. E.; Isbrucker, R. A. *J. Nat. Prod.* **2001**, *64*, 171–174; (b) Isbrucker, R. A.; Gunasekera, S. P.; Longley, R. E. *Cancer Chemother. Pharmacol.* **2001**, *48*, 29–36; (c) Gunasekera, S. P.; Paul, G. K.; Longley, R. E.; Isbrucker, R. A.; Pomponi, S. A. *J. Nat. Prod.* **2002**, *65*, 1643–1648; (d) Gunasekera, S. P.; Longley, R. E.; Isbrucker, R. A. *J. Nat. Prod.* **2002**, *65*, 1830–1837; (e) Gunasekera, S. P.; Mickel, S. J.; Daeffler, R.; Niederer, D.; Wright, A. E.; Linley, P.; Pitts, T. *J. Nat. Prod.* **2004**, *67*, 749–756.
86. Paterson, I.; Delgado, O. *Tetrahedron Lett.* **2003**, *44*, 8877–8882.
87. (a) See Ref. 28; (b) Burlingame, M. A.; Shaw, S. J.; Sundermann, K. F.; Zhang, D.; Petryka, J.; Mendoza, E.; Liu, F.; Myles, D. C.; LaMarche, M. J.; Hirose, T.; Freeze, B. S.; Smith, A. B., III. *Bioorg. Med. Chem. Lett.* **2004**, *14*, 2335–2338; (c) Smith, A. B., III; Freeze, B. S.; LaMarche, M. J.; Hirose, T.; Brouard, I.; Xian, M.; Sundermann, K. F.; Shaw, S. J.; Burlingame, M. A.; Horwitz, S. B.; Myles, D. C. *Org. Lett.* **2005**, *7*, 315–318; (d) Smith, A. B., III; Freeze, B. S.; LaMarche, M. J.; Hirose, T.; Brouard, I.; Rucker, P. V.; Xian, M.; Sundermann, K. F.; Shaw, S. J.; Burlingame, M. A.; Horwitz, S. B.; Myles, D. C. *Org. Lett.* **2005**, *7*, 311–314; (e) Shaw, S. J.; Sundermann, K. F.; Burlingame, M. A.; Myles, D. C.; Freeze, B. S.; Xian, M.; Brouard, I.; Smith, A. B., III. *J. Am. Chem. Soc.* **2005**, *127*, 6532–6533; (f) Smith, A. B., III; Freeze, B. S.; LaMarche, M. J.; Sager, J.; Kinzler, K. W.; Vogelstein, B. *Bioorg. Med. Chem. Lett.* **2005**, *15*, 3623–3626; (g) Shaw, S. J.; Menzella, H. G.; Myles, D. C.; Xian, M.; Smith, A. B., III. *Org. Biomol. Chem.*, in press.
88. (a) Curran, D. P.; Furukawa, T. *Org. Lett.* **2002**, *4*, 2233–2235; (b) Minguez, J. M.; Giuliano, K. A.; Balachandran, R.; Madiraju, C.; Curran, D. P.; Day, B. W. *Mol. Cancer Ther.* **2002**, *1*, 1305–1313; (c) Minguez, J. M.; Kim, S.-Y.; Giuliano, K. A.; Balachandran, R.; Madiraju, C.; Day, B. W.; Curran, D. P. *Bioorg. Med. Chem.* **2003**, *11*, 3335–3357; (d) See Ref. 42q.
89. IC_{50} data for the A549, HCT116, MIP101, 1A9, and 1A9PTX22 cell lines were drawn from: Kinder, F. R., Jr.; Bair, K. W.; Chen, W.; Florence, G. J.; Francavilla, C.; Geng, P.; Gunasekera, S.; Lassota, P. T.; Longley, R.; Palermo, M.; Paterson, I.; Pomponi, S.; Ramsey, T. M.; Rogers, L.; Sabio, M.; Sereinig, N.; Sorensen, E.; Wang, R.; Wright, A. Presented at American Association for Cancer Research 93rd Annual Meeting, San Francisco, CA, 2002. Poster #3650.
90. Kinder, F. R., Jr.; Bair, K. W.; Chen, W.; Florence, G. J.; Francavilla, C.; Geng, P.; Gunasekera, S.; Lassota, P. T.; Longley, R.; Palermo, M.; Paterson, I.; Pomponi, S.; Ramsey, T. M.; Rogers, L.; Sabio, M.; Sereinig, N.; Sorensen, E.; Wang, R.; Wright, A. Presented at American Association for Cancer Research 93rd Annual Meeting, San Francisco, CA, 2002. Poster #3650.
91. (a) Kinder, F. R. WO 2,002,012,220, 2002. (b) Kinder, F. R., Jr.; Kapa, P. K.; Loeser, E. M. WO 2,002,098,843, 2002. (c) Kinder, F. R., Jr.; Bair, K. W.; Ramsey, T. M.; Sabio, M. L. WO 2,003,014,102, 2003.
92. Dang, L. H.; Bettegowda, C.; Huso, D. L.; Kinzler, K. W.; Vogelstein, B. *Proc. Natl. Acad. Sci. U.S.A.* **2001**, *98*, 15155–15160.
93. Dang, L. H.; Bettegowda, C.; Agrawal, N.; Cheong, I.; Huso, D. L.; Frost, P.; Loganzo, F.; Greenberger, L.; Barkoczy, J.; Pettit, G. R.; Smith, A. B., III; Gurulingappa, H.; Khan, S.; Parmigiani, G.; Kinzler, K. W.; Zhou, S.; Vogelstein, B. *Cancer Biol. Ther.* **2004**, *3*, 326–337.
94. Newman, D. J.; Cragg, G. M.; Snader, K. M. *J. Nat. Prod.* **2003**, *66*, 1022–1037.

Biographical sketch

Brian Scott Freeze was born in Youngstown, OH in 1974. After receiving both a B.S in Biology and a Masters in Chemistry from Youngstown State University, he proceeded to earn a Ph.D. in 2005 under the direction of Professor Amos B. Smith, III at the University of Pennsylvania. His thesis research focused on the total synthesis of (+)-discodermolide and the production of novel analogues. He is currently employed as a medicinal chemist at Millennium Pharmaceuticals, Inc. in Cambridge, MA.

Amos B. Smith, III (born on 26 August 1944) attended Bucknell University, where he was awarded the University's first combined four-year B.S.–M.S. degree in Chemistry in 1966. After a year in medical school (University of Pennsylvania), he earned his Ph.D. degree (1972) and completed a year as a Research Associate at Rockefeller University. In 1973, he joined the Department of Chemistry at the University of Pennsylvania; currently, he is the Rhodes-Thompson Professor of Chemistry, a Member of the Monell Chemical Senses Center, and the Associate Director of the Penn Center for Molecular Discovery (PCMD). From 1988 to 1996 he served as Chairman of the Department of Chemistry and in 1998 he became the first Editor-in-Chief of the American Chemical Society's journal, *Organic Letters*. In 2001, he was appointed as an Honorary Member of the Kitasato Institute (Tokyo, Japan). Smith's research interests, recorded in more than 530 publications, encompass three diverse areas: natural product synthesis, bioorganic chemistry, and materials science. To date, his Laboratory has achieved the total synthesis of more than 90 architecturally complex natural products. Smith has been a Visiting Professor at Columbia, Cambridge (UK), and Auckland (NZ) Universities and has received a number of awards, including the ACS Arthur C. Cope Scholar Award (1991), the Alexander von Humboldt Research Award for Senior U.S, Scientist (1992), the ACS Award for Creativity in Organic Chemistry (1997), the Centenary Medal, Royal Society of Chemistry (2002), the Yamada-Koga Prize (2003), the University of Pennsylvania first Provost's Award for Distinguished Teaching and Mentoring of Ph.D. Students (2004), the Order of the Rising Sun, Gold Rays with Neck Ribbon from the Government of Japan (2004), Fellow in American Academy of the Arts and Sciences (2006), and the Royal Society of Chemistry Simonsen Medal (2008).